Electronic and Structural Properties of Substituted Oligo- and Polythiophenes

THESIS

Submitted in partial fulfillment

of the requirements for the degree of

Doctor of Philosophy

By

SAISUDHAKAR MUKKA

ID. No: 2012PHXF0507H

Under the supervision of

Prof. K. Sumithra

BIRLA INSTITUTE OF TECHNOLOGY AND SCIENCE, PILANI

Hyderabad campus, Telangana, INDIA

2018

Birla Institute of Technology and Science, Pilani,

Hyderabad Campus, Jawahar Nagar, Shamirpet Mandal, Hyderabad, Telangana State, 500078.

CERTIFICATE

This is to certify that the thesis entitled **"Electronic and Structural Properties of Substituted Oligo- and Polythiophenes"** submitted by Saisudhakar Mukka, ID.No. 2012PHXF0507H for the award of Ph.D degree of the institute embodies the original work done by him under my supervision.

Signature in full of the supervisor -

Name in Capital block letters - K. SUMITHRA

Designation - Associate Professor

Acknowledgements

Foremost, I would like to express my sincere gratitude to my Supervisor Prof. K. Sumithra for the continuous support of my Ph.D. study and research, for her patience, motivation, enthusiasm, and immense knowledge. Her guidance helped me in all the time of research and writing of this thesis.

I am thankful to acknowledge my doctoral advisory committee members Dr. Subhas Ghosal and Dr. Amit Nag for their support and encouragement during this period. I thank Prof. Manab Chakravarty, Head of the Department, Chemistry Division, BITS Pilani, Hyderabad campus and also other faculty members.

I am grateful to former vice-chancellor Prof. Bijendra Nath Jain, vice-chancellor Souvik Bhattacharyya of BITS Pilani, former director Prof. V. S. Rao, present director Prof. G Sundar of BITS Pilani Hyderabad Campus for allowing me to carry out my doctoral research work in the institute.

I would like to express my sincere thanks to Prof. Vidya Rajesh, Associate Dean, Academic Research (Ph.D. Programme), Prof. Yogeswari, Dean, SRCD, BITS-Pilani, Hyderabad campus, Prof. S. K.Verma, Dean, Academic Research (Ph.D. Programme), BITS Pilani for their continuous support and encouragement during my research work.

I specially thank T. Vikramaditya, for helping me in the work, thesis writing and was very much supportive in all aspects.

I acknowledge Department of Science and Technology (DST), Council of Scientific and Industrial Research (CSIR) and BITS, Pilani, Hyderabad campus for funding my fellowship.

I would like to acknowledge non-teaching staff Ashok Krishna, Sudheer, and Shanthakumari, of (chemistry department), Praveen, Bhagya Lakshmi (RCD Division), Krishna, Anil, Haritha, Madhu, Uday Kumar (Library staff), Hari (Stores), Ramesh, Suresh (IPC- Division).

I thank my parents and family members for their support throughout my Ph. D.

I thank all my friends Avinash, Bsri, Durga, Anusha, Purkayastha, Swagatika, Preeti, Reshma, Brindha, Uday, Karthik, Shanmukh, Abhijeet, Prasad, Krishna, Uma, Varma, Ravi, Rahul, Shiva, Karuna, Gangaram, Mahesh, Nagesh, Naidu, Suresh, Santhosh, Ravikiran, Swapna, Srinivas Rao, Sathvika, Shweta, Yadagiri, Pooja, Santhanam, Varalakshmi, Subramanyam, Subbarao, Kiran, Hemanth.

Saisudhakar Mukka

Abstract

The study of oligothiophene and polythiophene based molecules have attracted much attention in organic electronics industry due to their stability and ease of modification. Thiophene based molecules have been used in solar cell and light emitting device due to their tunable electronic and optical properties and also in field effect transistors due to their charge mobilities. The drawbacks associated with unsubstituted thiophene molecules are their lack of solubility in common organic solvents and are difficult to process. These drawbacks can be minimized by asymmetric substitution on thiophene units. This structural modification on oligo- or polythiophenes can alter their physical properties and improve their solubility. Cyclothiophenes are another family of thiophene based molecules which are present in circular form. These molecules have advantages over their linear counterparts as they do not have any end perturbing effects and they can also act as defect free conjugated polymers. Cyclothiophene systems with cavities are used in the nanometer range molecular recognition and host guest chemistry. Self-assembly of such macro cyclic systems could lead to the formation of nanotubes, which may be useful in biological and material science applications.

The electronic and optical properties of oligo and polythiophenes are extensively studied using density functional theory. Pure local density approximation (LDA) and generalized gradient approximation (GGA) methods systematically underestimate the band gaps. Therefore we have used the hybrid functional to study the electronic and structural properties of oligo- and polythiophenes. In order to study the excited state properties of conjugated systems, time-dependent density functional theory is employed. The hybrid functional B3LYP and meta-hybrid functional M06 overestimate the charge transfer excited state properties for extended π-conjugated systems. We have used long-range corrected functionals CAM-B3LYP to study the excited state properties and used the polarizable continuum model by incorporating state-specific and linear response approaches.

The effect of electronic donating (methoxy, ethoxy) and withdrawing (nitro, phenyl, cyano) substituents on all thiophene units in head tail – head tail (HT-HT) form of oligothiophene backbone are studied. The band gaps depend on the planarity, type of the substitution and bond length alternation. The oligothiophenes substituted with electron donating alkoxy group prefer more quinoid character than unsubstituted oligothiophenes. Electron withdrawing substituted oligothiophenes have less quinoid character than that of unsubstituted oligothiophenes which results in higher band gap. The most important criteria

for an oligomer to exhibit low band gaps is planarity. In order to understand the planarity behaviour, dihedral angles between sulphur atoms on adjacent thiophene units in oligomer are studied. The oligothiophenes retain planarity after substitution with alkoxy, cyano and nitro groups whereas phenyl substited oligothiophene deviates from planarity due to steric repulsions between phenyl and thiophene rings.

The charge separation effects are observed as a result of lack of symmetry in some of the substituted oligothiophenes. Oligothiophenes substituted with electron donating groups are found to show interesting delocalization phenomena and lead to lower band gaps than the oligothiophenes with terminal donor-acceptor substituents showing the push-pull effects. The band gap of oligothiophenes can be tuned by changing the nature of the substituents and its position. Oligothiophenes with electron donating substituents can be better materials with lower electronic band gaps than the corresponding polythiophenes.

The electronic properties of polythiophenes are studied with various substituents like alkyl, alkoxy, halo and aromatic groups in head head – tail tail (HH-TT) and head tail – head tail HT-HT form using density functional theory. The polymer is modelled as an infinite system in one-dimensional by taking a dimer as a unit cell using periodic boundary condition. The stability of the polymeric system is calculated with respect to the HH-TT form. Alkoxy substitution of polythiophene retains planarity and lowers the band gap compared to the unsubstituted polythiophene. This is due to the strong mesomeric effect by alkoxy group which increases the electron density on polymer and thereby increasing the conjugation. Alkyl and halo groups are electron donating and weak electron withdrawing groups respectively show no impact on the band gap. Bulky aromatic groups play crucial role in determining the band gap of polymer. Polythiophene lost planarity on substitution with phenyl or para-methoxy phenyl groups which increases the band gap of the polymer. The increase in deviation from the planarity and band gaps are more in HH-TT form than HT-HT form. Upon phenoxy substitution, polymer found to be planar due to decreases in the repulsion between thiophene and bulky phenyl group. The band gaps obtained from the extrapolation of oligomer band gaps result in inaccurate values whereas band gaps calculated with periodic boundary condition are accurate.

Time-dependent density functional theory is used to study the optical properties of a series α-oligothiophenes using various exchange-correlation functionals like hybrid functional B3LYP, meta hybrid functional M06, long-range corrected functionals ωB97XD

and CAM-B3LYP with various levels of basis sets with the inclusion of polarization and diffusion functions. We have considered polarizable continuum model with state-specific and linear response approaches to calculate absorption and emission properties. The accuracy of B3LYP and M06 functionals are foud to decrease with increase in chain length. The inclusion of "d" functions in the basis set improved results while the inclusion of "p" functions in the basis set with all the functionals and solvent formalisms have no effect on the optical properties. The long-range corrected CAM-B3LYP produced accurate results and ωB97XD functional consistently underestimated the wavelength maxima values. We have not observed any trend in the improvement of optical properties with increase of the basis set level. Thus, in essence, we have observed that the accuracy of different functionals varies depending upon the basis set chosen and solvent formalism employed, in determining the optical absorption and emission properties of these π-conjugated systems.

We have studied the electronic and optical properties of cyclic and linear isothianaphthenes of chain length 6, 8, 10, 12, 14 in syn and anti-forms employing density functional theory. Linear isothianaphthenes do not exhibit planarity in their structure. This is due to the steric repulsions between the adjacent monomers. The deviation from the planarity is more in syn-linear isothianaphthenes compared to that of trans isomers. The band gaps are decreased with the increase of chain length in both syn and anti linear forms. In the case of linear isothianaphthenes, anti-forms exhibited lower band gaps than corresponding syn-forms, due to less steric repulsions between adjacent isothianaphthene units compared to the syn-forms which adopt a slightly more planar configuration, thus facilitating a better π-conjugation. In the case of cyclic isothianaphthenes, anti-forms are found to be more stable than the corresponding syn counterparts. Cyclic syn-isothianaphthenes adopted crown shaped geometry for smaller monomeric units, but acquires a coplanar geometry at around n=12 and exhibited lower band gaps compared to that of corresponding anti-forms which are of cylindrical bangle like geometry. Band gaps of syn and anti-cyclic isothianaphthenes are found to be largely dependent on the geometry and strain energies.

In another study involving computational modelling of thiophene based donor-acceptor molecules towards photovoltaic applications, oligothiophenes of chain length 2-4 are considered as π-spacer between the triphenylamine donor and cyanoacrylic acid acceptor. The band gaps are reduced as the length of the π-spacer increases. The optical properties are improved when the donor strength of thetriphenylamine moiety is increased by substituting with methyl and methoxy groups but the HOMO energy level of the molecule is increased

thereby disfavouring the electron injection from the HOMO of electrolyte. In order to bring the HOMO and LUMO levels for favourable electron injection, thiophene units of π-spacer are substituted with strong electron withdrawing cyano group. With this modification, the electronic levels are made favourable for electronic injection with their absorption spectra in the visible region. Upon cyno substitution, one of the thiophene based donor-acceptor molecules exhibit the band gap 1.4 eV which falls in the Shockley-Queisser theoretical limit for solar cell application.

LIST OF ABBREVATIONS

AO – Atomic orbital

B3LYP - Becke-Lee-Yang and Parr

B88 - Becke parameter

BLA - Bond length alterations

CB – Conduction band

CGTO – contracted Gaussian types of orbitals

CT – Cyclothiophene

DFT – Density functional theory

FET – Field effect transistors

GGA - Generalized gradient approximation

GTO - Gaussian types of orbitals

HOMO – Highest occupied molecular orbital

ITN – Isothianapthene

KS - Kohn-Sham

LCAO - linear combination of atomic orbital approach

LDA - Local density approximation

LED – Light emitting diodes

LR – Linear response

LSDA – Local spin density approximation

LUMO – Lowest unoccupied molecular orbital

MGGA - Meta- generalized gradient approximation

MO - Molecular orbital

MOT - Molecular orbital theory

MP2 - Moller-Plesset

OFET – Organic filed effect transistors

PAT - Poly(3-alkylthiophene)

PBC – Periodic boundary condition

PBE - Perdew-Burke-Ernzerhof

PCM - Polarizable continuum model

PES - Potential energy surface

PITN – Polyisothianapthene

PT – Polythiophene

PVC – Photovoltaic cells

SALC - Symmetry-adapted linear combination

SS – State specific

STO - Slater type of orbitals

TD-DFT – Time-dependent density functional theory

UHF - Unrestricted Hartree–Fock

XCF - Exchange correlation functional

LIST OF FIGURES

LIST OF TABLES

Tables **Page No.**

TABLE OF CONTENTS

Contents

Chapter 1: Overview on electronic structure and optical properties of substituted oligo- and polythiophenes and their applications

Chapter 2: Computational Methodology

Chapter 5: Comprehensive evaluation of the effect of various exchange correlation functionals and basis sets on the optical properties of oligothiophenes

Chapter 6: Electronic structure calculations of linear and cyclic isothianaphthenes

Chapter 7: Computational modelling of thiophene based donor-acceptor molecules towards photovoltaic applications

Chapter 1

Review on electronic structure calculations of substituted oligo- and polythiophenes and their applications

1.1. Introduction

Organic semiconducting materials have received great attention since the discovery of polyacetylene derivative as a conducting material [1,2]. These materials offer numerous advantages over their inorganic counterparts such as easy fabrication, light weight, low cost, tunability, flexibility, solubility, and processability [3-7]. Generally, semiconducting materials exhibit a band gap in the range of 1-3 eV. Different types of organic π-conjugated molecular systems such as polyacetylene, polypyrrole, polyfuran etc. have been investigated in the past few years because of their promising electronic, electrical and optical properties [4,5].

Among the various organic π-conjugated materials, thiophene based systems are considered to be most promising candidates because of their environmental stability and synthetic availability in addition to their excellent electrical and optical properties [1,4,5]. These organic π-conjugated materials are considered to be potential analogs in various applications like field effect transistors (FETs) [6], light emitting diodes (LEDs) [7], photovoltaic cells (PVCs) [8] etc. The oligo- and polythiophene derivatives provide an extended π-conjugation, inter and intramolecular interaction, high charge carrier mobilities and low resistive losses [9,10]. The major drawback of these compounds containing extended π-conjugation is their lack of solubility in common organic solvents due to the formation of highly stable stacks by intermolecular π-π interactions between the molecules. This drawback can be addressed by the chemical functionalization of such π-conjugated systems.

Band gap is the fundamental property in organic conjugated systems which play a vital role in building devices [11]. The tuning of desired band gap results in enhancing the intrinsic charge carrier population and also attain stabilization in both oxidized and reduced states [12,13]. The band gap is one of the important factors in solar cell devices to achieve good power conversion efficiency [14]. However, narrowing the band gap in solar cells can also reduce the open circuit voltage which can result in the reduction of power conversion

efficiency [15]. The optimal band gap for solar cell applications has been reported to be 1.4 eV by Shockley and Queisser [16].

Band gap is critical parameter in OLED applications to determine the colour of the emitted light. So tuning of the band gap by structural modification of polymer affects the colour of the emission light. This kind of materials finds application in the light emitting diodes [7]. Among the aromatic and hetero-aromatic conjugated polymers, polythiophene has the lowest band gap of 2.1-2.2 eV [17,18]. The advantage of thiophene based materials is that they allow easy tuning of HOMO and LUMO energy levels by chemical functionalization to get the desired device performances [19]. Conjugated polymers are thermally stable and have been used to make electrical and optical devices like light emitting diodes and field effect transistors. In comparison with other organic conjugated polymers, polythiophenes offer many attractive characteristics in light emitting diode applications such as unique electrical and electro-optical properties, relatively good environmental stability and structural versatility [1,4,5]. However, poor electroluminescence and low quantum yield limit their use in these applications. Suitable functionalization on polythiophene backbone [20,21] helps to overcome this drawback.

1.2. Structural aspects of substituted oligo and polythiophenes

As unsubstituted oligothiophenes and polythiophenes are often associated with low solubility, it can be improved by the asymmetric substitution at 3rd or 4th carbon (β-position) on thiophene rings (Figure 1.1).

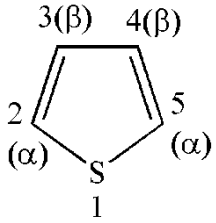

Figure 1.1 Chemical structure of thiophene monomer

Asymmetric 3-substituted thiophenes can result in three possible diads when two monomers are linked between 2- and 5-positions to yield, head-tail, head-head and tail-tail couplings as shown in the Figure 1.2. Coupling of head-tail diad results in the formation of $(HT\text{-}HT)_n$ polymer which is usually minor products and coupling with head-head dimer or tail-tail dimer results in the formation of $(HH\text{-}TT)_n$ polymer as shown in the Figure 1.3. Various synthetic methodologies are reported in the literature to synthesize $(HH\text{-}TT)_n$ polymer in good yields of almost 100%.

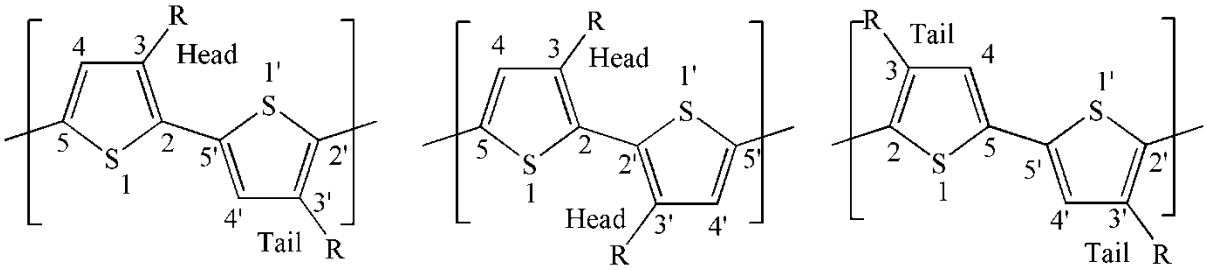

Figure 1.2. 2,5' or head–tail (HT) coupling; 2,2' or head–head (HH) coupling; 5,5' or tail–tail (TT) coupling [22].

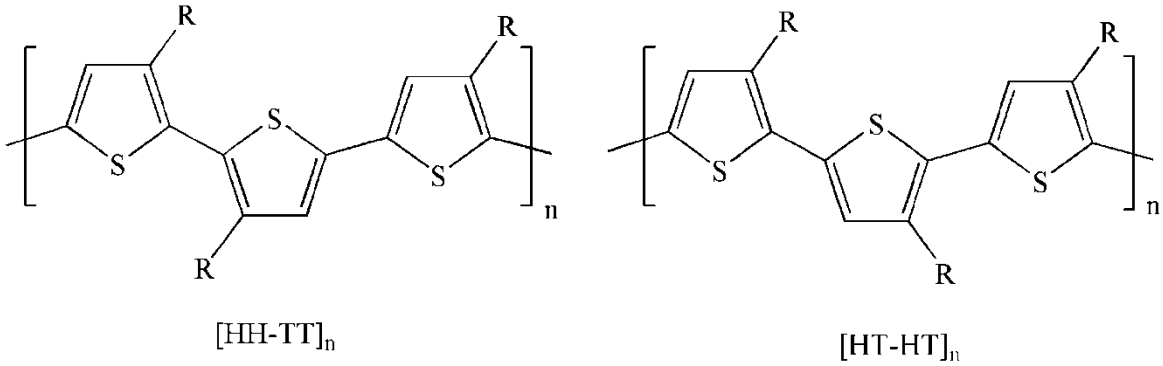

Figure 1.3. The possible polymers resulting from the coupling of three dimers (head-tail, head-head, and tail-tail).

1.3. Synthesis of oligothiophenes and polythiophenes

Stepwise synthesis of oligothiophenes requires a great effort compared to that of conventional polythiophenes [23]. Oligomeric systems have the advantage over polythiophenes in regio-specificity, precise control over chain length, and ease with which they can be characterized. Oligomers are normally more soluble than polymers, there-by having an increased processability which is a key factor for use in concerned devices. This can be attributed to the fact that oligothiophenes can be synthesized with a high degree of purity (including regioisomer control) [24], in contrast to polythiophenes. Polythiophenes can be synthesized electrochemically [25], by applying a potential across a solution of the monomer to be polymerized, or chemically [26], using oxidants or cross-coupling catalysts. Oligothiophenes are generally synthesized by either oxidative homocoupling or metal-catalyzed C-C-coupling reactions [27]. Various characterization methods such as electronic spectroscopy and cyclic voltammetry are generally used to analyze the electronic properties

of these materials. The lack of solubility of oligomers or polythiophenes can be overcome by the asymmetric substitution on thiophene rings in the 3rd position.

1.4. Literature Review

Thiophene acts as a promising building block for the synthesis and design of organic π-conjugated materials due to their excellent electronic, optical and redox properties [15]. The soft sulphur atom in thiophene ring has high polarizability which makes it prominent material as electron donating charge transporting system [28,29]. Numerous studies [21-30] have been carried out theoretically and experimentally on thiophene-based systems because of their potential applications in organic field effect transistors (OFETs) [30], organic light emitting diodes (OLEDs) [31], solar cells [32], sensors etc. The fundamental property which is essential to exhibit excellent properties for various electronic devices is the electronic band gap. Unsubstituted polythiophene has a band gap of 2.1 eV [33] and it can be altered by various substitution patterns.

1.4.1. Electronic and structural properties of oligo- and polythiophenes

The electronic properties of materials are governed by the band gap and therefore it is necessary to design oligomeric and polymeric systems to understand the changes in the band gap with respect to their chemical structure. Chou [34] and co-workers have studied theoretically the effect of various electron withdrawing and donating substituents on polythiophene and its derivatives employing periodic boundary conditions (PBC). The electron donating 3-substituted polythiophenes decrease the band gap whereas electron withdrawing group increases the band gap as compared to the unsubstituted polythiophenes. Steric effects of the substitution also have an appreciable impact on the π-conjugation of the polymer backbone resulting in band gap changes. As the structure deviates from the planarity there is an increase in the band gap [16]. End substitutions also play a crucial role in the development of molecules with well accepted band gaps. For example, asymmetrically substituted nitro compounds behave as push-pull systems and exhibit intense intramolecular charge transfer in the visible region whereas, nitro end substituted symmetrical oligothiophenes exhibit low energy π-π^* in the visible region [17]. These nitro-substituted systems form stable cations and anions and can be used as effectively as p- and n-channel semiconductors [35]. Oligothiophene with monomers having end substituted donor and acceptor groups at α-position are highly polarizable and can behave as push-pull molecules [18]. Such systems exhibit interesting non-linear optical properties and high second-order

polarizabilities which play a crucial role in two-photon absorption spectra [18]. These properties are dependent on the strength of the donor-acceptor groups and effect of the delocalization along the conjugated spacer [36,37]. Electron withdrawing groups like dicynomethylene [38] tricyanovinyl [39] groups at the terminal position of oligothiophenes facilitate the electron mobilities and promote the π-π interactions. These molecules are suitable for use as n-type transport materials.

In order to understand the effect of the interactions between the substituents and polymer backbone, Casanova and co-workers have studied the carboxylic substituted oligothiophenes in TT-HH and TH-TH form [40]. The carboxylic acid substituted oligothiophenes are expected to have similar electronic properties to those of unsubstituted oligothiophenes. Carboxylic acid enhances the solubility and π-π stacking interactions. The introduction of carboxylic acid substitution on oligo- or polythiophene increases the energy gap slightly. Alemán and co-workers have studied the effect of halogens on oligothiophene in tail-tail, head-head, head-tail fashion using experimental methods and density functional theory calculations [41]. Strong steric repulsions observed when bromine is substituted in head-head fashion while fluorine shows conformational flexibility and intermediate behaviour is observed with chlorine substitution. Costanzo and co-workers have studied the electronic and optical properties of substituted oligothiophenes in HH-TT form using semi-empirical calculations [42]. The thiol and thiomethyl substitutions lead to redshift and methyl substitution lead to blue shift in optical absorption with respect to corresponding unsubstituted oligomer. Regio-regularity is an important factor that helps to tune the band gap and thereby the structural parameters in polymers. Hadziioannou and co-workers have synthesized the various poly-alkylthiophenes [43] and studied the optical spectra. A blue shift has been observed when increasing the steric hindrance in head-head form of polymer whereas redshift is observed in head-tail form. The presence of head-head coupling in polymer increases the torsional angle and disturbs the conjugation and lead to increase of band gap from 3.4 eV to 3.5 eV.

Large differences in geometrical parameters have been observed depending on the length, type of the substitution, the pattern between the substituted and unsubstituted oligothiophenes [44]. For example, the substituent with large size can increase the distortion and decrease the effective π-conjugation in the polymer backbone. As a result, polythiophene with the larger substituent exhibits stronger steric effects and a blue shift in the emission spectrum [45]. Rittmeyer and co-workers [46] have investigated the effect of single bonded

substituents like methyl, amino, nitro, and phenyl as well as vinyl, bridged between thiophenes, on structural and electronic properties of oligo- and polythiophenes using periodic density functional theory calculations employing Perdew-Burke-Ernzerhof (PBE) functional. The nitro group shows a significant decrease in the HOMO-LUMO gap for monomer and dimer whereas slight increase for polymer when compared to the unsubstituted molecules. Groups like methyl, chlorine, and amine have no impact on the band gap either for the oligomer or polymer. Band gap is found to be decreased drastically on phenyl substitution and with vinyl bridge on polythiophenes [23].

Unsubstituted oligothiophenes have planar geometry in crystalline form which is responsible for their high π-delocalization and intermolecular interactions are introduced on chemical modification with appropriate groups. The position of the substituent on thiophene ring also has an impact on the electronic structure and properties of oligothiophenes. In addition, the introduction of substitution on thiophene ring may induce the conformational twist in the polymer backbone that disturbs the conjugation. If the substitution is at β-carbons of the oligomer, twist in dihedral angle observed is found to be more when compared to the end substituted oligothiophenes [47]. This is due to the steric hindrance between the molecules in the solid state [48]. Unubstituted oligothiophenes suffer from the chemical stability along with decreased solubility due to their high chemical activity at both ends of unsubstituted α-carbons. The stability of such unsubstituted oligothiophenes can be enhanced by blocking the end α-carbons with substituents [49] and this can increase the stability, crystal order and charge mobilities in the oligomers [50].

Substitution of long alkyl chains at 3rd position of thiophene ring in polythiophenes decreases the intermolecular interactions but enhances the solubility and processability. Such kind of substitutions may retard the conductivity of the polymers [51]. The effects of substitution of various functional groups on polythiophene have been studied in the literature. Alkoxy groups have shown the advantages over the alkyl group substitutions on polythiophene backbone such as higher stability, fluorescence etc [52,53]. Insertion of fluorocarbon side chain also improves the orientation and hydrophobic nature which helps in self-assembly of the polymer molecules and carrier mobilities [54,55]. Oligothiophenes can form self-assemblies with metal atoms due to their electron richness and their outstanding ability to acquire positive charge [56]. Self-assembly induces the white photoluminescence due to the intra and interchain interactions. These types of supramolecules are useful in charge transport devices [57].

Thiophene-based oligo- and polymers can be modified by doping or functionalization however doped materials are comparatively unstable and are associated with poor processability [58]. These disadvantages are overcome by chemical modification like substitution, fusion, ladder polymerization, donor-acceptor polymerization, topological methods [33] etc. to design low band gap materials [51-58]. The high polarizability of the sulphur atom on thiophene rings enhances the stability in the π-conjugated systems and provides excellent charge transport properties like electron coupling, reorganization energies, which is the key factor for its application in organic and molecular electronics [59]. Investigations by Zhang and co-workers [60] on end substituted oligo heterocycles concluded that substitition affects the charge transfer and intermolecular interactions. Influence of end substitution does not depend on the heteroatom but rather on the substituent electron donating or withdrawing group. End substituted oligomers with electron donating groups like methyl results in same intermolecular interactions as unsubstituted ones whereas electron withdrawing substitutions like cyano-substituted dimers result in strong intermolecular interactions compared to the methyl substituted oligomers [60]. Bendikov [61] and co-workers have studied the electronic structural properties of a series of oligothiophene di-cations in singlet and triplet states using density functional theory. According to these studies, oligothiophene di-cations up to 20-mer adopt singlet state as their ground state and singlet, triplet states are degenerate for longer oligomers and short oligothiophenes are found to form majorly bipolarons.

The type of substitution on the backbone of the polymer has an impact on their electronic and optical properties has been shown by the incorporation of electron withdrawing groups which improves the electron mobilities as well as the atmospheric stability [62,63]. Luschtinetz and co-workers [64] have investigated the C-H…N-C hydrogen bonding interaction in various thiophene-based molecules using quantum mechanical calculations. The effect of hydrogen bonding is found to be less in polymeric systems compared to oligomers and the impact of substitution on the hydrogen bonded systems is negligible in the thiophene oligomers. It is well established that the hole and electron mobilities play a crucial role in electronic devices like organic field effect transistors [33]. The molecular orientation is the one of the important factor for the high charge carrier mobilities in organic field effect transistors. Since the discovery of the first operational field affects transistors, with organic semiconductor as the active channel, oligo and polythiophenes have been emerged as one of the most promising materials [65] in this arena.

Oligothiophenes with high purity and liquid crystalline nature yields high charge carrier mobilities [33]. Generally, the charge transfer mobility of an organic polymer occur via a hopping mechanism on electron coupling between stacked molecules which depends on reorganization energy of the polymer. Hutchison and co-workers [66] have investigated the effect of inclusion of heteroatom and substitution of –F, -CN, $-CF_3$, $-NH_2$ on charge transfer rate using density functional calculations. It is found that the length-dependence of the intrinsic hole transfer rates in oligothiophenes of varying chain lengths is dominated by changes in the reorganization energy of the oligothiophenes.

Zade and co-workers [67] have computationally studied the effect of substituents on the planarity and electronic structure of the oligo- and polythiophenes and found that neutral thiophene systems are more sensitive to the substituents than the charged systems. Polythiophene deviates from planarity on substitution and as a result the electronic band gap increases [66]. Oligomeric systems can be used as models of the corresponding polymeric systems as in unsubstituted α-sexithiophene are used in the organic field effect transistor [61]. The field mobilities are found to be greater in conjugated α-sexithiophene compared to that of polythiophenes. Horowitz and co-workers [68] have fabricated various oligothiophenes, quarterthiophene, sexithiophene, and octathiophene of different chain length and studied the effect of chain length on field effect mobilities and found that charge mobilities are increased linearly with the increase of oligothiophene chain length.

1.4.2. Optical properties of oligo- and polythiophenes

The optical properties of polythiophenes are also extensively studied in the literature due to their numerous applications in the OLEDs and solar cells [11,12]. Various groups have studied the effect of substitution on optical properties of thiophene-based molecules. A polymer with different substitutions can show changes in the conjugation and thereby in the optical properties. Oligo or polythiophenes with shorter effective conjugation results in blue shift and that with higher conjugation observe red shift in emission [69]. Electron withdrawing group in polythiophenes shows redshift whereas electron donating substituent shows blue shift in the emission spectra. Bulky substitution on polymer backbone can create the disturbance in the conjugation due to steric hindrance and can lead to blue shift in the emission spectra [70]. Macchi and co-workers [71] have studied the optical properties of methyl substituted oligothiophenes experimentally and theoretically. Their studies show that oligomer adopts mirror symmetry at low temperature in excited and ground states whereas

mirror symmetry is lost at room temperature due to thermal population of normal modes. Fabiano and co-workers have studied the singlet and triplet excitation energies of oligothiophenes using time-dependent density functional theory (TD-DFT) calculations and compared the results with calculations done by coupled cluster methods and also with experimental data [72]. It is found that B3LYP (Becke 3-parameter Lee, Yang, Paar) functional underestimated the excitation energies and the errors increases with the chain length. This shows that the functional, B3LYP, fails to explain the long range interactions in the conjugated systems [73]. Semi-empirical calculations shows that modified polythiophene with bridging groups like –CH= causes the reduction of band gap [74]. This is because of the increase in the quinoid character compared to the aromatic character of bridged polythiophenes.

Becker and co-workers have studied the optical properties of a series of α-oligothiophenes experimentally along with theoretical calculations on stability, twist and optical properties using ten different methods on few oligothiophene systems [75]. According to their theoretical studies, trans oligomers are stable, and their calculated transition energy values with the basis set Slater-type orbital – three primitive Gaussians (STO-3G) are the best when compared with other methods. Wong and co-workers have investigated the absorption and fluorescence properties of oligothiophene biomarkers using long-range corrected functionals [76]. Their investigations concluded that long-range corrected functionals accurately describe excited state properties compared to the conventional hybrid functionals which has a constant fraction of Hartree-Fock exchange. A comparative study between state specific and linear response formalisms in calculating the vertical transition energies in solution employing coupled cluster methods has also been done [77]. The linear-response formalism is generally used to study the solvent effect and to evaluate the transition probabilities whereas the state-specific approach is better for the description of specific states and excited state potential energy surfaces of solvated systems.

Bendikov and co-workers have computationally studied the absorption and emission spectra of a series of α-oligofurans using conventional hybrid functional B3LYP which are structurally similar to oligothiophenes [78]. According to their studies, by increasing in the chain length of oligofuran, the deviation of absorption and emission properties from the experimental values increases and oscillator strengths also increases with increasing the chain length, however this is in disagreement with the experimental quantum yield of oligofurans. This disagreement between experiment and theory is due to the increase in degrees of

freedom with increase in chain length. Mannix and co-workers [79] have studied the excitation energies of organic sensitizers using different range separated density functional theory (DFT) functionals, with different Hartree-Fock contributions. It is found that a proper choice of functional separation parameter and Hartree-Fock exchange percentages are necessary for accuracy in the calculation of excited state properties [79] and the accuracy is found to be significantly system dependent. Azzam and co-workers have also studied the optical properties of a set of conjugated molecules with various hybrid and long-range corrected functionals [80]. As per their studies B3LYP functional gives better results than other functionals.

1.4.3. Oligo- and polythiophene applications towards the light emitting diodes

Ohmori and co-workers [81] have studied the electroluminescence properties of poly(3-alkylthiophene) (PAT) for the first time in the literature since their discovery. This is the first ever soluble and fusible conducting polymer. The emission intensity of this polymer is found to be enhanced with the increase of alkyl chain length on the backbone of the polymer. Polymeric systems also have some advantages over oligomeric systems such as physical properties which can be altered, ease to fabricate and emit all the colors in the visible region but with poor stability, high impurity levels and low luminescence limit. Geiger and co-workers have reported the first oligothiophene based light emitting diode [31] in the year 1993. Electroluminescence properties of end capped oligothiophenes were studied systematically and concluded that transport properties, spectral distribution depend on the morphology of the OLED material [8]. Thiophene-based materials are also used in biological fields as ligands for the identification of protein aggregation diseases and tools for the development of novel diagnostics using fluorescence [82].

An efficient OLED requires high luminescence efficiency and good charge transport properties. Oligothiophenes exhibit poor luminescence efficiencies in solid state due to strong intermolecular interactions. These luminescence efficiencies can be increased with alkyl substitution on the oligomer backbone. Such substitution also increases the intermolecular distance and reduces the intermolecular repulsions [83]. Shorter oligothiophenes with a low degree of crystallinity results in higher luminescence efficiency than that of longer oligomers or polythiophenes with a high degree of crystallinity. Chen and co-workers have synthesized and studied electroluminescence properties of alkyl substituted polythiophenes in regio-regular and regio-irregular form. Both the forms exhibit almost the

same order of electroluminescence efficiency. This indicates that structure order is not a prerequisite for higher efficiency of polythiophenes and polythiophene with comparatively higher head-tail ratio exhibited higher electroluminescence efficiency [84].

1.4.4. Biological applications of polythiophenes

Polythiophenes and its derivatives have tremendous biological applications due to their transport properties and low cytotoxicity [85]. These polymers have been used in many biological applications such as diagnostics [86,87], drug delivery [88], therapy and imaging, implant devices and artificial organs [89]. The reduction in electrical impedance of electrodes coated with polythiophenes is stable and establishes the permanent connection between devices and biological tissues. Charge transport phenomenon is a common process in biological systems and transport of ions and electrons across the cell membranes and other biomolecules plays a crucial role in the biological systems. Conjugated polymers are excellent candidates in the biomedical applications due to charge transport ability [90]. Along with this ability, conjugated polymers easily blend with tissues and organs and their self-assembling properties form biomimetics [91]. Moreover, conjugated polymers are known to be biocompatible and water soluble upon functionalization.

Polythiophenes, polypyrroles and polyanilines are the three classes of conjugated polymers used in bioelectronics [92]. Polythiophenes hold an advantage of easy chemical modification of thiophene unit over other two polymers [93,94]. Small size and thin films are required for applications in bioelectronics. Polythiophenes can form thin films with nanowire morphology and adopt micro or nanostructure size at electrode interface which can favourably alter the surface properties at electrodes. Light weight and printability on flexible substrates make polymers as ideal candidates in sensing applications. Polythiophene derivative, poly(3,4-diethoxythiophene) form stable complex with epithelial Hep-2 cells and no cytotoxicity was observed and such kinds of polymers are used in bioelectrodes [95]. Biocompatibility and optical properties of polythiophene help in the presence of oligonucleotides to detect the mutation in Hepatitis B virus [91]. Polythiophene fluorescence phenomena are used in the bio sensing applications to detect the DNA sequence and oligonucleotide chain length [92]. Water-soluble polythiophene derivatives have been used as anticancer agents for simultaneous therapeutic and imaging applications [90].

1.4.5. Isothianaphthenes and cyclothiophenes

Another polymer, closely related to polythiophene, is polyisothianaphthene. Polyisothianapthene is a low band gap (~1.0 eV) [96] conducting polymer where the monomer can be thought of as a thiophene unit fused with a benzene ring commonly known as Benzo[*c*]thiophene. The aromatic nature of the six-membered benzene ring is expected to affect the electronic structure of the polymer in the following ways [97]. Firstly, various resonance contributors would be expected to lead to higher stability and more nearly equal bond lengths along the pseudo polyene backbone. Secondly, the polarizability of the benzene ring would tend to reduce the repulsive electron-electron interactions between the two π-electrons on the same ring or on neighbouring carbons along the backbone. Due to these peculiar properties, isothianaphthenes exhibit higher stabilities and lower band gaps compared to that of oligothiophene counterparts.

Oligo- and polythiophenes are among the extensively studied π-conjugated systems due to their interesting electronic and optical properties and their potential applications in electronics [98]. Cyclothiophenes were first synthesized by Bäurle and co-workers [99] which have the advantage over the linear systems that they are not affected by the end perturbing effects and can act as defect free conjugated polymers [68]. Owing to their interesting semiconducting and optoelectronic properties, cyclothiophenes are found to be suitable for a variety of applications in the area of material science [100]. Moreover, the self-assembling [101] properties have made them suitable candidates for application in novel molecular circuits [102]. They emit bright colors from yellow to red [16] due to which they can also be potential candidates in the field of OLEDs. In addition, they can also serve as building blocks for the synthesis of complex structures like catenanes and knots [103].

Redox-active nano-rings have attracted considerable attention for their single-molecule electronics, nanofabrication, and unusual electronic and optical properties [55]. Cyclothiophenes are one among them as building blocks in an infinite π-conjugated system with a large inner cavity, and hence their physical properties are strongly affected by their structures in solution and in the solid state [104]. Cyclothiophenes have both moderate molecular rigidity and flexibility, can change their conformation according to an external parameter [105]. The absorption spectra for the oligothiophenes and cyclothiophenes show a systematic redshift with increasing number of thiophene units. The π-π transition of linear oligothiophenes and ring-shaped cyclothiophenes exhibit an interesting relation between their

linear optical absorption spectra [50,106]. In particular, the energy of the absorption band of a cyclothiophene with a given size corresponds to the one of an oligothiophene chain of about half the length. It means that cyclothiophene spectra are blue shifted with respect to oligothiophene spectra with the same number of repeat units. As like linear oligothiophenes, cyclothiophenes absorption band is red shifted and become more intensive with increasing number of size. Fluorescence efficiencies of cyclothiophenes are much lower than linear oligothiophenes [56]. Cyclothiophenes display bright yellow to red colors and are dedicated for oxidation reactions to form cationic or dicationic compounds.

A recent extensive study of Bendikov and co-workers of a series of even-numbered cyclothiophenes has also paid attention to anti-cyclo[N]thiophenes and to their structural and spectral characteristics in comparison to syn-isomers. While the anti-cyclo[N] thiophenes are energetically disfavoured with respect to syn-isomers up to ring sizes of N=20, the strain free anti-isomer with N=30 is significantly more stable than the syn-isomer [107]. Fabian and co-workers have investigated the structural and optical behaviour of cyclothiophenes under different symmetry using density functional theory [55]. They found that cyclothiophenes with minimum energy are of lower symmetry and become increasingly planar with growing ring size. In contrast to neutral compounds, cations and di-cations of cyclothiophenes with N ≥5 exhibit pronounced electron delocalization along the carbon backbone.

1.4.6. Applications of oligothiophenes in solar cells

Thiophene-based systems are extensively used as a π-spacer in dye sensitized solar cells between the donor and acceptor moieties because of their effective conjugation, and rigidity. Thiophenes π-spacer with donor-acceptor substitutions at terminals exhibits a red shift in absorption spectra along with the increase in the extinction coefficient [108]. Thiophene-based molecules can be used as donor molecules in p-n heterojunctions in solar cell applications [13]. Oligothiophenes have to follow two strategies to observe red shift in their absorption and fluorescence spectra. One is an increase of oligothiophene chain length and the other is the substitution of donor and acceptor moieties on two ends of the oligothiophene [109]. First, thiophene-based solar cell was synthesized in the year 1995 with α-octathiophene as a donor and perylene as an acceptor which exhibited 0.8% power conversion efficiency [10]. Excellent power conversion efficiency up to 10% have been achieved with oligothiophene based molecules [110]. Due to their excellent fluorescent properties, oligothiophenes coupled with donor and acceptor molecules are used as biomarkers and in photobleaching [111,112].

Dell [113] and co-workers have delineated the role of molecular backbone symmetry on the charge transfer of a family of bithiophene derivatives which bound to gold electrodes. The conductance of bithiophenes is found to be strongly dependent on the conformational fluctuations and reduced symmetry of bithiophene, which restricts the inter-ring torsional angle and influences their transport behavior. Oligothiophenes and polythiophenes are also used in bulk hetereojunction solar cells where fullerenes are used as electron acceptors. A regio-regular poly(3-hexylthiophene) blended with a fullerene derivative ($PC_{61}BM$) led to 5% of power conversion efficiency. Because of high cost, difficulty in synthesis and structural modification of fullerene derivatives, bulk hetero junction solar cells are of less use in solar cells.

Although the effects of some substituted oligo and polythiophene are studied experimentally and theoretically [34-42], but a systematic study of effect of substitution on oligo and polythiophenes with various substituents is lacking. By employing density functional calculations and periodic boundary calculations, we have carried out a comprehensive evaluation of the effect of various substitutions on oligo- and polythiophenes. We have also extended our computational study to investigate the optical properties of oligothiophenes, where we have done a benching marking calculations using time-dependent density functional theory formalism. In addition we have done electronic structure calculations of linear and cyclic isothianaphthenes and attempted few application based work with thiophene based donor acceptor molecules.

The control of band gap through structural modification is very important in the design of low band gap materials with intrinsic conductivity. Since the effects of substitution on all the monomers of the oligomeric systems are unknown in the literature, we have considered such systems and noted down some very interesting electronic properties. In this thesis, we have studied the effect of substitution of electron donating groups like methoxy and ethoxy and electron withdrawing groups like nitro, phenyl and cyano groups on oligothiophene of chain length 2-9 in the regio-regular HT–HT form. These groups are substituted on all monomers and special cases like terminal substitutions with an electron donating group at one end and an electron withdrawing group on the other end are also considered. Although band gaps can be altered by the substitution at the terminal edges of the oligomer [114] the main problem of solubility of thiophenes is not fully addressed through this mechanism. On the other hand, substitution with different groups throughout the length of oligomer would not only enhance the solubility but also alter the band gaps.

Substituted polythiophenes are available in two configurations, head tail – head tail and head head – tail tail. We have studied electronic properties of substituted polythiophenes in both head tail – head tail and head head – tail tail forms. The effect of substituents like alkoxy, alkyl, halo, and aromatic groups on band gaps and planarity are studied using periodic boundary condition. The extrapolated band gaps of oligothiophenes to polythiophenes are compared with the band gaps of PT calculated with DFT-PBC values.

A proper choice of exchange correlation functional, solvent formalism and basis set determine the accuracy in the calculation of optical properties of π-conjugated compounds. Many of the computational studies concentrated on any one of these aspects, whereas the accuracy can depend on various parameters. In this thesis, we have considered all these factors and calculated absorption and emission properties of thiophene oligomers and compared the results with the existing experimental results. The main aim of this work is to to choose proper time-dependent density functional theory formalism in order to calculate accurate optical properties especially for molecules with extended π-conjugation which are widely used in the field of organic electronics. We investigate the absorption and emission of oligothiophenes of chain length (2-7) with different functionals and basis sets. The most popular hybrid functionals B3LYP, M06 and range-separated hybrid functionals (RSH), CAM-B3LYP and ωB97XD employing different basis sets are considered in order to assess the effect of functionals together with the inclusion of polarization and diffusion functions in basis sets, in predicting the absorption and emission properties.

Although extensive computational and experimental studies on various substituted linear oligo- and polythiophenes have been carried out, studies on cyclic systems are rare. Even though the experimental study with butyl substituted cyclothiophenes [105] and theoretical studies of methyl substituted cyclothiophenes [102] have been carried out, there is no related interesting work on cyclic isothionaphthenes. First time ever, we have explored the electronic structure properties of cycloisothionaphthenes. Cyclic systems are novel as they can approximately model a polymeric system with many monomer units. Without perturbing end effects and with few relevant conformations adopted in the cyclic form and comparable band gaps with the polymer entity, they could replace the polymeric systems for many applications. In this thesis, we have investigated in detail, the structural and electronic properties of both cyclic and linear oligomeric systems of isothionaphthenes and their structure-property relationship in altering the band gaps, employing density functional theory.

Oligothiophenes are used as π-spacer in dye sensitized solar cells because of their rigidity in maintaining the planarity and effective π-conjugation. Therefore it allows the flow of charge carriers from donor to acceptor moiety with ease. We have studied the electronic and optical properties of oligothiophene based triphenylamine donor and cyanoacrylic acid acceptor molecules. The effect of thiophene chain length and donor strength by substituting electron donating groups like methyl and methoxy on triphenylamine on electronic and optical properties are also studied. The electronic properties like band gap, open circuit voltage are calculated with B3LYP functional. The optical properties like absorption, light harvesting efficiency, excited state life time, oscillator strength are calculated with CAM-B3LYP functional employing time-dependent density functional theory.

1.11. References

[1] C. K. Chiang, C. R. Jr. Fincher, Y. W. Park, A. J. Heeger, H. Shirakawa, E. J. Louis, S. C. Gau, A. G. Macdiarmid, Phy. Rev. Lett., 1977, 39, 1098.

[2] H. Shirakawa, E. J. Louis, A. G. Macdiarmid, C. K. Chiang, A. J. Heeger, Chem. Commun., 1977, 578.

[3] N. Somanathan, S. Radhakrishnan, Int. J. Mod. Phys., B 2005, 19, 4645.

[4] H. Tumura, I. Hamada, H. Shang, K. Oniwa, Md. Akhtaruzzaman, T. Jin, N. Asao, Y. Yamamoto, T. Kanagasekaran, H. Shimotani, S. Ikeda, K. Tanigaki, J. Phys. Chem. C, 2013, 117, 8072.

[5] V. Promarak, A. Punkvuang, D. Meunmat, T. Sudyoadsuk, S. Saengsuwan, T. Keawin, Tetrahedron Lett., 2007, 48,919.

[6] P. K. H. Ho, J. S. Kim, J. H. Borroughes, J. H. Becker, S. F. Y. Li, T. M. Brown, F. Cacialli, R. H. Friend, Nature, 2000, 404, 481.

[7] L. Ding, M. Jonforsen, L. S. Roman, M. R. Andersson, O. Inganas, Synth. Met., 2000, 110, 113.

[8] F. Wurthner, Angew. Chem. Int. Ed. Engl., 2001, 40, 1037.

[9] G. Barbarella, M. Zambianchi, L. Antolini, P. Ostoja, P. Maccahnani, A. Bongini, E. A. Marseglia, E. Tedesco, G. Gigli, R. Cingolani, J. Am. Chem. Soc., 1999, 121, 8920.

[10] M. Halik, H. Klauk, U. Zschieschang, G. Schmid, S. Pomomarenko, S Krichmeyer, W. Weber, Adv. Mater., 2003, 15, 917

[11] M. A. D. Oliveria, H. A. Duarte, J.-M. Pernaut, W. B. D. Almeida, J. Phys. Chem. A, 2000, 104, 8256.

[12] P. Garcia, J.-M. Pernaut, P. Hapiot, V. Wintgens, P. Garnier, F. Garnier, D. Delabouglise, J. Phys. Chem., 1993, 97, 513.

[13] P. Audebert, P. Hapiot, J. –M. Pernaut, P. Garcia, K. Monneir, Chem. Mater., 1994, 6, 1549.

[14] M. D. Irwin, B. Buchholz, A. W. Hains, R. P. H. Chang, T. J. Marks, Proc. Natl. Acad. Sci. USA, 2008, 105, 2783.

[15] R. Kroon, M. Lenes, J. C. Hummelen, P. W. M. Blom, B. D. Boer, Polym. Rev., 2008, 48, 531.

[16] W. Shockley, H. J. Queisser, J. Appl. Phys., 1961, 32, 510.

[17] G. Tourillon, F. Garnier, J. Electroanal. Chem., 1984, 407, 161.

[18] F. Wudl, M. Kobayashi, N. Colaneri, M. Boysel, A. J. Heeger, Mol. Cryst. Liq. Cryst., 1985, 118, 199.

[19] J. E Anthony, Chem. Mater., 2010, 23, 583

[20] J. Pei, W. Yu, W. Huang, A. J. Heeger, Synth. Met., 1999, 105, 43.

[21] M. Mazzeo, V. Vitale, F. D. Sala, D. Pisignano, M. Anni, G. Barbarella, L. Favaretto, A. Zanelli, R. Cingaolani, G. Gigli, Adv. Mater., 2003, 15, 2060.

[22] D. Ficho, *Hand book of Oligo- and Polythiophenes* Wiley-VCH, Weinheim, Germany. 1999.

[23] L. Zhang, N. S. Colella, B. P. Cherniawski, S. C. B. Mannsfeld, A. L. Briseno, ACS Appl. Mater. Interfaces, 2014, 6, 5327.

[24] I. Osaka, R. McCullough, Acc. Chem. Res., 2008, 41, 1202.

[25] G. Schopf, G. Kobmehl, Adv. Polym. Sci., 1997, 129, 1.

[26] T. A. Chen, R. A. OBrien, R. D. Rieke, Macromolecules, 1993, 26, 3462.

[27] S. Kotha, K. Lahiri, D. Kashinath, Tetrahedron, 2002, 58, 9633.

[28] F. Zhang, D. Wu, Y. Xu, X. Feng, J. Mater. Chem., 2011, 21, 17590.

[29] J. E. Anthony, Chem. Mater., 2010, 23, 583.

[30] G. Horowitz, D. Fichou, X. Peng, Z. Xu, F. Garnier, Solid State Commun., 1989, 72, 381.

[31] F. Geiger, M. Stoldt, H. Schweizer, P. Bäuerle, E. Umbach, Adv. Mater., 1993, 5, 922.

[32] N. Noma, T. Tsuzuki, Y. Shirota, Adv. Mater., 1995, 7, 647.

[33] G. Tourillon, F. Garnier, J. Electroanal. Chem., 1982, 135, 173.

[34] Y-M. Chou, W-H. Chen, C-C Liang, J. Mol. Struct. THEOCHEM, 2009, 894, 117.

[35] J. Casado, T. M. Pappenfus, L. L. Miller, K. R. Mann, E. Ortl, P. M. Viruela, R. P-. Amerigo, V. Hernandez, J. T. L. Navarrete, J. Am. Chem. Soc., 2003, 125, 2524.

[36] M. Y. Balakina, J. Li, V. M. Geskin, S. R. Marder, J. L. Bredas, J. Chem. Phys., 2000, 113, 9598.

[37] V. Hernandez, J. Casdo, F. Effenberger, J. N. Lopez, J. Chem. Phys., 2000, 112, 5105.

[38] T. M. Pappenfus, R. J. Chesterfield, C. D. Frisbie, K. R. Mann, J. Casado, J. D. Raff, L. L. Miller, J. Am. Chem. Soc., 2002, 124, 4184.

[39] M. M. Bader, R. Custelcean, M. D. Ward, Chem. Mater., 2003, 15, 616.

[40] J. Casanovas, D. Zanuy, C. Aleman, Polymer, 2005, 46, 9452.

[41] J. Casanovas, D. Aradilla, J. Poater, M. Solà, F. Estranyce, C. Alemán, Phys. Chem. Chem. Phys., 2012, 14, 10050.

[42] F. Costanzo, D. Tonelli, G. Scalmani, J. Cornil, Polymer, 2006, 47, 6692.

[43] G. G. Malliaras, J. K. Herrems, J. Wildeman, R. H. Wierings, S. S. Lampours, G. Hadziioannou, Adv Mater., 1993, 5, 721; R.E. Gill, G. G. Malliaras, J. Wildeman, G. Hadziioannou, Adv Mater., 1994, 6, 132; A. Hilberer, H.-J. Brouwer, B. J. van der Scheer, J. Wildeman, G. Hadziioannou, Macromolecules, 1995, 28, 4525.

[44] A. Facchetti, M. H. Yoon, C. L. Stern, G. R. Hutchison, M. A. Ratner, T. J. Marks, J. Am. Chem. Soc., 2004, 126, 13480.

[45] H. Saddeh, T. Goodson, L. Yu, Macromolecules, 1997, 30, 4608.

[46] S. P. Rittmeyer, A. Grob, Beilstein J. Nanotechnol., 2012, 3, 909.

[47] S. Hotta, K. Waragai, Adv. Mater., 1993, 5, 896.

[48] G. Barbarella, M. Zambianchi, A. Bongini, Adv. Mater., 1991, 3, 494.

[49] S. Hotta, K. Waragai, J. Mater. Chem., 1991, 1, 835.

[50] F. Garnier, A. Yassar, R. Hajaloui, F. Deloffre, B. Servet, S. Ries, P. Alnot, J. Am. Chem. Soc., 1993, 115, 8716

[51] A. Patil, A. J. Heeger, F. Wudl, Chem. Rev., 1988, 88, 183.

[52] Y. Yu, E. Gunk, B. Zinger and L. L. Miller, J. Am. Chem. Soc., 1996, 118,1013.

[53] A. Iraqi, D. Clark, R. Jones and A. Krier, Synth. Met., 1999, 102, 1220.

[54] X. M. Hong, J. C. Tyson and D. M. Collard, Macromolecules, 2000, 33, 3502.

[55] Y. Sakamoto, S. Komatsu, T. Suzuki, J. Am. Chem. Soc., 2001, 123, 4643.

[56] A. Mishra, C. Ma, and P. Bäuerle, Chem. Rev., 2009, 109, 1141.

[57] M. Melucci, G. Barbarella, M. Zambianchi, M. Benzi, F. Biscarini, M. Cavallini, A. Bongini, S. Fabbroni, M. Mazzeo, M. Anni, G. Gigli, Macromolecules, 2004, 37, 5692.

[58] I. F. Peripichika, D. F. Peripichika, H. Meng, F. Wudl, Adv. Mater., 17, 2005, 2281.

[59] A. Mishra, C. Ma, P. Bäuerle, Chem. Rev., 2009, 109, 1141.

[60] G-L. Zhang, H. Zhang, D-P. Li, D. Chen, X-Y. Yu, B. Liu, Z-S, Li, Theor. Chem. Acc., 2008, 121, 109.

[61] S. S. Zade, M. Bendikov, J. Phys. Chem., B 2006, 110, 15839.

[62] X. Cai, M. W. Burand, C. R. Newman, D. A. da Silva Filho, T. M. Pappenfus, M. M. Bader, J-L. Bredas, K. R. Mann, C. D. Frisbie, J. Chem. Phys., B 2003, 110, 14590.

[63] Y-A. Duan, Y. Geng, H-B Li, X-D. Tang, J-L. Jin, Z-M. Su, Org. Electron., 2012, 13, 1213.

[64] R. Luschtinetz, S. Gemming, G. Seifert, Comp. Theor. Chem., 2013, 1005, 45.

[65] D. Fichou, G. Horowitz, F. Nishikitani, F. Garnier, Chemtronics, 1988, 3, 176.

[66] G. R. Hutchison, M. A. Ratner, T. J. Marks, J. Am. Chem. Soc., 2005, 127, 2339.

[67] S. S. Zade, M. Bendikov, Chem. Eur. J., 2007, 13, 3688.

[68] G. Horowitz, R Hajlaoui, D. Fichou, A. E. Kassmi, J. Appl. Phys., 1999, 85, 3202.

[69] B. L. Groenendaal, F. Jonas, D. Freitag, H. Pielartzik, J. R. Reynolds, Adv. Mater., 2000, 12, 481.

[70] M. R. Andersson, M. Berggren, O. Ingankis, G. Gustafsson, J. C. Gustafsson-Carlberg, D. Selse T. Hjertberg, O. Wennerstrtimt, Macromolecules, 1995, 28, 7525.

[71] G. Macchi, B. M. Medina, M. Zambianchi, R. Tubino, J. Cornil, G. Barbarella,

J. Gierschner and F. Meinardi, Phys. Chem. Chem. Phys., 2009, 11, 984.

[72] E. Fabiano, F. D. Sala, R Cingolani, M. Weimer, A. Gorling, J. Phys. Chem. A, 2005, 109, 3078.

[73] Z. L. Cai, K. Sendt, J. R. Reimers, J. Chem. Phys., 2002, 117, 5543.

[74] M. Kertesz, Y. S Lee, J. Phys. Chem., 1987, 91, 2690.

[75] R. S Becker, J. S. deMelo, A. L Maçanita, F. Elisei, J. Phys. Chem., 1996, 100, 18683.

[76] B. M. Wong, M. Piacenza, F. D. Sala, Phys. Chem. Chem. Phys., 2009, 11, 4498.

[77] M. Caricatoa, J. Chem. Phys., 2013, 139, 044116.

[78] S. Sharma, M. Bendikov, Chem. Eur. J., 2013, 19, 13127.

[79] M. P. Balanay, D. H. Kim, J. Phys. Chem. C, 2011, 115, 19424.

[80] C. E. A. Azzam, A. Planchat, B. Mennucci, C. Adamo, D. Jacquemin, J. Chem. Theory Comput., 2013, 9, 2749.

[81] Y. Ohmori, M. Uchida, K. Muro, K. Yoshino, Solid State Commun., 1991, 80, 605.

[82] T. Klingstedt, A. Åslund, R. A. Simon, L. B. G. Johansson, J. J. Mason, S. Nyström, P. Hammarströma, K. P. R. Nilsson, Org. Biomol. Chem., 2011, 9, 8356.

[83] A. Yassar, G. Horowitz, P. Valat, V. Wintgens, M. Hmyene, F. Deloffre, P. Srivastava, P. Lang, F. Garnier, J. Phys. Chem., 1995, 99, 9155.

[84] F. Chen, P. G. Mehta, L. Takiff, R. D. McCullough, J. Mater. Chem., 1996, 6, 1763.

[85] P. Sista, K. Ghosh, J. S. Martinez, R. C. Rocha, J. Nanosci. Nanotechnol., 2014, 14, 250.

[86] H. Guan, M. Cai, L. Chen, Y. Wang, Z. He, Luminescence, 2010 25, 311.

[87] I. Charlebois, C. Gravel, N. Arrad, M. Boissinot, M. G. Bergeron, M. Leclerc, Macromol. Biosci., 2013, 13, 717.

[88] R. C. Barthus, L. M. Lira, and D. T. S. I. Cordoba, J. Braz. Chem. Soc., 2008, 19, 630.

[89] L. Liu, M. Yu, X. Duan, and S. Wang, J. Mater. Chem., 20, 6942, 2010.

[90] G. Scarpa, A.-L. Idzko, S. Goetz, S. Thalhammer, Macromol. Biosci., 2010, 10, 378.

[91] D. Tuncel, H. V. Demir, Nanoscale, 2010, 2, 484.

[92] S. E. Moulton, M. J. Higgins, R. M. I. Kapsa, G. G. Wallace, Adv. Funct. Mater., 2012,

22, 2003.

[93] C. A. Cutler, A. K. Burrell, D. L. Officer, C. O. Too, G. G. Wallace, Synth. Met., 2002 128, 35.

[94] M. Nishiki, W. Oi, K. Ito, J. Inclusion Phenom. Macrocyclic Chem., 2008, 61, 61.

[95] V. L. J. del, D. Aradilla, R. Oliver, F. Sepulcre, A. Gamez, E. Armelin, C. Aleman, F. Estrany, Eur. Polym. J., 2007, 43, 2342.

[96] S. S. Zade, M. Bendikov, J. Org. Chem., 2006, 71, 2972.

[97] M. Kobayashi, N. Colaneri, M. Boysel, F. Wudl, A. J. Heeger J. Chem. Phys., 1985, 82, 5717.

[98] S. Foumine, P. Guadarrama, P. Flores, J. Phys. Chem. A, 2007, 111, 3124.

[99] G. Fuhrmann, T. Debaerdemaeker, P. Bäuerle, Chem. Commun., 2003, 948.

[100] S. Foumine, P. Guadarrama, P. Flores, J. Phys. Chem. A, 2007, 111, 3124.

[101] M. Bednarz, P. Rwineker, E. Mena-Osteritz, P. Bäuerle, J. Lumin., 2004, 110, 225.

[102] E. Mena-Osteritz, Adv. Mater., 2002, 14, 609.

[103] J. Fabian, H. Hartmann, J. Phys. Org. Chem., 2007, 20, 554.

[104] K. Nakao, M. Nishimura, T. Tamachi, Y. Kuwatani, H. Miyasaka, T. Nishinaga, M. Iyoda, J. Am. Chem. Soc., 2006, 128, 16740.

[105] W-H. Michele, A. Bhaskar, G. Ramakrishna, T. Goodson, M. Imamura, A. Mawatari, K. Nakao, H. Enozawa, T. Nishinaga, M. Iyoda, J. Am. Chem. Soc., 2008, 130, 3252.

[106] J. Krömer, I. Rios-Carreras, G. Fuhrmann, C. Musch, M. Wunderlin, T. Dabaerdemaeker, E. Mena-Osteritz, P. Bäuerle, Angew.Chem., Int. Ed., 2000, 39, 3481.

[107] S. S. Zade, M. Bendikov, J. Org. Chem., 2006, 71, 2972.

[108] N. Koumura, Z-S Wang, S. Mori, M. Miyashita, E. Suzuki, K. Hara, J. Am. Chem. Soc. 2006, 128, 14256; Q. Feng, Q. Zhang, X. Lu, H. Wang, G. Zhou, Z-S Wang, Appl. Mater. Interfaces, 2013, 5, 8982.

[109] M. Piacenza, M. Zambianchi, G. Barbarella, G. Gigli, F. Della Sala, Phys. Chem.

Chem. Phys., 2008, 10, 5363.

[110] W. Zeng, Y. Cao, Y. Bai, Y. Wang, Y. Shi, M. Zhang, F. Wang, C. Pan, P. Wang, Chem. Mater., 2010, 22, 1915.

[111] A. Cazzato, M. Capobianco, M. Zambianchi, L. Favaretto, C. Bettini, G. Barbarella, Bioconjugate Chem., 2007, 18, 318.

[112] G. Barbarella, M. Zambianchi, A. Ventola, E. Fabiano, F. Della Sala, G. Gigli, M. Anni, A. Bolognesi, L. Polito, M. Naldi and M. Capobianco, Bioconjugate Chem., 2006, 17, 58.

[113] E. J. Dell. B. Capozzi, K. H. Dubay, T. C. Berkelbach, J. R. Moreno, D. R. Reichman, L. Venkataraman, L. M. Campos, J. Am. Chem. Soc., 2013, 135, 11724.

[114] S. Radhakrishnan, R. Parthasarathi, V. Subramanian, N. Somanathan, Comp. Mater. Sci., 2006, 37, 318.

Chapter 2

Computational Methodology

2.1. Introduction

Electronic, structural and optical properties of oligo- and polythiophenes can be investigated using various electronic structure calculations. Density functional theory (DFT) is extensively used to study the oligo- and polythiophene-based organic π-conjugated systems. The advantage of DFT is that it takes less computational time than wavefunction based ab initio calculations and predicts the ground state and excited state properties almost as accurate as Moller-Plesset (MP2) with the consideration of appropriate exchange-correlation terms. Theoretical studies can give great insights about the electronic band gap, structural geometry, absorption, emission spectra and contribution of molecular orbital in transitions and charge distribution etc. There are different methodologies in the DFT framework such as local density approximation (LDA), generalized gradient approximation (GGA) and Hybrid functionals and long-range corrected functionals etc. Although these DFT methodologies are widely used, the drawback is that the LDA or GGA methods underestimate band gaps in semiconductors, insulators and strongly correlated systems [1-4]. This drawback arises from the lack of semi-local functional contribution and derivative discontinuity of the exchange –correlation potential with respect to the electron occupancy [5,6]. We have used hybrid functional B3LYP to calculate the electronic band gaps of oligo- and polythiophenes, which incorporates the non-local Hartree-Fock (HF) exchange and produce more accurate band gaps than the LDA or GGA approaches. In this chapter we discuss the basic concepts of DFT and various exchange-correlational functionals, basis sets and band structure calculations that we have employed to study the electronic structure properties of oligo and polythiophenes.

2.2. Density functional theory – Thomas-Fermi Model

According to Hohenberg-Kohn theorems, ground state properties of an atom or molecule can be calculated from its exact electron density and the energy calculated using trail electron density is always greater than or equal to the true energy of the system. DFT is based on electron density ρ(x,y,z) which is derived from Hohenberg-Kohn theorems. *Ab-initio* wave function approaches cannot be measured physically whereas DFT techniques, use electron density which can be measured employing techniques like X-ray diffraction or

electron diffraction [7]. The advantage of DFT over wave-function based approach is that electron density is a function of only three spatial coordinates (x,y,z) irrespective of the size of the molecule [8,9] whereas wave function based approaches depend on 4n coordinates, where "n" represent the number of electrons in atom or molecule and 4 indicates the three spatial coordinates and one time coordinate. Therefore the wave function of an atom with ten electrons will have 40 variables whereas the electron density is a function of only three variables which simplifies the calculations in DFT and provides an advantage over the wave function based methods.

The predecessor to the current DFT [8,9] is the Thomas-Fermi model developed independently by Thomas and Fermi in 1927. However this model is failed to explain the properties of molecules because earlier DFT techniques which employ orbital free models, where the energy functional is divided into three components such as kinetic energy term T[ρ], electrons-nuclei attraction term, $E_{ne}[\rho]$, and electron–electron repulsion term, $E_{ee}[\rho]$. The $E_{ee}[\rho]$ term is further divided into Coulomb and exchange parts, J[ρ] and K[ρ], including correlation energy in all the terms. Kinetic and exchange energies considered based on uniform electron gas.

$$T_\rho = \pi \frac{3}{10} (3\pi^2)^{\frac{2}{3}} \int \rho^{\frac{5}{3}}(r) dr. \tag{2.1}$$

$$E_{ne}[\rho] = \sum_{a}^{N_{nuclei}} \int \frac{Z_e\,(R_a)\rho(r)}{|R_a - r|}\, dr. \tag{2.2}$$

$$E_{ee}[\rho] = \frac{1}{2} \iint \frac{\rho\,(r)\rho\,(r)'}{|r - r'|} dr\, dr'. \tag{2.3}$$

Calculations obtained from this orbital free model, where the energy components obtained from the functional of electron density, yielded poor results and hence wave function based approaches were preferred over DFT calculations. In 1965 Kohn and Sham suggested that the electron kinetic energy should be calculated from an auxiliary set of orbitals which represent the electron density. This approach gave satisfactory results with the experiments and laid the foundation of modern DFT based on Kohn-Sham orbitals. In the Kohn- Sham formalism, kinetic energy functional is split into two parts, one can be calculated exactly and the other is the correction term (Explained in section 2.3). But kinetic energy calculated from the auxiliary set of orbitals again introduces the complexity from 3 to 3N variables.

2.3. DFT: Kohn-Sham approach

The idea in this approach is fictitious non-interacting reference system where electrons do not interact with each other and ground state electron density ρ_r is considered as exactly as in the real ground state system ρ_o ($\rho_r = \rho_o$). Since the electrons are non-interacting they can be treated exactly and any deviation in energy caused due to the assumption of non-interacting electrons can be added further by exchange-correlation term (correction term) which is rather a small fraction compared to the total energy.

Electronic ground state energy of the real molecule is given by the sum of electron kinetic energy, nucleus-electron attraction energy, and electron-electron repulsion energies and is given by

$$E_0 = < T[\rho_0] > + < V_{Ne}[\rho_0] > + < V_{ee}[\rho_0] >. \quad (2.4)$$

The first term ($T[\rho_0]$) in the Eq. (2.4) represents kinetic energy of the electrons, the second term ($V_{Ne}[\rho_0]$) represents Coulombic attraction between nucleus and electron and the final term ($V_{ee}[\rho_0]$) indicates Coulombic repulsions between the electrons. The second term is given by the expression,

$$V_{Ne}[\rho_0] = \sum_{i=1}^{2n} \sum_{\text{nuclei A}} \frac{Z_A}{r_{iA}} = \sum_{i=1}^{2n} v\,(r_i). \quad (2.5)$$

Z_A/r_{iA} is the potential energy due to the interaction of electron "i" with nucleus "A" at the varying distance r; $v(r_i)$ is the external potential for the attraction of electron "i" to all the nuclei. The density function $\rho(r)$ can be introduced into $<V_{Ne}>$ (in the Eq. 2.5) by using the fact that [10]

$$\int \psi \sum_{i=1}^{2n} f(r_i)\psi \, d\tau = \int \rho(r) f(r) dr. \quad (2.6)$$

Here $f(r_i)$ is a function of the spatial coordinates of electron "i" of the system and "ψ" is the total wave function. Eq. (2.6) represents the Coulombic force of attraction between electrons and the nuclei in terms of $\rho(r)$. Now the total energy is given by,

$$E_0 = < T[\rho_0] > + \int \rho(r) v(r) dr + < V_{ee}[\rho_0] >. \quad (2.7)$$

But the Eq. (2.7) cannot be used to calculate the energy because of the functionals corresponding to first (kinetic energy) and last term i.e., the Coulombic force of repulsion between electrons in the Eq. (2.7) is unknown. Moreover the Eq. (2.7) is built on the assumption that electrons are non-interacting, thus the energy calculated using the above formula does not give proper results. Therefore Eq. (2.7) has to be modified by considering the corrections of first and last terms. In the real systems electrons are interacting, therefore there will be the difference in kinetic energy calculated with respect to the real systems and the kinetic energy calculated for the reference system where the electrons are non-interacting. Kinetic energy deviation of the real from the reference system is given by

$$\Delta< T[\rho_0] > \equiv\ T[\rho_{real}] - T[\rho_{reference}]. \tag{2.8}$$

The deviation of Coulombic repulsion is given as follows, the classical electrostatic repulsion energy is the summation of the repulsion energies for pairs of infinitesimal volume elements $\rho(r_1)dr_1$ and $\rho(r_2)dr_2$ separated by a distance r_{12}, multiplied by one-half. Similarly, the deviation in Coulombic repulsion is given by

$$\Delta< V_{ee}[\rho_0] > \equiv < V_{ee}[\rho_0] >_{real} - \frac{1}{2} \iint \frac{\rho_0\,(r_1)\rho_0\,(r_2)}{r_{12}} dr_1\, dr_2. \tag{2.9}$$

Employing the classical charge-cloud repulsion formula, it gives an inappropriate picture of electrons in that smearing an electron out into cloud forces it to repel itself, as any two regions of the cloud interact repulsively. This physically incorrect electron self-interaction can be compensated by using a good correlation functional. Now the modified ground state electronic energy is given by,

$$E_0 =< T[\rho_0] >_{ref} + \int \rho(r)v(r)dr\ + \frac{1}{2} \iint \frac{\rho_0\,(r_1)\rho_0\,(r_2)}{r_{12}} dr_1\, dr_2 + \Delta< T[\rho_0] > \ +\Delta< V_{ee}[\rho_0] >. \tag{2.10}$$

The sum of the kinetic energy deviation from the reference system and the electron–electron repulsion energy deviation from the classical system is called as Exchange-correlation energy (E_{XC}) is given by,

$$E_{XC} \equiv \Delta< T[\rho_0] > \ +\Delta< V_{ee}[\rho_0] >. \tag{2.11}$$

Incorporating (E_{XC}) into the equation Eq. (2.10), we get

$$E_0 = \int \rho(r)v(r)dr + < T[\rho_0] >_{ref}\ + \frac{1}{2} \iint \frac{\rho_0\,(r_1)\rho_0\,(r_2)}{r_{12}} dr_1\, dr_2 + E_{XC}. \tag{2.12}$$

The first term in the Eq. (2.12) is the sum of Coulombic force of attraction of nuclei with infinitesimal charge cloud which can be calculated from ρ_0 employing the expression,

$$\int \rho(r)v(r)dr = -\sum_{a}^{N_{nucleus}} Z_A \int \frac{\rho_{r1}}{r_{1A}}\, dr_1. \qquad (2.13)$$

The second term in the Eq. (2.12) is the kinetic energy of non-interacting electrons of the reference system, given by the expression,

$$< T[\rho_0] >_{ref} = -\frac{1}{2}\sum_{i=1}^{2n} < \psi_1^{KS}(1)|\nabla_1^2|\psi_1^{KS}(1) >. \qquad (2.14)$$

The expected kinetic energy of non-interacting electrons is given by Eq. (2.14), as the electrons are non-interacting and the wavefunction can be written as a single Slater determinant similar to the wavefunction constructed in the HF methodology. The only difference in the DFT is that the orbitals involved in the construction are Kohn-Sham (KS) orbitals. The third term in the Eq. (2.12) represents the Coulombic force or repulsion between the electrons, which can be calculated using the classical formula, if the density ρ_0 is known. The only term which is unknown is the exchange-correlation E_{XC} functional, which is smaller compared to the first three terms; since the exact functional is unknown, the most approximate to determine the E_{xc} energy is the main problem in DFT and devising an appropriate exchange-correlation functional is needed to calculate this energy.

2.4. Exchange and correlation Functionals

Exchange-correlation functions are represented by mathematical forms containing different parameters. These parameters are evaluated based on the functional's requirement to satisfy the conditions like; the energy functional should be self-interaction-free; when the density becomes constant, the uniform electron gas result should be recovered, etc [9] or by fitting the parameters to experimental data. But in practice, a combination of these approaches is often used.

2.4.1. Local Density Approximation (LDA)

The simplest approximation in the DFT is LDA [9], where the electron density is confined with an infinitesimal distance beyond a point. Exchange-correlation energy can be calculated from the formulae derived for a uniform electron density in this methodology. It is

based on the assumption that at every point in the molecule the energy density is given by a homogeneous electron gas which had the same electron density ρ at that point. It is the energy density i.e., the energy (exchange plus correlation) per electron. LDA does not assume that the electron density in a molecule as homogeneous; it arises only in Thomas-Fermi molecule.

2.4.2. Local Spin Density Approximation (LSDA)

The electrons of opposite spin are placed in different Kohn–Sham orbitals, similar to the unrestricted Hartree–Fock (UHF) method. The advantage of LSDA [9] is that it can handle systems with one or more unpaired electrons like radicals. For species in which all the electrons are paired, the LSDA is equivalent to the LDA. LSDA geometries, frequencies, and electron distribution properties are found to be reasonably good, but the dissociation energies, including atomization energies, are very poor.

2.4.3. Gradient-Corrected Functionals

Modern DFT calculations use gradient corrected functionals which use both electron density and its gradient (the first derivative of ρ with respect to its position). These functionals are called GGAs. In GGA methods, the first derivative of the density is included as a variable, and in addition, the Fermi and Coulomb holes integrate to the required values of −1 and 0. These functionals have also called as non-local functionals since it considers the electron density beyond the vicinity of each point in the system. The exchange-correlation energy can be written as sum of exchange energy and correlation energy functional, both negative i.e, $E_{xc} = E_x+E_c$. $|E_x|$ is much larger than $|E_c|$. The results have been improved when gradient is applied to the exchange energy. The major advance in DFT is the introduction of Becke parameter (B88), which improves the accuracy of exchange energy functional. The gradient correlated funnctionals like P86 combined with Becke parameter results GGA functionals.

Exchange-correlation functionals can be further improved by making functionals depend on higher order derivatives of electron density. Functionals which use the second derivative of ρ are called meta- generalized gradient approximation (MGGA) functionals [9]. Although this functional improves the accuracy of results, functionals are dependent on Laplacian of ρ at present. MGGA functionals side skips the problem by not depending on ρ but on KE density τ. This can be obtained as

$$\tau(r) = \frac{1}{2} \sum_{i=1}^{\text{occupied}} \left|\nabla \psi_i^{KS}(r)\right|^2, \qquad (2.15)$$

where ψ_i^{KS} represent Kohn-Sham orbitals.

2.4.4. Hybrid functional B3LYP

Exchange energy corresponding to HF is added to GGA functionals. These are also called adiabatic correction methods. In the adiabatic process of wave function approach, wave function remains the same on potential energy surface (PES). Adiabatic correction method shows that the exchange-correlation energy $E_{XC}(\rho)$ can be taken as a weighted sum of the DFT exchange-correlation energy and HF exchange energy. Hybrid DFT functionals which include an energy contribution from HF-type electron exchange, calculated from the KS wave function of the non-interacting electrons. Since these electrons have no Coulomb interaction, but electrons with a spin of one-half, show "Pauli repulsion" represented by the exchange K integral. Hybrid functionals are functionals (of the GGA level or higher) that contain HF exchange, the correction energy to the classical Coulomb repulsion [9]. The percentage of HF exchange energy to use is a main characteristic of the various hybrid functionals.

There are two methodologies for assigning values of parameters for exchange-correlation functional either by requiring the functional to fulfil the criteria discussed above or by fitting the parameters to experimental data, but in practice a combination of these approaches is often used. The B3LYP functional has a total of eight purely empirical parameters. This exchange-energy functional was developed by Becke [11] with Lee, Yang, and Paar with three parameters (LYP) [12]

$$E_{XC} = a_0 E_{X,HF} + (1 - a_0) E_{X,Slater} + a_X \Delta E_{X\,Becke88} + (1 - a_C) E_{c,VWN} + a_C \Delta E_{C,LYP}. \qquad (2.16)$$

$E_{x,HF}$ is the HF exchange energy based on Kohn-Sham orbitals, $E_{x,Slater}$ is the uniform electron gas exchange-correlation energy, $\Delta E_{xBecke88}$ is Becke's 1988 GGA for exchange [13] $E_{c,VWN}$ is Vosko-Wilk-Nusair 1980 correlation functional [14] and $\Delta E_{c,LYP}$ is the LYP correlation functional. The parameters $a_o = 0.20$, $a_x = 0.72$ and $a_c = 0.81$ are determined by Becke using the least square fit to 56 experimental values of atomization energies, 42 ionization potentials, and 8 proton affinities.

2.4.5. Meta-hybrid functional M06

Meta hybrid functionals are analogous to hybrid functionals but HF exchange is added to meta GGA functional. Meta-hybrid functionals include electron density ρ, and its first and second derivative or kinetic energy density and HF change in exchange-correlation energy. Minnesota [15,16] functionals come under meta- hybrid functionals. M06 [17] is an example of a meta-hybrid functional and broadly used to study the main group thermochemistry, thermochemical kinetics, non-covalent interactions, and excited states. Its exchange-correlation energy is given by

$$E_{XC}^{\text{metal hybrid}} = \frac{X}{100} E_X^{HF} + \left(1 - \frac{X}{100}\right) E_X^{DFT} + E_C^{DFT}. \quad (2.17)$$

E_X^{HF} is HF exchange energy, which is 27% for M06 functional, $E_X^{DFT}$is DFT exchange energy derived from Kohn-Sham equations, which is of 73% for M06 functional and E_C^{DFT} correlation energy.

2.4.6. Long range-corrected hybrid functionals

In the case of ground-state studies, conventional exchange-correlation functionals give accurate results with DFT calculations. But when it comes to excited state properties, these conventional exchange-correlation functionals fail to describe the charge transfer phenomena and underestimate the long-range charge transfer states. In the exchange-correlation functional, electron repulsion operator $\frac{1}{r_{12}}$ is written as [18],

$$\frac{1}{r_{12}} = \frac{1 - [\text{erf}(\mu r_{12})]}{r_{12}} + \frac{\text{erf}(\mu r_{12})}{r_{12}}. \quad (2.18)$$

where μ is the range parameter which balances the contribution of DFT and HF and erf is the standard error function. The smaller the μ value greater is the short range contribution. The first term indicates the short-range electron-electron interaction and second term describes the long-range interactions. The hybrid functional B3LYP has been extensively used to study the various ground state properties but it is unsuccessful to study the charge transfer excited states. The reason for these failures is that the long-range interaction term behaves as $-0.2r^{-1}$ instead of $-r^{-1}$. These shortcomings of conventional exchange-correlation functionals can be overcome by the long-range corrected functionals. Long-range corrected hybrid functionals include full HF exchange term only for long-range electron-electron interactions.

2.4.7. ωB97XD long-range corrected functional

The functional ωB97X [19] is the one of the long-range corrected functionals which is used to study the atomization energies, ionization potentials, electron affinities, proton affinities, enthalpy of formation, the thermochemistry of a set of inorganic and organic molecules, non-covalent interactions in complexes, and kinetics of chemical reactions. The ωB97X functional has the contribution of HF in short-range as well as in long-range exchange term. The ωB97X functional exchange correlation energy is given by

$$E_{XC}^{\omega B97X} = E_X^{LR-HF} + c_x E_x^{SR-HF} + E_x^{SR-B97} + E_c^{B97}. \quad (2.19)$$

The inclusion of empirical dispersion correction term in ωB97X functional results in ωB97XD [20] long-range corrected functional. Range parameter μ value is 0.4 for ωB97XD functional. General form of DFT with empirical dispersion corrections (DFT-D) functional after inclusion of dispersion correct term

$$E_{DFT-D} = E_{KS-DFT} + E_{disp}. \quad (2.20)$$

is computed as the sum of a KS-DFT part using ωB97X functional and an empirical atomic-pairwise dispersion correction.

2.4.8. Coulomb-attenuating method (CAM-B3LYP)

The CAM-B3LYP [21] is one of the hybrid exchange-correlation functionals which combines the qualities of hybrid functional B3LYP and long-range corrections. Two parameters α and β are included in the equation (2.21) to describe the long-range interactions included in the exchange functional of CAM-B3LYP functional. The new long-range hybrid functional CAM-B3LYP proposed by Yanai and co-workers. The CAM-B3LYP exchange-correlation parameter r_{12}^{-1} is given by

$$\frac{1}{r_{12}} = \frac{1 - [\alpha + \beta . \mathrm{erf}(\mu r_{12})]}{r_{12}} + \frac{\alpha + \beta . \mathrm{erf}(\mu r_{12})}{r_{12}}. \quad (2.21)$$

where α is a parameter which allows the incorporation of HF exchange contribution over the whole range by a factor of α and β incorporates DFT counterpart over the whole range by a factor 1-(α+β). The parameters α and β describe the importance of HF and DFT contributions to short-range and long-range interactions.

2.5. Basis sets

Basis functions approximate atomic orbitals (AOs) in a molecule and linear combination of basis functions approximate the molecular orbitals. This approach is called as linear combination of atomic orbitals approach (LCAO). AOs are represented by atom-centered Gaussians in most quantum chemistry programs for example in Gaussian09 [22]. Slater type of orbitals (STO) represents electron density well in valence region and beyond (not so well near nucleus) however evaluating these STOs are difficult because a typical STO function is given below,

$$\emptyset_{abc}^{STO}(x,y,z) = N\, x^a y^b z^c e^{-\zeta r}. \tag{2.23}$$

"N" represents the normalization constant, a,b,c control angular momentum (L = a+b+c) and Zeta (ζ) controls the width of the orbital (the function is difficult to solve mathematically). Gaussian types of orbitals (GTO) are used in the place of Slater type of orbitals where they can be mimicked by using linear combination of Gaussian functions. Gaussian type of orbitals are given by the Eq. (2.26)

$$\emptyset_{abc}^{GTO}(x,y,z) = N\, x^a y^b z^c e^{-\zeta r^2}. \tag{2.24}$$

A combination of "n" Gaussians to mimic an STO is often called an "STO-nG" basis, even though it is made of contracted GTO's (CGTO) given by,

$$\emptyset_{abc}^{CGTO}(x,y,z) = N \sum_{i=1}^{n} c_i x^a y^b z^c e^{-\zeta r^2}. \tag{2.25}$$

where c_i represent contraction coefficient. We have used Pople basis sets in our calculations developed by late Nobel Laurate John Pople [23] which are based upon CGTOs. In most of our calculations we used 6-31G (d) basis sets, where 6 represent the core orbital which is a CGTO made of 6 Gaussians, and the valence orbitals are described by two orbitals — one CGTO made of 3 Gaussians, and the other with one single Gaussian. "d" indicates the polarization functions on non-hydrogen atoms. Adding more basis functions per atom allow orbitals to "change size" and adding polarization functions allow orbitals to change shape.

2.6. Band structure studies

Molecular orbital theory (MOT) describes the electronic energy levels of isolated molecules. But in solid state materials, interactions between neighboring molecules become

very important. Many of the important properties like superconductivity, magnetism, metallic conductivity, etc. depend upon intermolecular interactions. The solid state equivalent to a molecular orbital (MO) diagram is called the band structure diagram [24]. Electronic band structure provides the insight and understanding of very important physical properties of solids. Similar to the molecular orbital theory where the energy levels in a MO diagram are dependent upon the energy levels of the AOs, the symmetry and interatomic distances in a molecule, the electronic band structure depends on the energy levels of the constituent AOs and the crystal structure. Band structure is mostly studied by physicists and the terminology of physicists differs from the chemists. A rough comparison of the way chemists and physicists view solids is given in the table below.

Chemist	Physicist
MO Diagram	Band Structure Diagram
Molecular Orbital	Wave vector
Chemical bonding	Potentials
Qualitative	Quantitative (Mathematical)

Table 2.1. Terminology in Band structure used by chemists and physicists.

2.6.1. Preliminaries of Band structure

Let us consider a simple 1-D chain of hydrogen atoms. If there are N atoms in the chain there will be N energy levels and N electronic states or N "MOs". The wavefunction of the electronic state [24] is given by Eq. (2.37),

$$\Psi_k = \sum e^{ikna} \chi_n. \tag{2.26}$$

Here "a" corresponds to the lattice constant (spacing between H atoms) and n is a counter for each AO in the chain. χ represents basis functions and n corresponds to a number of atoms in the chain. Each Ψ_k is a symmetry-adapted linear combination (SALC) of AOs, where the symmetry operator, in this case, is translational symmetry. The process of symmetry adoption is called in the solid-state physics as, "forming Bloch functions"[25,26]. The variable k represents the labels of respective SALCs, it also gives the information about the phase of the orbitals as shown in Figure 2.1 [24].

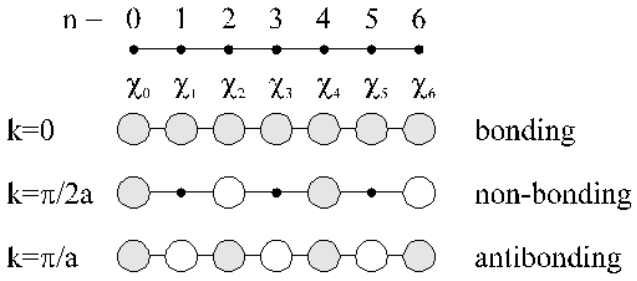

Figure 2.1 Illustration of bonding at different k points forming bonding, non-bonding, and antibonding orbitals.

At k = 0 all of the orbitals are in phase, while at k = π/a the orbitals are out of phase, at intermediate values the phase of the orbitals is different. The value of k also is related to the wavelength of the wave packet (λ) which in turn describes an electron in a given state, Ψ_k, given by the relationship,

$$\lambda = \frac{2\pi}{k}. \tag{2.27}$$

The unique values of k are in the interval $-\pi/a \leq k \leq \pi/a$ or $|k| \leq \pi/a$, called the first Brillouin zone. An example of a typical Band structure diagram [23] is shown below (Figure 2.2).

Here we observe (Figure 2.2) the lowest energy orbital is at k=0 and highest energy orbital at k=π/a. One of the interesting features of bands is how they "run". Let us consider the band structure diagram [24] of sigma interaction of "p" functions shown below (Figure 2.3). From the Figure 2.3, it is clear that k = 0 corresponds to highest energy and π/a the lowest. Another important feature of band structure plots is it gives the information about bonding interactions between orbitals in the case of polymer or crystal the overlap is considered between neighbouring unit cells.

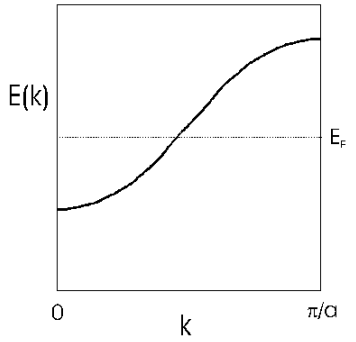

Figure 2.2. Band structure diagram Energy vs k vector in the first Brillouin zone is shown.

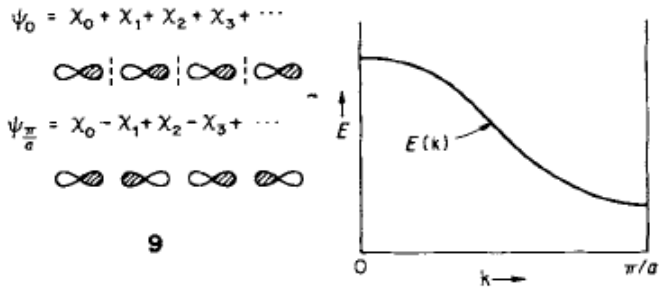

Figure 2.3. Band structure diagram formed by "p" functions (frontier orbitals). Overlap of frontier orbitals at k points 0, π/a is also shown.

Bandwidth is defined as the energy gap between the lowest and highest energy orbital. As the orbital overlap is increased (decreasing the interatomic spacing) the bonding interaction is stabilized while the antibonding is further destabilized. This will cause the bandwidth to increase.

2.7. Time-dependent density functional theory (TD-DFT)

Theoretical investigations of absorption and emission spectra by means of quantum mechanical calculations have become a very standard approach widely used to help the assignment of the experimental spectra and to get insights of the underlying optical and electronic properties of technologically important molecules. Time- dependent DFT (TD-DFT) is already established as the most widely used, effective approach to investigate the optical spectra and excited state properties of organic molecules in gas phase, solution and also in complex environments [27-31].

The advantages of DFT and its time dependent formalism are combined in TD-DFT [32-34] to make it well suited for accurate description of structures, energies and electronic excitations over the past few years [35-37]. It is originally developed by Runge and Gross and can be easily applied to time-dependent quantum mechanical scenarios by establishing a relation between the time-dependent densities with the potentials. The accuracy of this theory is limited because of the adiabatic approximation and requires the appropriate exchange correlation functional (XCF). Even though TD-DFT predicts molecular excited states correctly, long-range charge transfer effects are not accurately defined [38-40].

It is also known [38-40] that the use of conventional XCF drastically underestimates the charge transfer excitation energies and yields incorrect asymptotic potential energy

surfaces. The selection of an appropriate XCF for modeling excited state properties has been the subject of several bench marks performed on different systems over the past few years [41-43]. It is now well established in the literature that the conventional functionals fail for long-range charge transfer states and also for the correct prediction for optically excited states [44-46].

Time-dependent DFT is used to study the effect of the electric and magnetic field on molecules to extract the excited state properties like absorption, emission spectra, and their oscillator strengths etc. Conventional DFT is restricted to study only the ground state properties of a molecule. TD-DFT is an alternative approach to study the properties of molecules in the presence of external fields. It is an extension of DFT and conceptual and computational foundations are analogous. TD-DFT is extensively used to study the excited state properties like absorption, emission, oscillator strength etc. These calculations are based on the fact that the linear response function that is, how the electron density changes when the external potential changes. Such calculations require, in addition to the exchange-correlation potential, the exchange-correlation kernel – the functional derivative of the exchange-correlation potential with respect to the density [33].

2.8. Runge-Gross Theorem

Runge-Gross theorem [32] provides the formal foundation of Time-dependent DFT. It shows that the density can be used as the fundamental variable in describing quantum many-body systems in place of the wavefunction and that all properties of the system are functionals of the density. The Runge-Gross theorem is the time-dependent analog of the celebrated Hohenberg-Kohn theorem. For every single particle potential $\upsilon(\mathbf{r},t)$ which can be expanded into a Taylor series with respect to the time coordinate $t=t_0$, correspondence to one body density $n(\mathbf{r},t)$ is defined by solving the time-dependent Schrödinger equation with an initial fixed state ($\Phi(t_0) = \Phi_0$). The evolution of the wave function ($\Psi(t=t_0) = \Psi_0$) is governed by the time-dependent Schrödinger equation:

$$\hat{H}(t)\Phi(t) = i\frac{d\Phi(t)}{dt}. \tag{2.28}$$

where $\hat{H}(t)$ is the Hamiltonian operator. As the system evolves in time from some initial point (t=0), it's one particle density changes. This electron density is given by

$$n(\mathbf{r},t) = N \int d^3r_2 \dots \int d^3r_N \, |\Phi(\mathbf{r},\mathbf{r}_2 \dots, \mathbf{r}_N, t)|^2. \tag{2.29}$$

and has the interpretation that $n(r,t)d^3r$ is the probability of finding any electron in a region d^3r around 'r' at time t. The density normalized the number of electrons

$$\int d^3\mathbf{r}\, n(\mathbf{r},t) = N. \tag{2.30}$$

We consider N nonrelativistic electrons, mutually interacting via Coulomb repulsion, in a time-dependent external potential. The theorem states that the densities $n(\mathbf{r},t)$ and $n'(\mathbf{r},t)$ evolving from a common initial state $\Phi(t=0)$ under the influence of two potentials $\upsilon(\mathbf{r},t)$ and $\upsilon'(\mathbf{r},t)$ eventually differ if the potentials differ by more than a purely time-dependent function:

$$\Delta\upsilon(\mathbf{r},t) = \upsilon(\mathbf{r},t) - \upsilon'(\mathbf{r},t) \neq c(t). \tag{2.31}$$

The corresponding current density must differ is given by

$$\mathbf{j}(\mathbf{r},t) = N \int d^3 r_N \Im\{\Psi(\mathbf{r},\mathbf{r}_2,\dots,\mathbf{r}_N,t)\nabla\Psi^*(\mathbf{r},\mathbf{r}_2,\dots\mathbf{r}_N,t)\}. \tag{2.32}$$

where $\Im\Psi$ denotes the imaginary part of Ψ. From the time-dependent Schrödinger equation, (2.28):

$$\frac{\partial n(\mathbf{r},t)}{\partial t} = -\nabla.\mathbf{j}(\mathbf{r},t). \tag{2.33}$$

The corresponding current densities of two potentials ($\upsilon(\mathbf{r},t)$ and $\upsilon'(\mathbf{r},t)$) are $\mathbf{j}$ and $\mathbf{j'}$ and their difference at t= 0 is,

$$\begin{aligned}\frac{\partial}{\partial t}\{\mathbf{j}(\mathbf{r},t) - \mathbf{j}'(\mathbf{r},t)\}_{t=0} &= -i\langle\Phi_0|\left[\hat{\mathbf{j}}(\mathbf{r},t),\{\hat{H}(0) - \hat{H}'(0)\}\right]|\Phi_0\rangle \\ &= -i\langle\Phi_0|\left[\hat{\mathbf{j}}(\mathbf{r},0),\{\upsilon(\mathbf{r},0) - \upsilon'(\mathbf{r},0)\}\right]|\Phi_0\rangle \\ &= -n_0(\mathbf{r},0)\nabla\{\upsilon(\mathbf{r},0) - \upsilon'(\mathbf{r},0)\}. \end{aligned} \tag{2.34}$$

At the initial time, the two potentials differ, the first derivative of currents must differ. Then the currents will change infinitesimally soon thereafter. Using the equation of motion and considering t=0, to find

$$\frac{\partial^{k+1}}{\partial t^{k+1}}\{\mathbf{j}(\mathbf{r}.t) - \mathbf{j}'(\mathbf{r},t)\}_{t=0} = -n_0(\mathbf{r})\nabla\frac{\partial^k}{\partial t^k}\{\upsilon(\mathbf{r},t) - \upsilon'(\mathbf{r},t)\}_{t=0.} \tag{2.35}$$

If (2.31) holds, and the potentials are Taylor expandable about t=0, then there must be some finite k for which the right-hand side (2.34) does not vanish (The corresponding current densities are different and their difference must be non-zero)

$$\mathbf{j}(\mathbf{r},t) \neq \mathbf{j}'(\mathbf{r},t). \qquad (2.36)$$

For two Taylor-expandable potentials that differ by more than just a trivial constant, the corresponding current densities must be different. This is the first part of the theorem, which establishes a one-to-one correspondence between current densities and external potentials. The second part discusses the one-to-one correspondence between densities and external potentials.

$$\frac{\partial^{k+2}}{\partial t^{k+2}}\{n(\mathbf{r},t) - n'(\mathbf{r},t)\}_{t=0} = \nabla.[n_0(\mathbf{r})\nabla\frac{\partial^k}{\partial t^k}\{\upsilon(\mathbf{r},t) - \upsilon'(\mathbf{r},t)\}_{t=0}]. \qquad (2.37)$$

The two densities will differ and give non-zero value if (T4) holds on the right-hand side for some k. Let us assume that obtained outcome is contradictory, $\frac{\partial^k}{\partial t^k}\{\upsilon(\mathbf{r},t) - \upsilon'(\mathbf{r},t)\}_{t=0} = u(r)$.

$$\nabla.[n(\mathbf{r},t)\nabla\frac{\partial^k}{\partial t^k}\{\upsilon(\mathbf{r},t) - \upsilon'(\mathbf{r},t)\}] = 0.$$

$$0 = \int d^3r\, u(r)\nabla[n_0(\mathbf{r},t_0)\ \ \nabla u(r)\,]$$

$$= -\int d^3r\, n(\mathbf{r},t_0)[\nabla u(r)]^2 + \frac{1}{2}\int n(\mathbf{r},t_0)[\nabla u^2(r)].df. \qquad (2.38)$$

If the initial density n(**r**,0) falls off rapidly enough to ensure that the surface integral vanishes and Range-Gross theorem conclude $n(\mathbf{r},0)[\nabla u(r)]^2 = 0$ This is a contradiction to u(r) ≠0 well behaved. Thus right hand side of the (2.44) cannot vanish which proves that densities n(**r**,t) and n′(**r**,t) become different infinitesimally later than t_0.

2. 9. Time-dependent Kohn-Sham system

Kohn-Sham approach considers a fictitious system of non-interacting electrons moving in a time-dependent effective potential, whose density is precisely that of the real system. This effective potential is known as the time-dependent Kohn-Sham potential. Kohn-Sham time-dependent equation is given by

$$i\frac{\partial\Phi_j(\mathbf{r},t)}{\partial t} = \hat{H}\Phi(\mathbf{r},t). \tag{2.39}$$

H is the Hamiltonian operator, $\hat{H} = -\frac{1}{2}\nabla^2 + \upsilon_{KS}(\mathbf{r},t).$ (2.40)

whose density, $n(\mathbf{r},t) = \sum_{j=1}^{N}\left|\Phi_j(\mathbf{r},t)\right|^2$ is defined to be precisely that of the real system. Kohn-Sham potential ($\upsilon_{KS}(\mathbf{r},t)$) consists of an external potential, Hartree potential and exchange-correlation potential which is functional of density.

$$\upsilon_{KS}(\mathbf{r},t) = \upsilon_{ext}(\mathbf{r},t) + \upsilon_H(\mathbf{r},t) + \upsilon_{XC}(\mathbf{r},t). \tag{2.41}$$

where Hartree potential is given by

$$\upsilon_H(\mathbf{r},t) = \int d^3r' \frac{n(\mathbf{r},t)}{|r-r'|}. \tag{2.42}$$

Exchange-correlation potential is given as the functional derivative of exchange-correlational action A_{XC} is represented by

$$\upsilon_{XC}(\mathbf{r},t) = \frac{\delta A_{XC}[n]}{\delta n(\mathbf{r},t)} \cong \frac{\delta E_{XC}[n_t]}{\delta n_t(\mathbf{r})} = \upsilon_{XC}(\mathbf{r}). \tag{2.43}$$

where A_{XC} is functional of a function 'n' over both time and space. E_{XC} is a function of n_t of space at fixed t. This local approximation in time is commonly referred as the adiabatic approximation.

2.10. Linear Response TD-DFT

Linear response TD-DFT is used when weak external electric is applied. This weak perturbation does not completely destroy the ground state geometry of the molecule. In this case, one can analyze the linear response of the system. The Perturbation introduced into Kohn-Sham Hamiltonian by turning on applied field $\delta\upsilon_{appl}(\mathbf{r},t)$ is, to linear order,

$$\delta\upsilon_{eff}(\mathbf{r},t) = \delta\upsilon_{appl}(\mathbf{r},t) + \delta\upsilon_{SCF}(\mathbf{r},t). \tag{2.44}$$

where $\delta\upsilon_{SCF}(\mathbf{r},t)$ is the linear response of the self-consistent field arising from the change in the charge density.

$$\delta P_{st}(\omega) = \sum_{ai}\delta P_{ai}(\omega)\Psi_a(\mathbf{r})\Psi_i^*(\mathbf{r}) + \sum_{ia}\delta P_{ia}(\omega)\Psi_i(\mathbf{r})\Psi_a^*(\mathbf{r}). \tag{2.45}$$

where $\delta P_{st}(\omega)$ is the linear response of the KS/HF density matrix in the basis of unperturbed molecular orbitals. Using elementary results from time-dependent perturbation theory, one can write down the linear response of the KS/HF density matrix to the applied field as

$$\delta P_{st}(\omega) = \frac{\Delta n_{st}}{(\epsilon_s - \epsilon_t) - \omega} \delta \upsilon_{st}^{eff}(\omega). \quad (2.46)$$

where Δn_{st} is the difference in the occupation number and is 1 for st = ai and -1 for st = ia. The equation (2.52) is somewhat more complicated due to the fact that the potential $\delta \upsilon_{SCF}$ depends on the response of the density matrix

$$\delta \upsilon_{st}^{SCF}(\omega) = \sum_{uv} K_{st,uv}(\omega) \delta P_{uv}(\omega)$$

$$= \sum_{bj} K_{st,bj}(\omega) \delta P_{bj}(\omega) + \sum_{jb} K_{st,jb}(\omega) \delta P_{jb}(\omega). \quad (2.47)$$

where K is the coupling matrix.

The most logical choice to study the charge transfer phenomena in the organic π-conjugated system is TD-DFT. The presence of extended π-conjugation results in large errors in charge transfer excitation energies because of the incorrect description of the distance coordinate matrix due mainly to the nonlocal nature of the interactions in the charge transfer state, particularly when using global hybrid exchange-correlation functionals such as B3LYP and PBE0 etc [47].

2.11. Electronic and optical parameters for solar cells

DFT and TD-DFT formalism can be used to study the electronic and optical properties dye sensitized solar cell molecules like electronic band gap, reorganization energy, absorption, light harvesting efficiency (LHA), Gibbs free energy change (ΔG^{Inject}), open circuit voltage (V_{OC}), exciton binding energy, excited state lifetime etc. The power conversion efficiency (PCE) of a dye molecule can be determined by the formula,

$$PCE(\eta) = \frac{J_{SC}.V_{OC}.FF}{P_{inc}}. \quad (2.48)$$

where J_{SC} is the short circuit current density, V_{OC} is open circuit voltage, FF is filled factor and P_{inc} is incident power density. Short circuit current (J_{SC}) depends on LHE (light harvesting efficiency), q is the electron charge, F(λ) is the incident photon flux.

$$J_{SC} = \int \mathrm{LHE}\,(\lambda)\Phi_{inj}n_{collect}d\lambda. \tag{2.49}$$

Light harvesting efficiency (LHE) [48] is the fraction of light absorbed by the dye at a particular wavelength. In the case of every dye, the highest oscillator strength observed at lowest excitation. LHE should be as maximum as possible so that these dyes will show a maximum of short circuit current which will increase the solar cell efficiency. The theoretical way to calculate the LHE of dye is,

$$\mathrm{LHE} = 1 - 10^{-f}. \tag{2.50}$$

where f represents oscillator strengths of particular wavelength transistion from occupied to unoccupied orbital of adsorbed dye molecules. Short circuit current also depends on the electron injection efficiency (Φ_{inj}). In order to evaluate the favorable electron injection from dye to the semiconductor TiO_2, ΔG_{Inject} can be calculated. The exergonic or negative value of ΔG_{Inject} leads to favorable electron injection. Preat and co-workers established a theoretical procedure [49] to calculate the ΔG_{Inject} which tells about the electron injection onto the semiconductor TiO_2. The free energy change can be calculated by

$$\Delta G_{Inject} = E^{dye*} - E_{CB}^{SC} = E^{dye} - \lambda_{max} - E_{CB}^{SC}. \tag{2.51}$$

where E^{dye*} is the oxidation potential of the dye in excited state and E_{CB}^{SC} is the reduction potential of the conduction band of the semiconductor TiO_2. E^{dye} is calculated using Born-Haber's cycle. Open circuit voltage (V_{OC}) is also one of the important parameters to influence the power conversion efficiency of a solar cell. Besides J_{SC}, the overall PCE of a molecule is also depends on the magnitude of V_{OC}. In dye sensitized solar cells, V_{OC} is directly proportional to the energy difference between the LUMO of the dye to the conduction band of the semiconductor [50].

$$eV_{OC} = E_{LUMO} - E_{CB}. \tag{2.52}$$

The efficiency of the dyes also depends on the excited state lifetime of the electrons. Usually, the electron injection is very fast from excited state of dye to the conduction band of semiconductor and takes place within 100 fs. The penetration of dye with the semiconductor

is more leading to faster electron recombination. Due to the electron recombination, the electron will not go to the electrodes and this leads to lower efficiency. In order to have high electron lifetime, the dye must be in cationic state until the regeneration. The excited state lifetime [51] is calculated by

$$\tau = {}^{1.499}/_{fE^2}. \tag{2.53}$$

where f is oscillator strength and E is lowest excited state energy of the optimized geometries of the excited singlet state

$$E_B = E_{Opt} - E_T. \tag{2.54}$$

Exciton binding energy is defined as the difference between optical gap (E_{opt}) and transport gap (E_T). E_{opt} is excitation energy and E_T is the energy gap between HOMO and LUMO. Exciton is a bound state of electron and hole which are attracted by electrostatic Coulomb attraction force. An exciton is formed when a photon is absorbed by an organic semiconducting molecule. Smaller exciton binding energies are required for dye sensitized solar cells. This ensures that hole and electron separation occurs and leads to better power conversion efficiency.

2.12 References

[1] J. P. Perdew, A. Zunger, Phys. Rev., B 1981, 23, 5048.

[2] M. S. Hybertsen, S. G. Louie, Phys. Rev. B, 1986, 34, 5390.

[3] G. Pacchioni, F. Frigoli, D. Ricci, J. A. Weil, Phys. Rev. B, 2000, 63, 054102.

[4] A. Filippetti, N. A. Spaldin, Phys. Rev. B, 2003, 67, 125109.

[5] J. P. Perdew, M. Levy, Phys. Rev. Lett., 1983, 51, 1884.

[6] L. J. Sham, M. Schluter, Phys. Rev. Lett., 1983, 51, 1888.

[7] R. F. W. Bader. *Atoms in molecules* Oxford, New York, 1990.

[8] E. G. Lewars. *Computational Chemistry-Introduction to the Theory and Applications of Molecular and Quantum Mechanics* Springer, Dordrecht Heidelberg, London, NewYork, 2011.

[9] F. Jensen, *Introduction to Computational Chemistry* John Wiley & Sons Ltd, England, 2007.

[10] I. N. Levine, *Quantum chemistry*, Prentice Hall, Upper Saddle River, NJ, 2000.

[11] A. D. Becke. J. Chem. Phys., 1993, 98, 5648.

[12] C. Lee, W. Yang, R. G. Parr. Phys. Rev. B, 1988, 37, 785.

[13] A. D. Becke. Phys. Rev. A 1988, 38, 3098.

[14] S. H. Vosko, L. Wilk, M. Nusair. Can. J. Phys., 1980, 58, 1200.

[15] Y. Zhao, N.E. Schultz, D.G. Truhlar, J. Chem. Phys., 2005, 123, 161103.

[16] Y. Zhao, N.E. Schultz, D.G. Truhlar, J. Chem. Theor. Comput., 2006, 2, 364.

[17] Y. Zhao, D. G. Truhlar, Theor. Chem. Acc., 2006, 120, 215.

[18] Y. Tawada, T. Tsuneda, S. Yanagisawa, T. Yanai, K. Hirao, J. Chem. Phys., 2004, 120, 8425.

[19] J.-D. Chai, H.-G. Martin, J. Chem. Phys., 2008, 128, 084106.

[20] J-D Chai, H.-G. Martin, Phys. Chem. Chem. Phys., 2008, 10, 6615.

[21] T. Yanai, D. P. Tew, N. C. Handy, Chem. Phys. Lett., 2004, 393, 51.

[22] M. J. Frisch, G. W. Trucks, H. B. Schlegel, G. E. Scuseria, M. A. Robb, J. R.

Cheeseman, J. A. Montgomery Jr., T. Vreven, K. N. Kudin, J. C. Burant, J. M. Millam, S. S. Iyengar, J. Tomasi, V. Barone, B. Mennucci, M. Cossi, G. Scalmani, N. Rega, G.A. Petersson, H. Nakatsuji, M. Hada, M. Ehara, K. Toyota, R. Fukuda, J. Hasegawa, M. I Shida, T. Nakajima, Y. Honda, O. Kitao, H. Nakai, M. Klene, X. Li, J. E. Knox, H. P. Hratchian, J. B. Cross, V. Bakken, C. Adamo, J. Jaramillo, R. Gomperts, R. E. Stratmann, O. Yazyev, A. J. Austin, R. Cammi, C. Pomelli, J. W. Ochterski, P. Y. Ayala, K. Morokuma, G. A. Voth, P. Salvador, J. J. Dannenberg, V. G. Zakrzewski, S. Dapprich, A. D. Daniels, M. C. Strain, O. Farkas, D. K. Malick, A. D Rabuck, K. Raghavachari, J. B. Foresman, J. Ortiz, Q. Cui, A. G Baboul, S. Clifford, J. Cioslowski, B. B. Stefanov, G. Liu, A. Liashenko, P. Piskorz, I. Komaromi, R. L. Martin, D. J. Fox, T. Keith, M. A. Al-Laham, C. Y. Peng, A. Nanayakkara, M. Challacombe, P. M. W. Gill, B. Johnson, W. Chen, M. W. Wong, C. Gonzalez, J. A. Pople, Gaussian Inc, Gaussian 09, Revision A.1, Wallingford, CT, 2009.

[23] J. B. Foresman, A. Frisch, *Exploring Chemistry with Electronic Structure Methods: A Guide to using Gaussian*, Pittsburgh, 1996.

[24] R. Hoffmann, Angew. Chem. Int. Ed., 1987, 26, 846.

[25] J. K. Burdett, Prog. Solid State Chem., 1984, 15, 173.

[26] T. A. Albright, J. K. Burdett, M. H. Whangbo, *Orbital Interactions in Chemistry*, Wiley-Interscience, New York, 1985.

[27] C. Adamo, D. Jacquemin, Chem. Soc. Rev., 2013, 42, 845

[28] B. Mennucci, Phys. Chem. Chem. Phys., 2013, 15, 6583.

[29] A. Pedone, G. Proampolini, S. Monti, V. Barone, Phys. Chem. Chem. Phys., 2011, 13, 16689.

[30] F. Labat, I. Ciofini, H. P. Hratchian, M. J. Frisch, K. Raghavachari, C. Adamo, J. Am. Chem. Soc., 2009, 131, 14290.

[31] S. Chibani, A. D. Laurent, A. Blondel, B. Mennucci, D. Jacquemin, J. Chem. Theory Comput., 2014, 10, 1848.

[32] E. Runge, E. K. U. Gross, Phys. Rev. Lett., 1984, 52, 997.

[33] M. Petersilka, U. J. Gossmann, E. K. U. Gross, Phys. Rev. Lett., 1996, 76, 1212.

[34] M. A. L. Marques, E. K. U. Gross, Annu. Rev. Phys. Chem., 2004, 55, 427.

[35] M. E. Casida, *Recent Advances in Density Functional Methods* World Scientific: Singapore, 1995.

[36] E. U. K. Gross, J. F. Dobson, M. Petersilka, *Density Functional Theory II*, Springer: Heidelberg, 1996.

[37] R. Bauernschmitt, R. Ahlrichs, Chem. Phys. Lett., 1996, 256, 454.

[38] C. Jamorski, J. B. Foresman, C. Thilgen, H. P. Lüthi, J. Chem. Phys., 2002, 116, 8761.

[39] A. Dreuw, J. L. Weisman, M. HeadGordon, J. Chem. Phys., 2003, 119, 2943.

[40] D. J. Tozer, J. Chem. Phys., 2003, 119, 12697.

[41] A. L. Sobolewski, W. Domcke, J. Chem. Phys., 2003, 294, 73.

[42] S. Grimme, M. Parac, Chem. Phys. Chem., 2003, 4, 292.

[43] Y. Kurashinge, T. Nakajima, S. Kurashinge, K. Hirao, Y. Nishikitani, J. Phys. Chem. A, 2007, 111, 5544.

[44] B. M. Wong, J. G. Cordaro, J. Chem. Phys., 2008, 129, 214703.

[45] C. E. A. Azzam, A. Planchat, B. Mennucci, C. Adamo, D. Jacquemin, J. Chem. Theory Comput., 2013, 9, 2749.

[46] M. Promkatkaew, S. Suramitr, T. Karpkird, M. Ehara, S. Hannongbua, Int. J. Quantum Chem., 2013, 113, 542

[47] M. P. Balany, D. H. Kim, J. Phys. Chem. C, 2011, 115, 19424.

[48] J. Feng, Y. Jiao, W. Ma, M. K. Nazeeruddin, M. Gratzel, S. Meng, J. Phys. Chem. C, 2013, 117, 3772.

[49] J. Preat, C. Michaux, D. Jacquemin, E. A. Perpete, J. Phys. Chem. C, 2009, 113, 16833.

[50] D. Cahen, G. Hodes, M. Gräetzel, J. F. Guillermoles, I. J. Riess, J. Phys. Chem. B, 2000, 104, 2053.

[51] K. Chaithanya, X-H Ju, B. M. Heron, RSC Adv., 2014, 4, 26621.

Chapter 3

Computational Modeling of Electronic Structure of α-Oligothiophenes with Various Substituents

3.1. Introduction

Thiophene based oligomers are considered as promising candidates in organic semiconducting materials because of their stability and synthetic availability. The advantages of oligomers are that their physical properties can be easily tuned to the desired properties by changing their structure, for example, solubilizing chains with chemical functionalization at sides, terminal groups, and also with different oligomer lengths. Because of their π-packing motif in solid state, these oligothiophenes have been used in field effect transistors owing to their charge carrier mobilities [1]. This due to the formation of intra- and intermolecular interactions which resulted from the high polrizability electrons on sulphur atom. These oligothiophenes are also used as a π-spacer in dye sensistized solar cells due to their effective conjugation [2-5]. Oligothiophenes are also used in biomarkers due to their high fluorescence efficiencies, optical stability and large stokes shift [6-9]. The oligothiophenes are extensively used in many more applications such as electromagnetic shielding and molecular electronics etc. [10-12]. Since they are stable at ambient conditions, have been used in new optical devices like [13] light emitting diodes and filed-effect transistors, electrode materials, organic semiconductors, materials for solar cells, materials with nonlinear optical (NLO) properties, etc. [10,12,14-16]. Luminescent conjugated polythiophenes and luminescent conjugated oligothiophenes have been utilized as ligands for identifying diseases associated with protein aggregates [17,18]. Recently Nilsson and co-workers synthesized the azide functionalized pentameric oligothiophenes [19]. This functionalized oligothiophene acts as a ligand and binds to the protein aggregation. Upon binding, oligothiophene-protein aggregation emits the light which can detect the diseases associated with protein aggregates [19].

This chapter discusses the effect of substitution of electron donating (methoxy, ethoxy) and withdrawing (nitro, phenyl, cyano) groups on oligothiophene of chain length from 2-9 in the region-regular head-tail – head-tail form. All the thiophene units are substituted with the functional groups in each oligothiophene. We have also studied terminal substitutions with an electron donating group at one end and an electron withdrawing group

at other end of 9-oligomer. Although band gaps can be altered by the substitution at the terminal edges of the oligomer [20-23], the main problem of solubility of thiophenes is not fully addressed through this mechanism, on the other hand substitution with different groups throughout the length of oligomer (like in HT–HT Form) would not only enhance the solubility but also alter the band gaps [12]. The different substituted molecules considered are given in Scheme 3.1. The electronic properties like HOMO, LUMO, band gap, electrostatic potential and structural properties like bond length alternations, torsional angles of oligomers are studied with most successful hybrid functional B3LYP and 6-31G(d) basis set using Gaussian 09 suite of program. The polymer is modelled as an infinite system and studied employing periodic boundary condition that could replace the discrete molecular orbital model in the continuous bands. Thus calculations for the polymer are done by generating a monomer with Gaussian type molecular orbital and extending it to infinite real polymer model using Density functional theory – Periodic boundary condition (DFT-PBC).

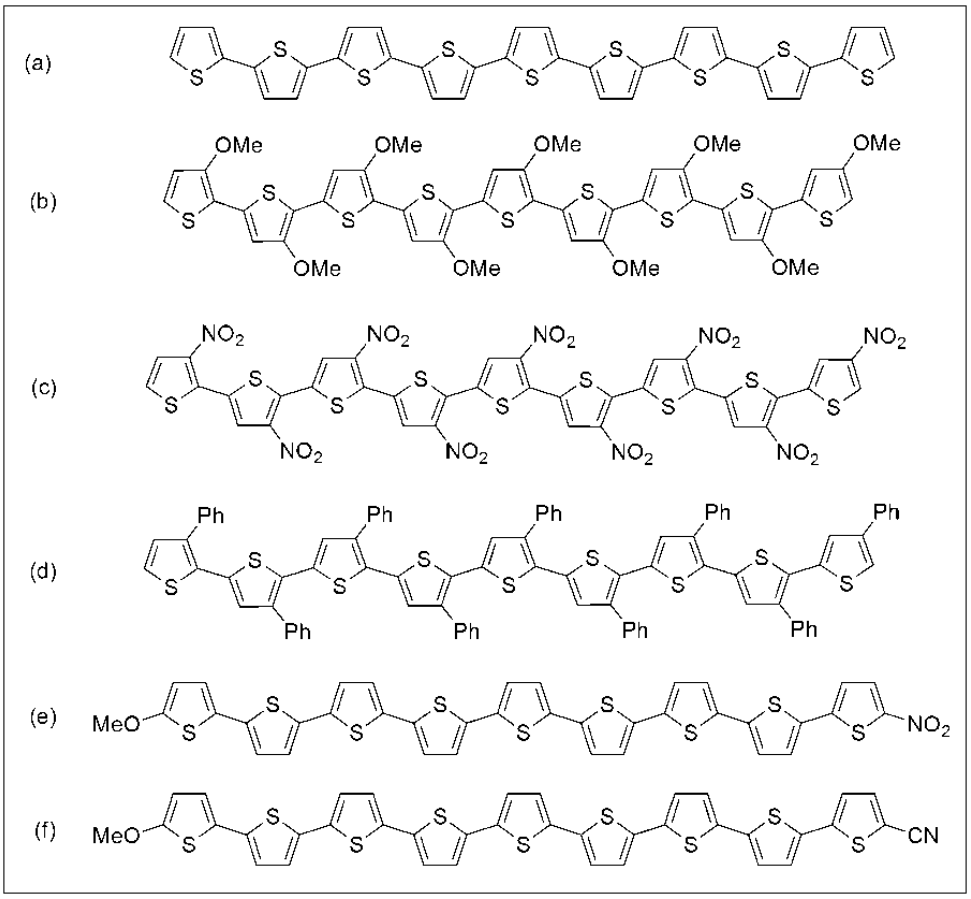

Scheme 3.1. The different substituted oligothiophenes 9-oligomer considered for the study.

3.2. Structural properties: Bond length alternations (BLA) in substituted α-oligothiophenes

The band gap in aromatic linear π-conjugated systems mainly depends on bond length alternations, deviation from the planarity and inductive and mesomeric effects associated with eventual substitution. In order to understand any electronic changes with respect to substitution and to examine the deviations from the planarity, we have first carried out bond length alternation (BLA) [24] studies for nTs and the energy changes associated with twist in dihedral angles. Oligomers of low band gap polymers prepared from planar monomer units are not sufficient to lower the band gaps. One of the methods to alter the band gaps is by substitution with different groups which can give rise to intra-molecular charge transfer along the oligomer or polymer chain backbone.

3.2.1. Quinoid and aromatic character in polythiophenes

Polythiophenes and oligothiophenes exist in the two forms such as quinoid form and aromatic form [25] as shown in Scheme 3.2. Quinoid form exhibits double bond character at interring bond whereas aromatic form shows more of single bond character. The contribution of these two forms was explained theoretically by Bredas and co-workers [26]. The band gap of polythiophene decreases linearly with increasing of quinoid character. Electron donating substitutions on oligothiophenes result in more quinoid character whereas electron withdrawing groups on the oligothiophene backbone exhibit more aromatic character as compared to the unsubstituted oligothiophenes.

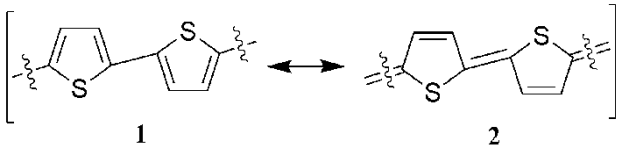

1 **2**

Scheme 3.2. Aromatic and quinoid forms of polythiophenes.

In order to understand the quinoid character and therefore the degree of π-conjugation a plot of bond lengths with respect to bond numbers in the sequential order for oligothiophenes with 9-monomer units with electron donating and electron withdrawing substituents are represented in Figures 3.1 and 3.2 respectively.

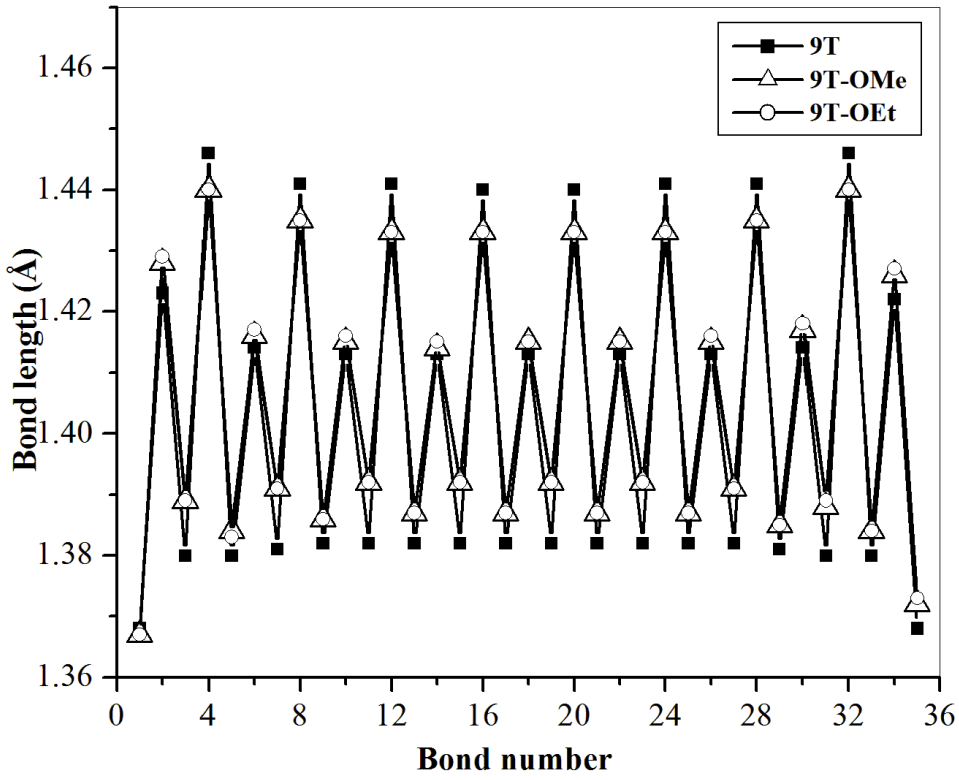

Figure 3.1. C-C Bond length alternation patterns of oligothiophene backbone containing 9 monomer units. BLA patterns of oligothiophenes substituted with electron donating methoxy and ethoxy groups are also included.

The overall BLA patterns are similar to those of other π-conjugated heterocyclic systems. From Scheme 3.2, it is clear that inter connecting bonds between two thiophene units have bond lengths lesser in quinoid form than in the aromatic form due to increase in double bond character. It can be clearly identified that bond lengths of the inter connecting bonds in the oligomers are smaller for oligothiophenes substituted with electron donating methoxy and ethoxy substituents compared to that of unsubstituted oligothiophenes. The average inter-ring bond distance for unsubstituted oligothiophene is found to be around 1.440 Å whereas that for oligothiophenes substituted with electron donating substituents are found to be 1.434 Å. The difference between single and double bonds is more evident in the unsubstituted oligothiophenes suggesting that the effective electron delocalization is more in the oligothiophenes substituted with electron donating groups. Simple oligomer backbone prefers an aromatic structure while the oligothiophenes substituted with electron donating groups prefers adopt planar quinoid form as shown in the optimized geometry of methoxy substituted oligothiophene in Figure 3.3.

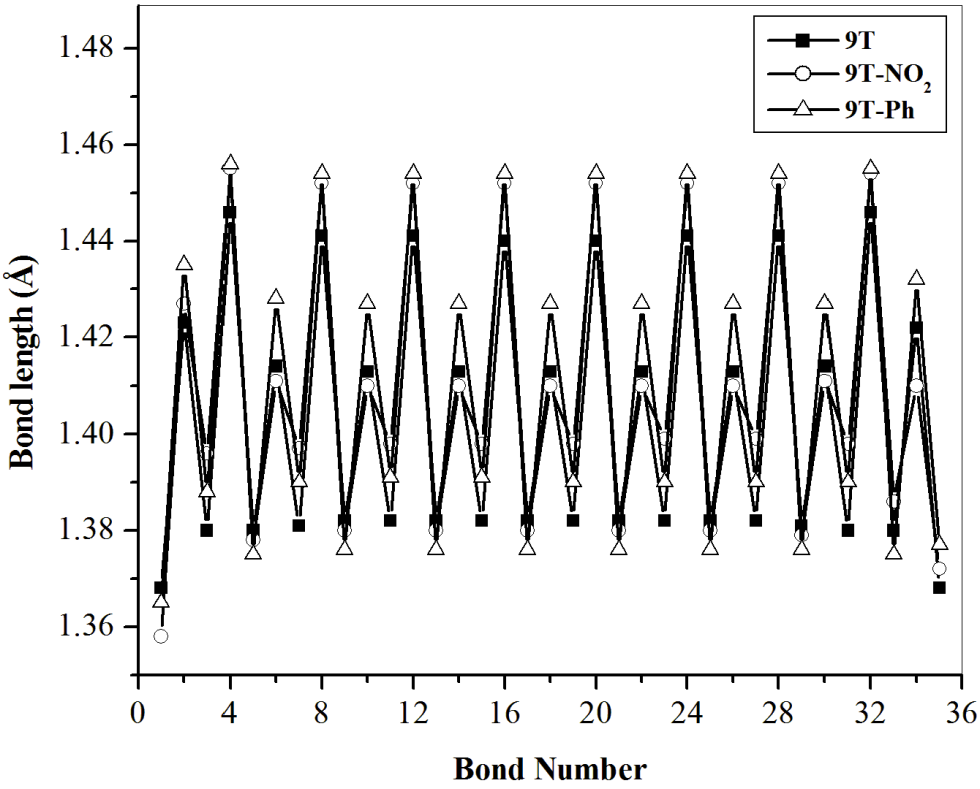

Figure 3.2. BLA patterns of oligothiophe substituted with electron withdrawing groups nitro and phenyl shown (9-monomer units) together with that of unsubstituted oligothiophene.

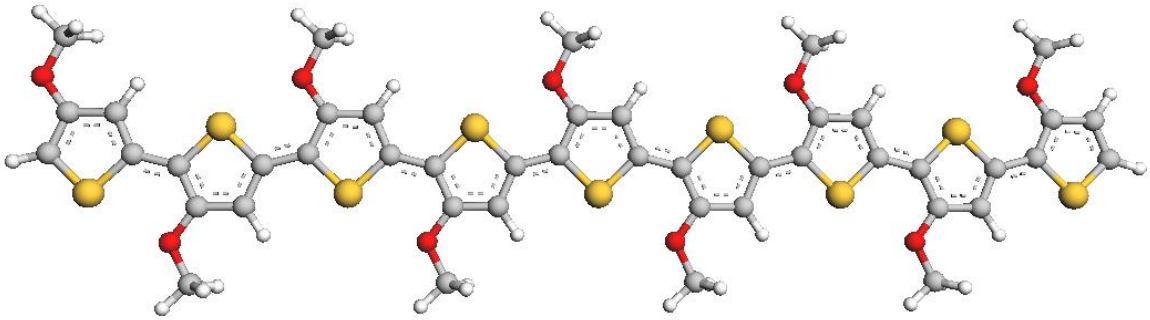

Figure 3.3. Geometry optimized structure of oligothiophene substituted with electron donating methoxy group. Note the quinoid behavior of the interconnecting bonds denoted by the dashed lines.

For example, alkoxy groups (methoxy and ethoxy) groups increase the electron density of the oligomer backbone by inductive and mesomeric effects thus resulting in the decrease of band gap. Methoxy and ethoxy substituted oligothiophenes shows similar band gaps and increasing the alkoxy side chain beyond methyl have not shown any further

significant decrease in band gap. The shorter inter-ring distances in methoxy substituted oligothiophenes are caused by higher contribution of the quinoid structure which prevent the molecule from twisting about the single bonds and thereby maintaining the planarity of the backbone. This in turn increases the double bond character of the inter-ring C–C bonds compared to that of the unsubstituted oligothiophenes which implies a higher conjugation in these substituted systems than in the corresponding oligothiophenes. On the other hand with the substitution of electron withdrawing groups like nitro and phenyl the inter ring bond distance is found to be more compared to that of unsubstituted oligothiophenes as shown in Figure 3.2. The inter bond distance of nitro substituted oligothiophenes is found to be 1.452 Å and phenyl substituted nT is 1.454 Å whereas it is 1.44 Å for the unsubstituted oligothiophenes.

The most important criteria for an oligomer to exhibit low band gaps is its planarity [27]. To understand more about how planarity of the backbone facilitate the low band gap oligomers, the energy changes associated with twist in dihedral angles are examined to find out the deviations from the planarity as it is an important factor for better conjugation. Oligomers or polymers which are found to be most stable in planar conformations show a lower band gap since planarity allows the delocalization of electrons throughout the molecule and enhances the conductivity. We have considered the dimer of unsubstituted, electron donating substituted and electron withdrawing substituted oligothiophene and plotted the energy changes associated with changes in the dihedral angle. The internal rotation is studied by scanning the inter-ring torsional angle in steps of 15^0 between 180^0 (anti-conformer) and 0^0 (syn conformer). The energies of various conformers are found with respect to the most stable form using the formula

Energy = Energy of the conformer (θ) - Energy of the most stable conformer

It is noted in the Figure 3.4 that for unsubstituted thiophene dimer and substituted dimers with methoxy, ethoxy and nitro, the most stable conformation is obtained at 180^0 with both the monomer units being anti towards each other and in the same plane. Since the planarity is retained upon substitution with these simple electron donating groups, planarity combined with conjugation effects results in the decrease of band gap. From Figure 3.4, it can be observed that methoxy, ethoxy and nitro substituted dimer assume the most stable form at 180^0 suggesting that the dimer would continue to be planar with band gaps almost remaining the same as unsubstituted thiophene oligomers. In the case of phenyl substituted

dimer the most stable conformation is obtained at around 42^0 which indicate that the dimer is twisted from the planarity which could be due to the steric repulsions arising from the bulky phenyl group.

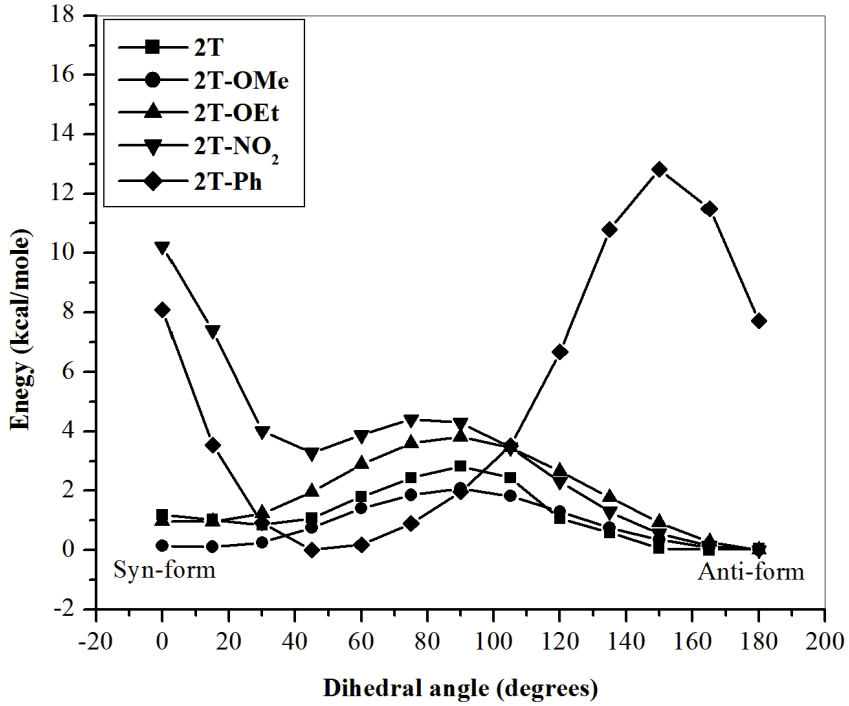

Figure 3.4. Energy changes associated with twist in the dihedral angle for unsubstituted thiophene dimer along with dimers substituted with methoxy, ethoxy, nitro and phenyl substituents.

Anti-conformation of phenyl substituted thiophene (at 180^0) dimer was destabilized by 7.7 kcal/mol from the stable form at 42^0. As a consequence of the loss in planarity and therefore conjugation, we see that phenyl substituted oligomers show higher band gaps. The study of twist in dihedral angle of the dimer gives us an excellent understanding to predict the geometry of higher oligomers. Taking both the substituted and unsubstituted 9-unit oligothiophene, we have calculated the dihedral angles of the oligomer unit which is found to be in very good agreement with the twisting studies performed on dimers. From Table 3.1, we find that the carbon backbone of unsubstituted oligomers and substituted oligomers with methoxy, ethoxy and nitro groups are in planar conformation whereas phenyl substituted oligomer deviates from the planarity with a dihedral angle of around $37^0 – 42^0$, which is in good agreement with the most stable conformation of dimer at an angle around 42^0. The non-planarity of the phenyl substituted oligothiophene can also be confirmed with its optimized geometry from Figure 3.5.

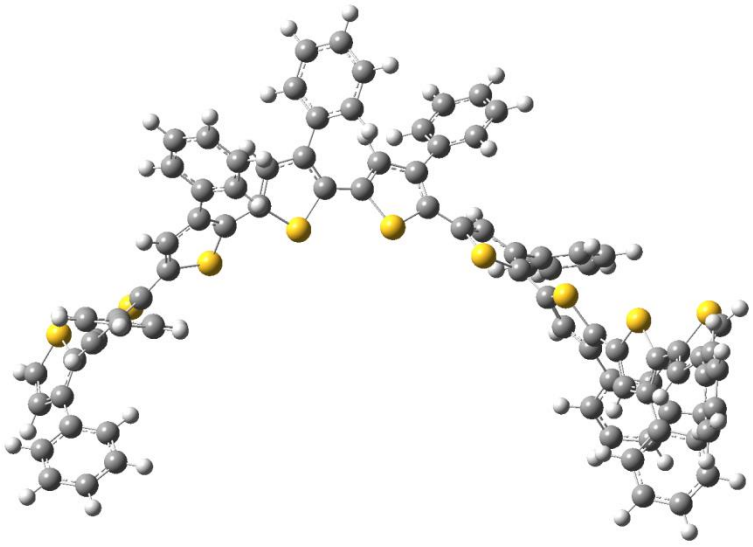

Figure 3.5. The optimized geometry of phenyl substituted oligothiophene 9-monomer

System	9T	9T-OMe	9T-NO_2	9T-Ph
1.D.A	179.99	180.00	179.99	42.45
2.D.A	179.99	179.99	179.99	39.05
3.D.A	179.99	180.00	179.99	37.32
4.D.A	179.99	179.99	179.99	37.72
5.D.A	179.99	179.99	179.99	38.67
6.D.A	179.99	179.99	179.99	39.56
7.D.A	179.99	179.99	179.99	38.62
8.D.A	179.97	179.99	179.98	38.41

Table 3.1. Dihdral angle (D.A) is calculated between two adjacent thiophene units of the 9-oligomer for unsubstituted and substituted systems in HT-HT form.

3.3. Electronic properties in substituted oligothiophenes

The evolution of electronic properties of α-oligothiophene systems upon substitution with various groups are also studied employing DFT. In particular the effects of electron donating groups like methoxy, ethoxy and electron withdrawing groups like nitro, cyano and phenyl on the electronic band gaps in the HT–HT regioregular forms are studied. In order to validate the current theoretical methodology to calculate the band gaps we have compared the band gaps of unsubstituted oligothiophenes (HOMO–LUMO gap) of different n (n = 2–9)

with the experimentally obtained results [28] for dimer and trimer. We find that the values obtained by DFT using B3LYP are very much close to the experimental values of these systems. These values are also matching with the existing computational values for unsubstituted oligothiophenes by Bendikov and Sharma [29] using the same methodology. Since it is evident that the same computational methodology to calculate the band gaps can be followed, investigations are carried out for the substituted head–tail oligothiophenes with various substituents and the results are summarized in Table 3.2.

No of monomer units	nT(eV)	nT-OMe or nT-OEt (eV)	nT-NO_2 (eV)	nT-Ph (eV)
2	4.23(4.12*)	3.88	3.68	4.31
3	3.44(3.44*)	3.09	3.18	3.70
4	3.03	2.65	2.89	3.39
5	2.78	2.36	2.71	3.29
6	2.62	2.16	2.59	3.13
7	2.50	2.01	2.49	3.06
8	2.41	1.90	2.43	3.02
9	2.35	1.80	2.38	2.98

Table 3.2. Band gaps of substituted oligothiophenes of various chain lengths (n corresponds to 2-9). Substituted oligothiophenes are designated as nT-R, where R is –OMe, -OEt, -NO_2 and -Ph. * The experimental band gap.

Among all the oligomeric systems studied, the system substituted with electron donating groups show the least band gap of about 1.8 eV for the 9 oligomeric system. The energy band gaps as a function of reciprocal of the number of monomeric units for various electron donating and electron withdrawing substituents are plotted in Figure 3.6.

We have also calculated the band gap of few monomers of electron withdrawing cyano substituted oligothiophenes. We have observed that the band gap of cyno substituted oligothiophenes follow the similar trend as the nitro substituted oligothiophenes. Their band gaps also lie above the band gap of corresponding unsubstituted oligothiophenes.

Oligothiophene backbone maintain the planarity on substitution of cyano group on each thiophene unit as in the nitro substituted oligothiophenes.

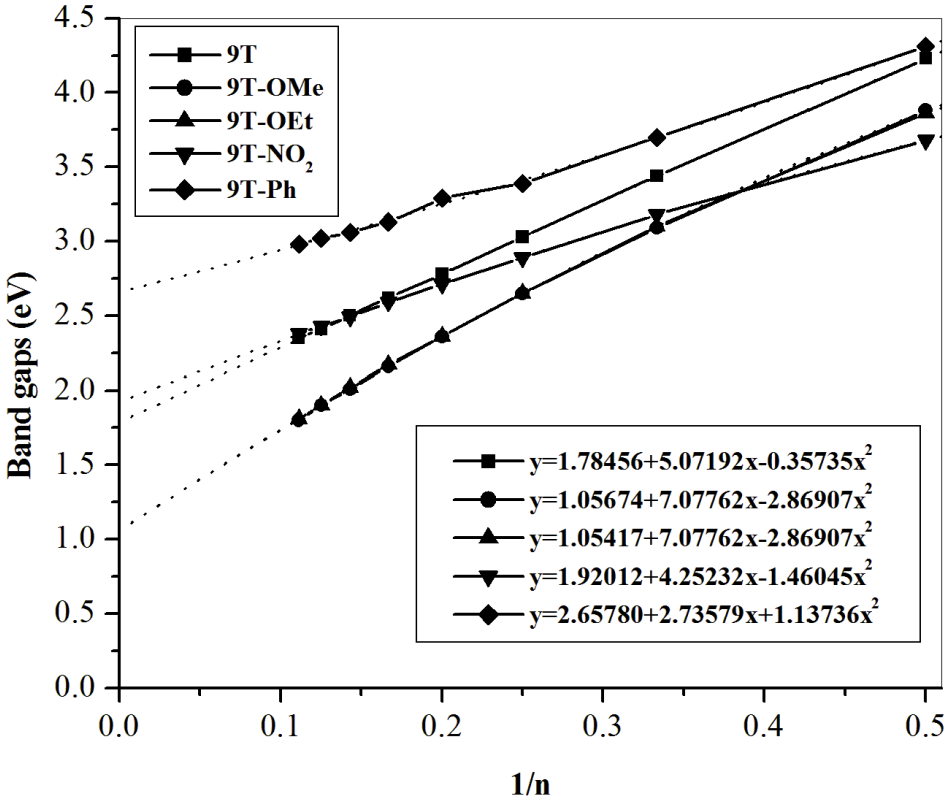

Figure 3.6. Calculated B3LYP/6-31G(d) HOMO-LUMO gaps versus the reciprocal of the number of oligomer units 1/n for unsubstituted and substituted oligomers from n=2 to n=9. The experimental band gap of polythiophene is 2.1 eV. Substituted oligothiophenes are designated as nT-R, where R is –OMe, -OEt, -NO_2 and -Ph. Calculated oligomeric polynomial scaling is given in the inset.

With the increasing chain length, the plotted band gap is found to linearly decrease and this can be attributed to the increase in conjugation and enhanced delocalization of electrons along the ring back bone as more monomeric units are added. Band gap is found to be lower for electron donating groups like methoxy and ethoxy groups compared to that of the unsubstituted system. Electron withdrawing groups found to show a different trend. For the nitro substituted oligomers the band gap is found to be slightly more than that of unsubstituted thiophene oligomers and similarly phenyl substituted systems shows an increase in band gap compared to that of unsubstituted oligothiophenes. This increase can be attributed to the loss of planarity and decreased π-conjugation along the chain backbone. Thus we can conclude that the loss of planarity is the main reason for oligomers to show a

higher band gap. In order to understand the trend further the frontier orbital energies are examined to see the changes with various substituents. The HOMO–LUMO energies are plotted as a function of number of monomers in Figure 3.7.

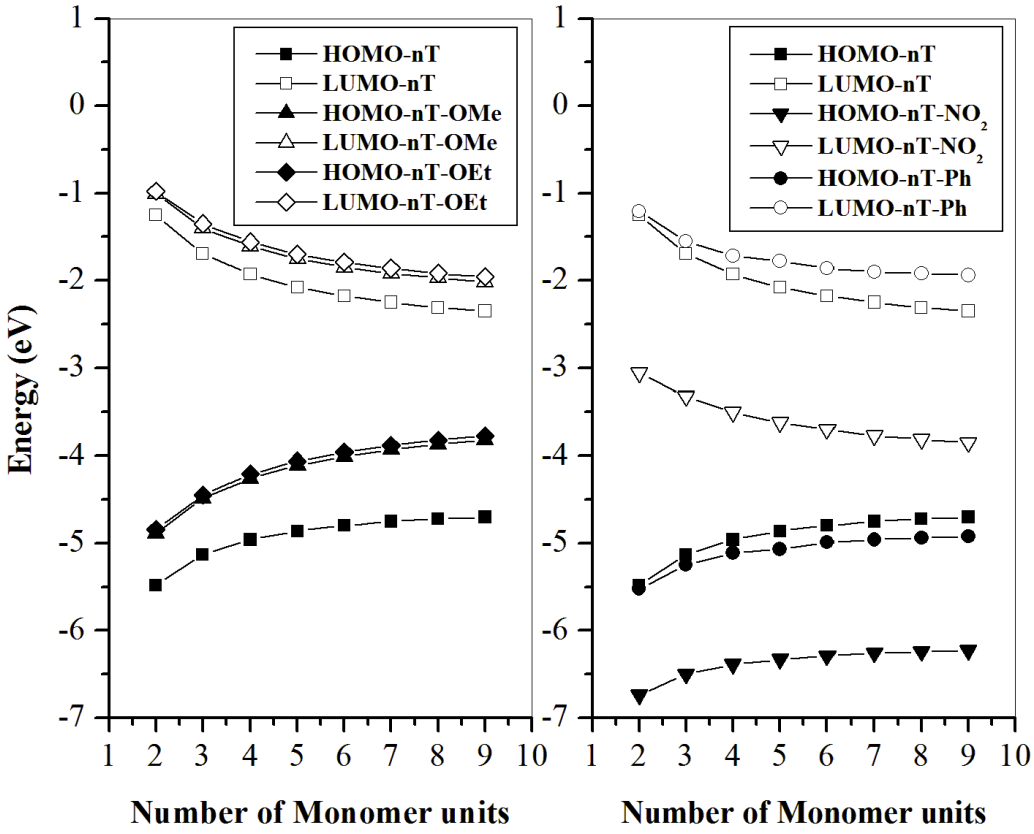

Figure 3.7. HOMO LUMO energy levels plotted for oligomers (2-9) for unsubstituted oligothiophenes and oligothiophenes substituted with electron donating groups (methoxy and ethoxy) and with electron withdrawing groups' nitro and phenyl. Substituted oligothiophenes are designated as nT-R, where R is –OMe, -OEt, -NO_2 and -Ph.

There is an increase in HOMO and LUMO energies observed for electron donating groups (methoxy and ethoxy) with respect to the unsubstituted oligothiophenes. Increase in HOMO energies are found to be more compared to that of increase in LUMO energies and thus there is a decrease in the band gap of oligothiophenes substituted with electron donating groups compared to that of the unsubstituted ones. The HOMO of the low band gap systems, 9T-OMe or 9T-OEt are having higher energies than that of the unsubstituted oligothiophenes indicating that these systems can be further doped. In the case of electron withdrawing substituents, HOMO and LUMO energies of nitro substituted thiophene is found to be lowest compared to that of unsubstituted oligothiophene. This could be an added advantage since

decrease in HOMO and LUMO levels improve air stabilities and abilities of electron injection compared to that of unsubstituted ones [30]. In the case of phenyl substituted nTs HOMO energy is found to be low and LUMO energy is found to be high compared to that of unsubstituted oligothiophene thus increasing the band gap. It is seen for oligomeric systems from n = 7, the HOMO of the oligothiophenes substituted with electron donating groups nT-OMe and nT-OEt and the LUMO of the electron withdrawing nT-NO2 are coinciding. This is an indication that these groups could be attached to the terminals of oligothiophenes to establish a push–pull effect [31] to enhance the charge transfer and delocalization properties so as to design better materials. The HOMO–LUMO energy gaps are represented in a different fashion for different substituents in Figure 3.8 to visualize the effect of various substituents.

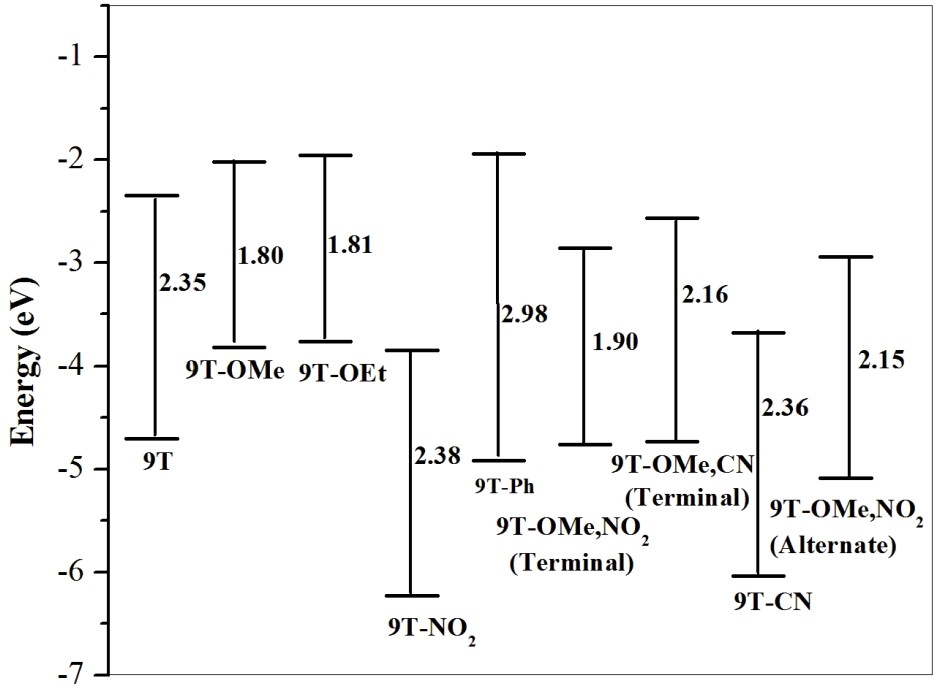

Figure 3.8. Comparison of the frontier orbital energies for 9T and substituted 9Ts. In the case of 9T-OMe, NO_2 and 9T-OMe, CN the substituent are only at the terminals to establish a push-pull effect. On all other cases, the substituents are present on all monomers. Note that the HOMO of 9T-OMe and 9T-OEt are coinciding with LUMO of 9T-NO_2. The band gaps are given in eV.

Even though the HOMO is much stabilized for the nT-NO_2 compared to all other systems, it has a band gap of 2.38 eV. When we study the push–pull effect with nitro or

cyano groups at one terminal and an electron donating group like methoxy at the other terminal, the energy gap appreciably decreases to 1.90 eV and to 2.16 eV respectively. HOMOs in these cases are more stabilized than in the case of 9T-OMe and 9T-OEt and are equally stabilized as an unsubstituted system. The values of these frontier energy levels are summarized for the 9T and also for the substituted systems in Table 3.3.

System	HOMO (eV)	LUMO (eV)	Band gap (eV)
9T	-4.70	-3.35	2.35
9T-OMe	-3.82	-2.02	1.80
9T-OEt	-3.77	-1.96	1.81
9T-NO_2	-6.23	-3.85	2.38
9T-Ph	-4.92	-1.94	2.98
9T-OMe, NO_2 (t)	-4.76	-2.86	1.90
9T-OMe, CN (t)	-4.73	-2.57	2.16
9T-CN	-6.04	-3.68	2.36
9T-OMe, NO_2(a)	-5.09	-3.68	2.15

Table 3.3. HOMO, LUMO energies and band gaps of various substituted and unsubstituted 9-oligomers. 9T-OMe, NO_2 and 9T-OMe, CN represent 9T substituted only at the terminals by –OMe, NO_2 and –OMe,CN. (t) Denotes the substituents are attached at the terminal edges of the oligomer (a) indicates two substituents are linked to thiophene units in alternate way in HT-HT form.

This includes the push–pull systems studied with terminal -OMe with -NO_2 and with -CN and a system with alternate electron donating (-OMe) and withdrawing groups (NO_2). To understand the effect of increasing chain length, we have also investigated the dependence of band gap on the chain length for the case with electron donating groups in the HT–HT form. The evolution of the decrease in band gap with the increase in the number of monomers is plotted in Figure 3.9.

For 9T-OMe, the band gap is at 1.80 eV but it decreases as ‘n’ increases and as it reaches n = 15 it shows considerable decrease with a value of 1.52 eV. The decreased energy

gap between HOMO and LUMO is an indicator of the increase in π-conjugation of the backbone as more monomeric units are added.

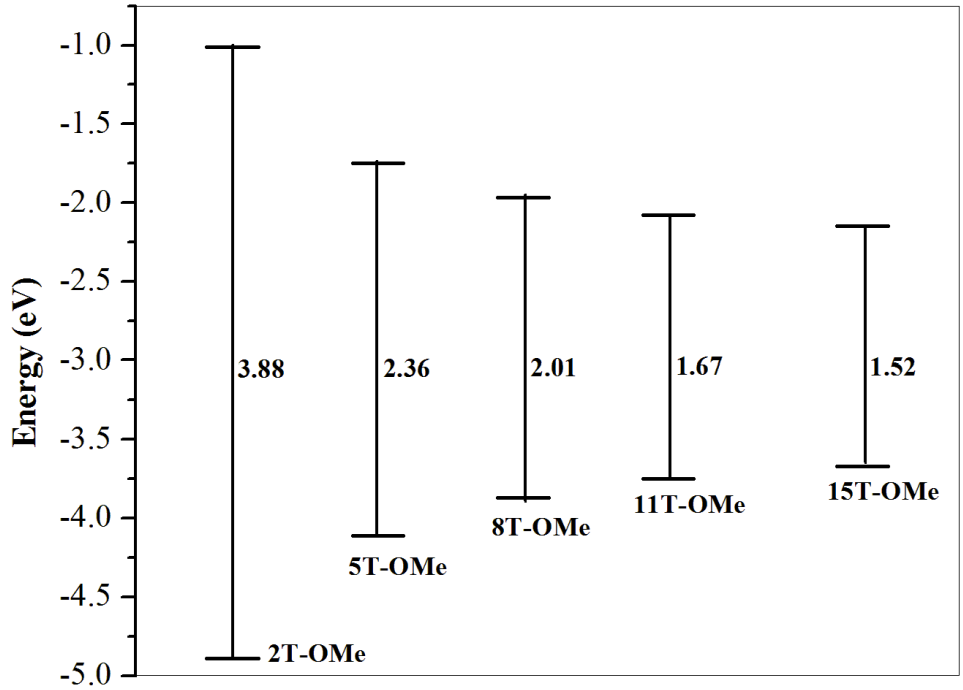

Figure 3.9. Evolution of the band gap (in eV) of methoxy substituted oligothiophenes with various chain lengths till n=15.

The values corresponding to n = 13 and 14 are 1.58 and 1.54 respectively showing that the decrease is less prominent as chain length is increased indicating that there is an ‘‘effective conjugation length’’ for the oligomer above which there may not be any further decrease in band gap. It is also interesting to note that the band gaps in some of the substituted oligomeric systems are considerably lower than the experimental band gap of polythiophene which is approximately 2.1 eV [32-34] which indicates that the oligo systems can be better materials than the corresponding polymers. The effective conjugation length for these oligomeric systems can be calculated from linear regression analysis. However this calculation can only be done for isolated chains without considering any intermolecular effects and with no disorder in the π-conjugated system. This can also be thought of as the maximum length in terms of monomer number up to which the backbone may remain planar. It is noted that the inverse relationship of 1/n represented in Figure 3.6 holds for oligomers because the length of the π-conjugated system and the number of electrons simultaneously increase as more monomer units are added. As noted by previous investigators [35,36], a simple extrapolation from oligomeric gaps, the band gap of the corresponding polymers

cannot be predicted. The extrapolated values from Figure 3.6 and the values calculated for the infinite system using DFT periodic boundary condition (DFT-PBC) for the polymeric systems are listed in Table 3.4.

System	Band gap (DFT-PBC) (eV)	Band gap (Extrapolation) (eV)
PT-unsubstituted	2.05(~2.1*)	1.78
PT-MeO	1.74	1.05
PT-EtO	1.76	1.05
PT-NO2	2.33	1.92
PT-Ph	2.11	2.65

Table 3.4. Band gaps calculated from PBC conditions and also by extrapolation from band gaps of oligomers. * denotes experimental band gap for polythiophene**.**

It can be observed that the band gaps predicted from extrapolation of oligomers will not give the accurate band gaps for the infinite polymeric systems. Band gaps obtained from extrapolation underestimates the exact band gap of the polymers leading to erroneous conclusions. In case of unsubstituted polythiophene band gap obtained from the extrapolated graph of 1.78 eV is far less than the experimentally obtained band gap of 2.1 eV whereas band gaps obtained from PBC calculation are closer to the experimental band gaps. In case of electron donating groups the band gap was found to decrease to 1.74–1.76 eV for alkoxy groups from the PBC study whereas extrapolated band gaps suggest a value of 1.05 eV. With electron withdrawing groups, nitro and phenyl substituted polythiophenes the band gaps are found to be 2.33, 2.11 eV and extrapolated band gaps gives a band gap of 1.92 and 2.65 eV. Overall the band gaps obtained from extrapolated values of oligomers seems to underestimate the band gaps of polymeric system, except for the phenyl substituted system.

It is seen that there is very good agreement with the experimental band gap of the unsubstituted polythiophene and the calculated value with PBC-DFT. For the unsubstituted polythiophene, there is some agreement in band gap of 15T (2.18 eV) with that of the experimental and PBC values. The extrapolated values are however very much different. Similarly for PT-OMe we have 1.74 calculated from the PBC and extrapolated values of the oligomer are only 1.05 eV and that of 15T-OMe is 1.52 eV. The empirically extrapolated

values of calculations with oligo systems does not hold good for infinite polymer chains since it does not accurately describe the asymptotic behavior. Thus the extrapolated band gaps for the substituted oligomeric systems may not describe the electronic properties of the polymeric systems. This can be understood as resulting from the increased degree of freedom and therefore the conformational entropy and also the increased flexibility as the chain length is increased which may need additional calculations to establish. It should therefore be noted that electronic properties of oligomeric systems are very much different from that of the corresponding polymers mainly owing to less conformational entropy of the oligomer.

In order to understand the charge distribution in various oligomeric systems the electrostatic potential mapped (ESP) surfaces are also investigated. It correlates with dipole moment, electronegativity, partial charges and site of chemical reactivity of the molecule and provides a visual method to understand the relative polarity of a molecule. While the negative electrostatic potential corresponds to an attraction of the proton by the concentrated electron density in the molecule (colored in shades of red in the ESP surface) the positive electrostatic potential corresponds to repulsion of the proton by atomic nuclei in regions where the electron density is low and the nuclear charge is incompletely shielded (in shades of blue). The electrostatic potential at different points on the electron density isosurface is shown by coloring the isosurface with contours. The electron density isosurface on which the electrostatic potential has been mapped for various substituted oligothiophenes are shown in Figure 3.10. The electron density on each thiophene unit of unsubstututed oligothiophene, in Figure 3.10(d), from the electro static mapped potential surface of push-pull oligothiophene molecule, we can conclude that the electron flow takes place from electron donating methoxy group to the electron withdrawing nitro group. This kind of push-pull molecules would be useful in the application of solar cell and non-linear optics.

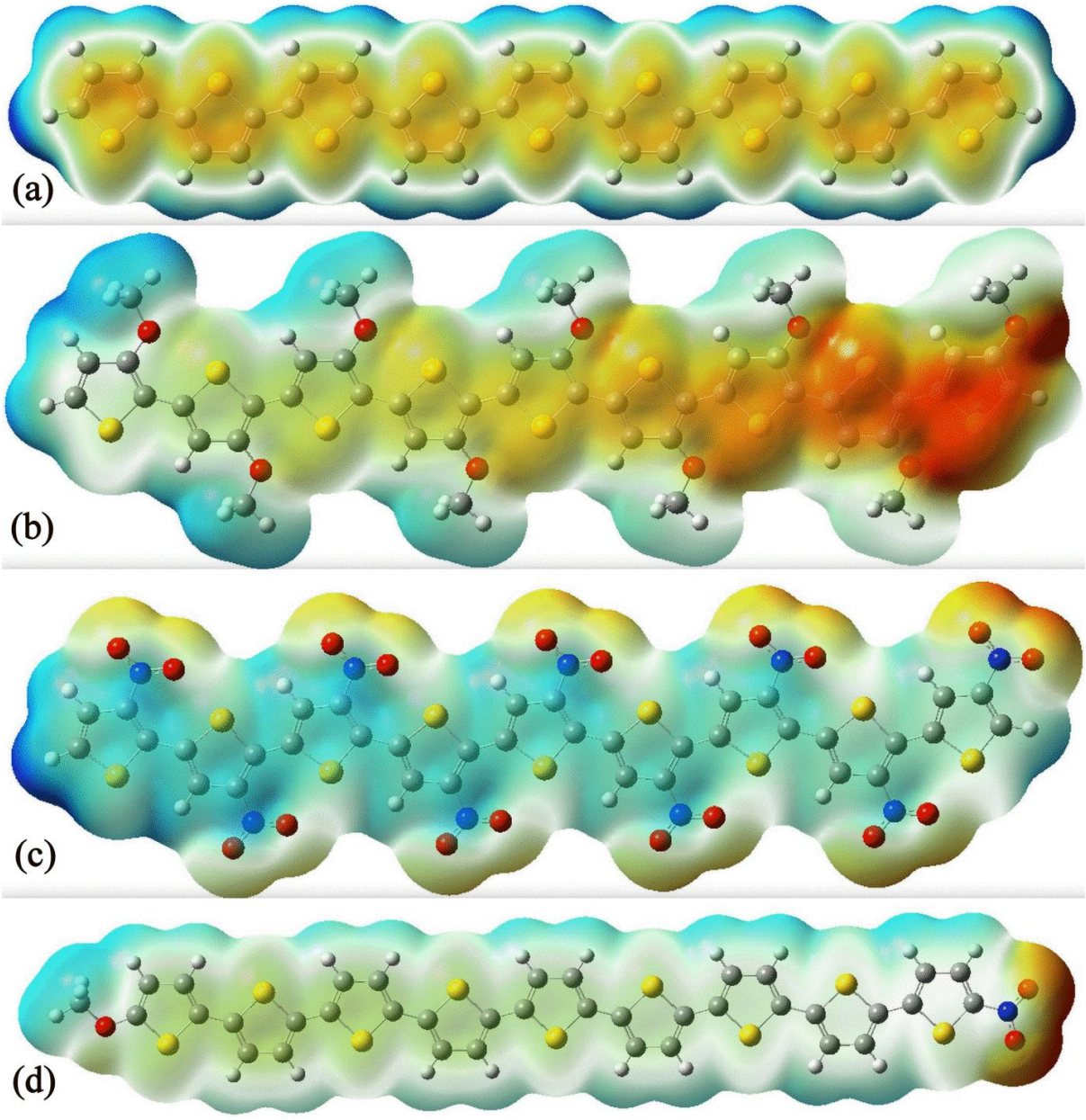

Figure 3.10. ESP mapped surfaces of (a) 9-Thiophene (b) 9T-OMe(HT-HT) (c) 9T-NO_2(HT-HT) and terminal substituted (d) 9T-OMe-NO_2(t).

In our case it is interesting to see that this is induced as a result of lack of symmetry in the HT–HT forms. This effect of concentration of charge density to the side of the chain vanishes as the symmetry is introduced. This effect is also visualized in the frontier Kohn–Sham molecular orbitals shown in Figure 3.11. It is clear that the HOMO is more localized on the rings on one side than the other and the LUMO is concentrated near the region where there is electron deficiency.

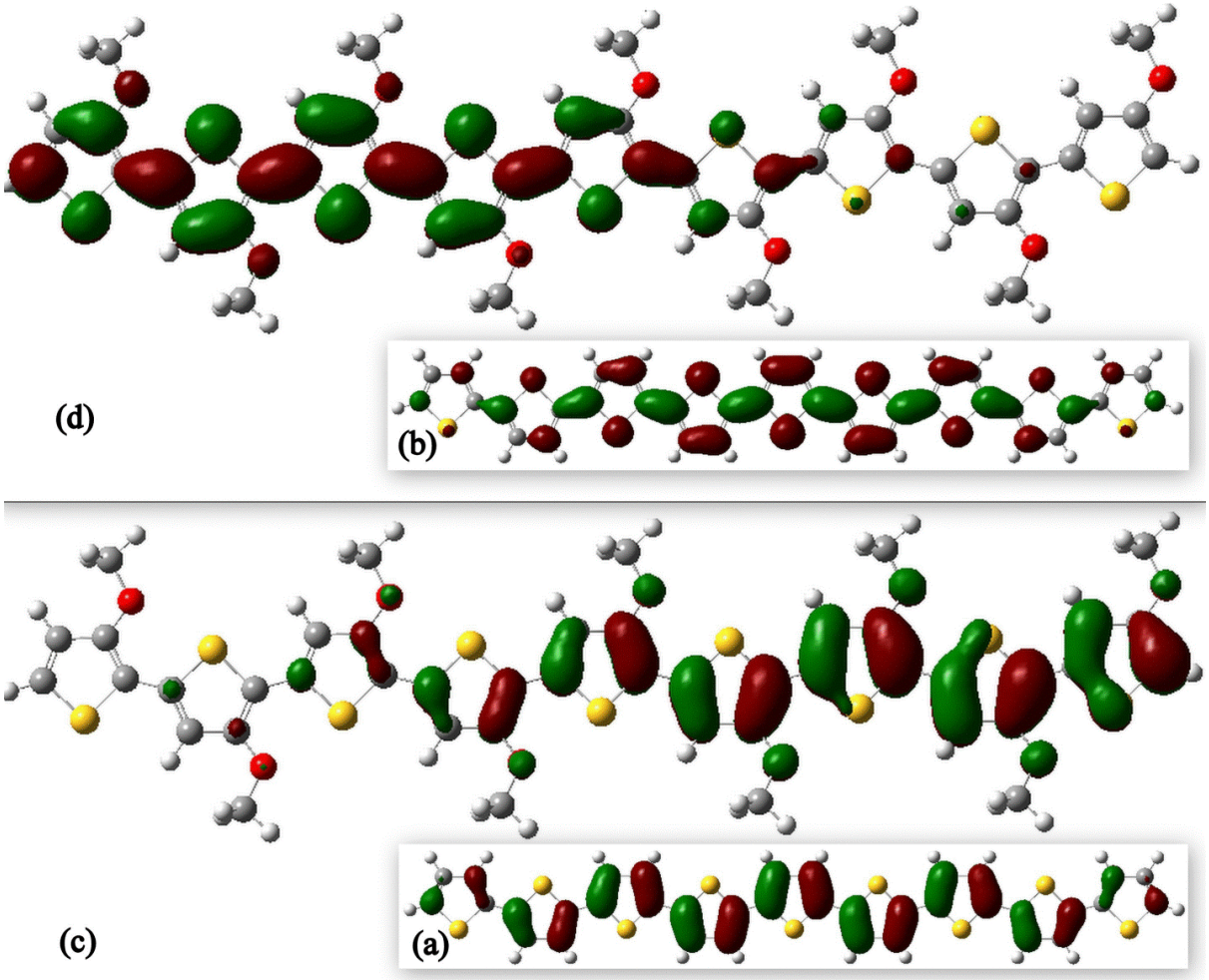

Figure 3.11. Frontier orbitals of methoxy substituted 9Ts. To compare the corresponding orbitals for the unsubstituted 9Ts, HOMO (a) and LUMO (b), are kept in the inset. (c) and (d) are the HOMO and LUMO of the methoxy substituted oligothiophene.

Therefore the most intense transition (HOMO-LUMO) can be attributed to charge transfer. It is interesting to note that a recent experimental investigation by Campos and co-workers [37] on the impact of molecular symmetry on single molecule conductance also corroborate this observation. They have found that reduced symmetry of bithiophene restricts the inter-ring torsion rotations when confined in a junction. As like the electron donating methoxy substituted oligothiophene, HOMO of nitro substituted oligothiophene is also concentrated on the ring and LUMO is concentrated near the electron deficient region, as shown in Figure 3.12.

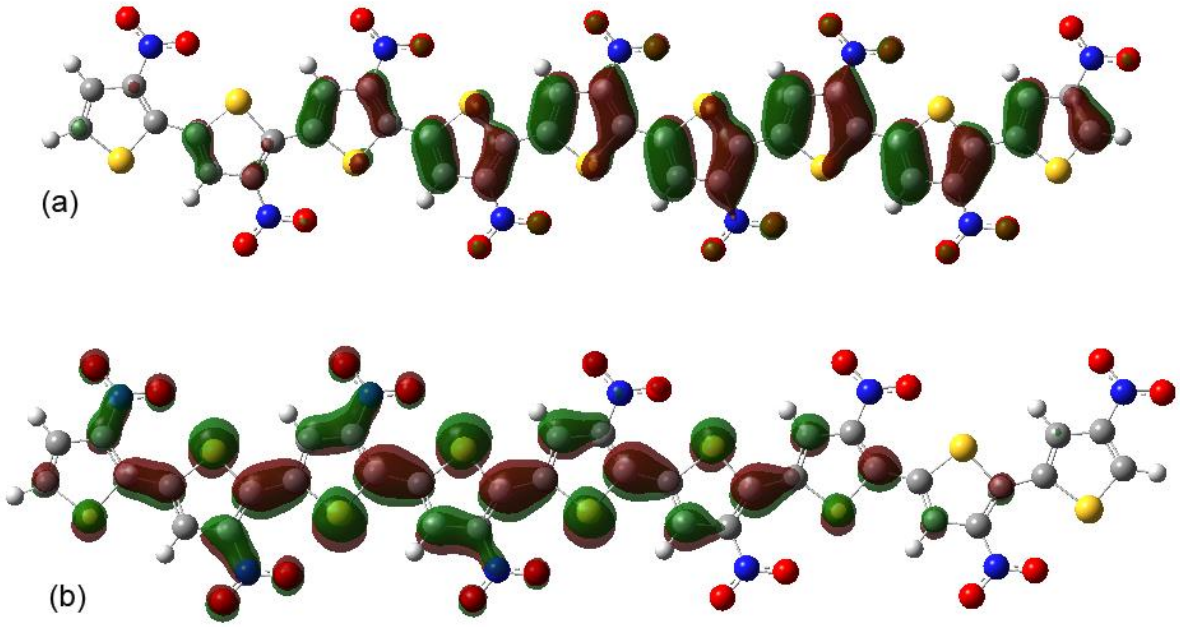

Figure 3.12. Frontier orbitals of nitro substituted 9-oligothiophene, HOMO (a) and LUMO (b).

We have also calculated the density of states (DOS) which again reflects the same band gaps calculated from the frontier orbitals. DOS plots for oligothiophenes and for substituted with electron donating and electron withdrawing groups (9-mer units) are given in Figures 3.13 and 3.14. The decrease in band gap from 2.35 eV to 1.80 eV when substituted with methoxy or ethoxy groups can be seen clearly from these plots. When substituted with electron withdrawing groups for example nitro substituted 9T, we observe a slight increase in band gap of 2.38 eV, whereas with phenyl substituted 9T have shown an increase of band gap of 2.98 eV.

3.4. Conclusions

The effects of electron donating and withdrawing substituents on the electronic structure of oligothiophenes in the regio regular HT–HT form are studied. Appreciable difference in the delocalization pattern is observed between unsubstituted and substituted oligothiophenes depending on the substitution pattern and also the nature of substituent. We observed that the lack of symmetry in the oligomeric configuration plays an important role in deciding the electronic band gaps. For the 3-substitued systems electron donating and electron withdrawing substituents are shown to decrease and increase electronic band gaps respectively compared to that of unsubstituted systems. There are interesting charge

separation effects introduced as a result of lack of symmetry in some of the substituted oligothiophenes.

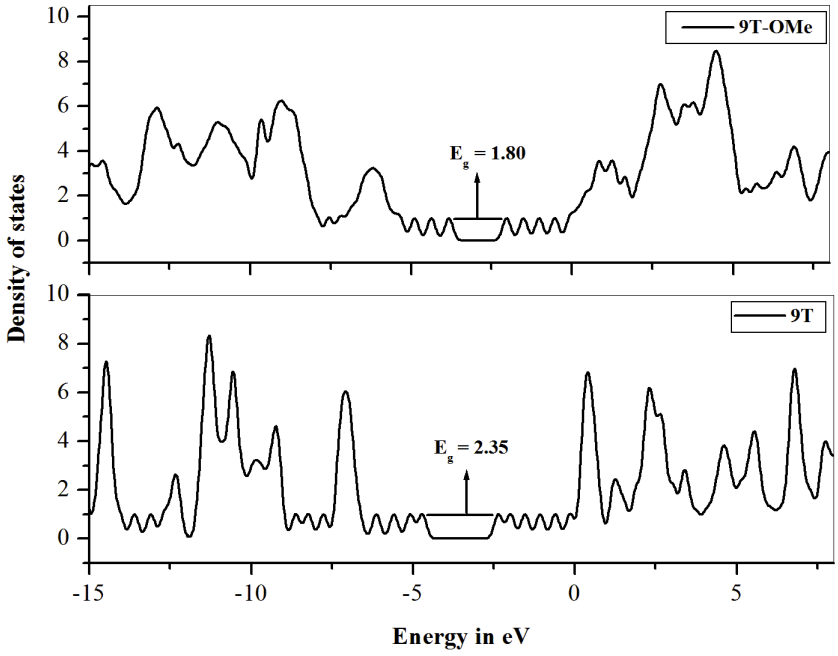

Figure 3.13. Density of states for unsubstituted oligothiophene (9T) and methoxy substituted thiophene (9T-OMe).

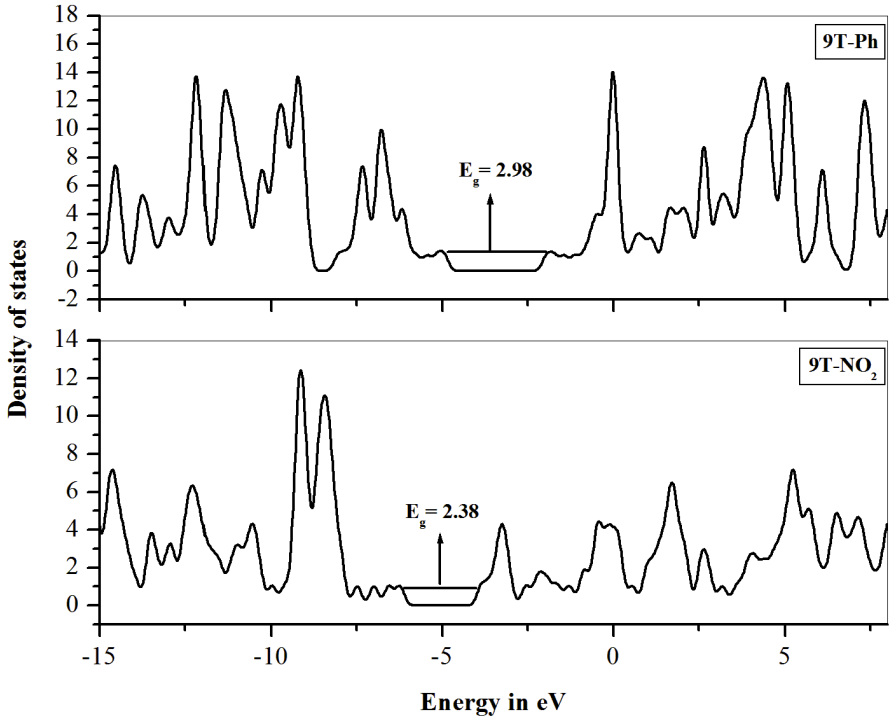

Figure 3.14. Density of states for substituted thiophenes with nitro (9T-NO_2) and Phenyl (9T-Ph).

Oligomers with low band gaps are found to retain the planarity whereas the higher band gap oligomers are found to deviate from planarity. HT–HT oligothiophene substituted with electron donating groups are found to show interesting delocalization effects and lead to lower band gaps than the regular conjugated oligomers with terminal donor–acceptor substituents showing the push–pull effect ESPs also provide insights of charge transfer attained in HT–HT forms than in donor–oligomer–acceptor architecture. The band gap of simple conjugated organic oligomers can be tuned by modifying the nature of the substituent. Oligothiophenes with electron donating substituents can be better materials with lower electronic band gaps than the corresponding substituted polythiophene. Theoretical procedure and strategy to predict the energy gap of new substituted oligothiophenes giving importance to the molecular symmetry is an important step for the better design of the material structure.

3.5. References

[1] G. Barbarella, M. Zambianchi, L. Antolini, P. Ostoja, P. Maccagnani, A. Bongini, E. A. Marsegila, E. Tedsco, G. Gigli, R. Cingolani, J. Am. Chem. Soc., 1999, 121, 8920.

[2] N. Koumura, Z-S. Wang, S. Mori, M. Miyashita, E. Suzuki, K. Hara, J. Am. Chem. Soc., 2006, 128, 14256.

[3] N. Koumura, Z-S. Wang, M. Miyashita, Y. Uemura, H. Sekiguchi, Y. Cui, A. Mori, S. Mori, K. Hara, J. Mater. Chem., 2009, 19, 4829.

[4] Q. Feng, Q. Zhang, X. Lu, H. Wong, G. Zhou, Z-S. Wang, ACS Appl. Mater. Interfaces, 2013, 5, 8982.

[5] C. Koenigsmann, T. S. Ripolles, B. J. Brennan, C. F. A. Negre, M. Koepf, A. C. Durell, R. L. Milot, J. A. Torre, R. H. Crabtree, V. S. Batista, G. W. Brudvig, J. Bisquert, C. A. Schmuttenmaer, Phys. Chem. Chem. Phys., 2014, 16, 16629.

[6] M. Zambianchi, A. Barberi, A. Ventola, L. Favaretto, C. Bettini, M. Galeotti, G. Barbarella, Bioconjugate Chem., 2007, 18, 1004.

[7] E. Fabiano, F. D. Sala, G. Barbarella, S. Lattante, M. Anni, G. Sotgiu, C Hättig, R. Cingolani, G. Gigli, J. Phys. Chem. B, 2006, 111, 18651.

[8] M. Piacenza, M. Zambianchi, G. barbarella, G. Gigli, F. D. Sala, Phys. Chem. Chem. Phys., 2008, 10, 5363.

[9] G. Barbarella, M. Zambianchi, A. Ventola, E. Fabiano, F. D. Sala, G. Gigli, M. Anni, A. Bolognesi, L. Polito, M. Naldi, M. Capobianco, Bioconjugate Chem., 2066, 17, 58.

[10] K. Magnusson, H. Appelqvist, A. Cieślar-Pobuda, M. Bäck, B. Kågedal, J. A.Jonasson, M. J. Los, K. P. R. Nilsson, Front. Chem., 2015, 3, 1.

[11] T. Taka, Synth. Met., 1991, 41, 1177.

[12] I. F. Perepichka (Editor), D. F. Perepichka, *Handbook of Thiophene-Based Materials: Applications in Organic Electronics and Photonics*, Volume 2, 2009.

[13] J. Pei, W. L. Yu, W. Huang, A. J. Heeger, Macromolecules, 2003, 33, 2462.

[14] J. Roncali, Acc. Chem. Res., 2000, 33, 147.

[15] J. Roncali, Chem. Rev. 1997, 97, 173; J. M. Tour, Chem. Rev., 1996, 96, 537.

[16] M. G. Vivas, S. L. Nogueira, H. S. Silva, N. M. B. Neto, A. Marletta, F. Serein-Spirau, S. Lois, T. Jarrosson, L. De Boni, R. A. Silva, C. R. Mendonca, J. Phys. Chem. B, 2011, 115, 12687.

[17] K. P. R. Nilsson, P. Hammarström, F. Ahlgren, A. Herland, E. A. Schnell, M. Lindgren, G. T. Westermark, O. Inganäs, ChemBiochem, 2006, 7, 1096.

[18] T. Klingstedt, C. Blechschmidt, A. Nogalska, S. Prokop, B. Häggqvist, O. Danielsson, W. K. Engel, V. Askanas, F. L. Heppner, K. P. R. Nilsson, ChemBioChem, 2013, 14, 607.

[19] B. G. Johansson, R. Simon, G. Bergström, M. Eriksson, S. Prokop, C-F. Mandenius, F. L. Heppner, A. K. O. Åslund, K. P. R. Nilsson, Biosens. Bioelectron., 63, 2015, 204.

[20] S. Radhakrishnan, R. Parthasarathi, V. Subramanian, N. Somanathan, Compos. Mater. Sci., 2006, 37, 318.

[21] G.-L. Zhang, H. Zhang, D-P. Li, D. Chen, X-Y. Yu, B. Liu, Z-S. Li, Theor. Chem. Acc., 121, 109.

[22] G. R. Hutchison, M. A. Ratner, T. J. Marks, J. Am. Chem. Soc., 2005, 109, 3126.

[23] J. Casanovas, D. Zanuy, C. Alemán, Polymer, 2005, 46, 9452.

[24] A. Karpfen, M. Kertesz, J. Phys. Chem., 1991, 95, 7680.

[25] G. F. Musso, G. Dellepiane, C. Cuniberti, M. Rui, A. Borghesi, Synth. Met., 1995, 72, 209.

[26] J. L Bredas, J. Cornil, D. Beljonne, D. D. Santos, Z. G. Shuai, Acc. Chem. Res., 32, 1999, 267.

[27] N. Somanathan, S. Radhakrishnan, Int. J. Mod. Phys. B, 2005, 19, 4645.

[28] A. Diaz, J. Crowley, J. Bargon, G.P. Gardini, J.B. Torrance, J. Electroanal. Chem., 1981, 121, 355.

[29] S. Sharma, M. Bendikov, Chem. Eur. J., 2013, 19, 13127.

[30] Y. A. Duan, Y. Geng, H.B. Li, X.D. Tang, J. L. Jin, Z.M. Su, Org. Electron., 2012, 13,

1213.

[31] H. Meier, Angew. Chem. Int. Ed., 2005, 44, 2482.

[32] G. Tourillon, F. Garnier, J. Electroanal. Chem., 1982 135, 173.

[33] G. Tourillon, F. Garnier, J. Electroanal. Chem., 1984, 161, 404.

[34] M. Kobayashi, N. Colaneri, M. Boysel, F. Wudl, A. J. Heeger, J. Chem. Phys., 1985, 82, 5717.

[35] U. Salzner, J.B. Lagowski, P.G. Pickup, R.A. Poirier, Synth. Met., 1998, 96, 177.

[36] G. R. Hutchison, Y. J. Zhao, B. Delley, A. J. Freeman, M. A. Ratner, T. Marks, J. Phys. Rev. B, 2003, 68, 035204.

[37] E. J. Dell, B. Capozzi, K. H. DuBay, T. C. Berkelbach, J. R. Moreno, D. R. Reichman, L. Venkataraman, L. M. Campos, J. Am. Chem. Soc., 2013 135, 11724.

Chapter 4

Electronic properties of substituted polythiophenes: A PBC-DFT study

4.1. Introduction

Conjugated polymers are considered as one of the most promising organic semiconductors due to their potential applications in optoelectronics [1-3]. Organic conjugated polymers are widely used in many areas like ranging from conducting fabrics [4], antistatic coatings for use in photographic films [5], electronic device fabrication [6,7] and low voltage electrochromic windows [8,9] to the organic light emitting diodes [10], photodiodes and photovoltaic devices [11. Conjugated polymers play a vital role in the biological applications due to their charge transporting [12] and optical properties [9,13]. Moreover these polymers are strong contenders in biological applications such as softness to easy blending with tissues/organs [14], self-assembly [15] in biomimetics and air stability and solubility in common solvents for facile manufacturing [16].

Among the conjugated polymers, polythiophenes play leading role in organic electronics due to their stability and ease of synthesis [17-19]. They are one among the polymers widely used in these applications due to their tunable optical properties and electrical conductivity [20,21]. Polymer molecules have the advantages over small molecules such as high viscosity, higher boiling points and high mechanical strengths [22]. Polythiophenes can be synthesized in three different processes, such as electropolymerization, metal-coupling reactions, and chemical oxidative polymerization [23]. By substitution with various groups, polythiophenes show further improvement in their solubility and processability. Such substitutions can be classified as regio-regular and regio-irregular. Polymers containing only head-tail couplings are considered as regio-regular and those polymers which contain a mixture of all possible couplings, are denoted as regio-irregular polymers. Substitution on polythiophenes has received the attention of researchers due to their variety of applications in field effect transistors, light-emitting diodes and solar cells, biosensors [1-3,11] etc.

In this chapter, the systematic study of the effect of various substituents on band gaps of polythiophenes in head-tail - head-tail (HT-HT) and head-head - tail-tail (HH-TT) forms with a focus to predict low band gap polythiophenes. The intrinsic optical properties of

materials are decided by the band gap and therefore it is essential to investigate the band gap as a function of the chemical structure of the polymer.

The effect of substituents on the electronic properties of polythiophenes is investigated employing periodic boundary condition (PBC) with density functional theory calculations. We have used one of the most successful functional, namely B3LYP hybrid functional and 6-31G(d) for electronic structure calculations of substituted polythiophenes. All these calculations are performed in gas phase using Gaussian 09 suite of program. The band structure studies are performed with 100K points in the first Brillouin zone. We have considered substituents like alkyl groups, halogens, aromatic groups and alkoxy groups shown in Scheme 4.1.

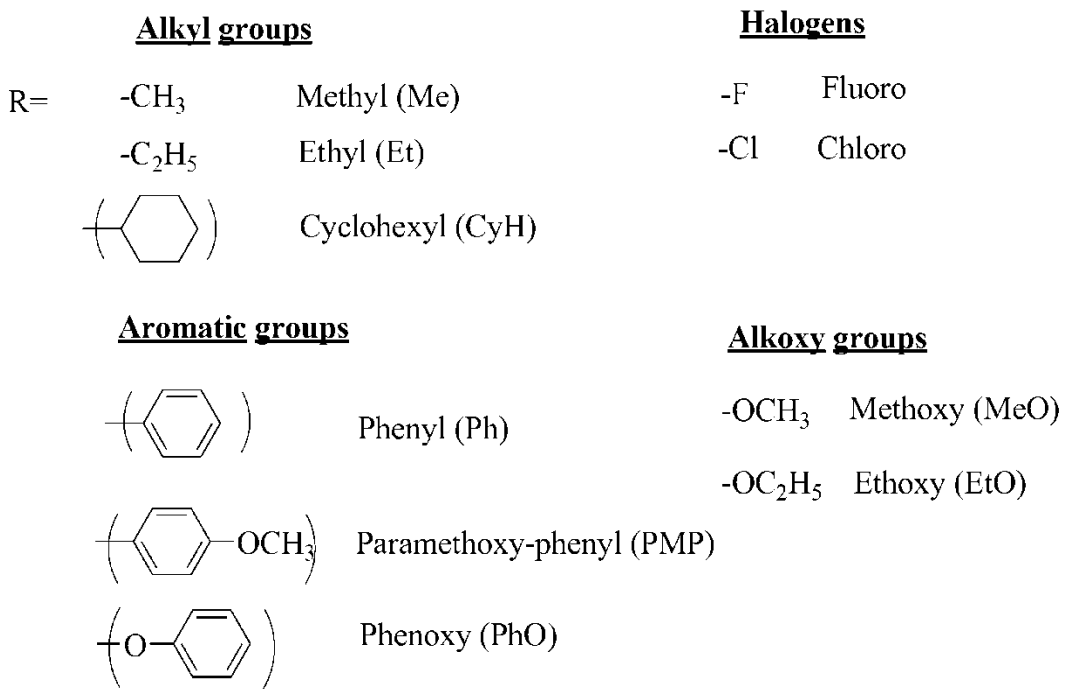

Scheme 4.1. Various substituents alkyl, halo, aromatic and alkoxy groups considered for DFT-PBC calculations.

We have considered the substituted thiophene dimer in head-tail and head-head forms and applied periodic boundary condition in one dimension to study infinite system. Polythiophenes are substituted with various groups shown in Scheme 4.1 and the band structure calculations are performed in order to understand the band gap changes upon substitution. Electronic band gaps for the polymer and the deviation in dihedral angles are observed in the dimeric system in the unit cell are tabulated. Deviation in dihedral angle (DDA) is calculated for the dimeric units by the formula, DDA =180^{o}- (dihedral angle

between two sulphur atoms of adjacent thiophene units). The stability of HH-TT form is also calculated with respect to HT-HT form using the following expression,

Stability in terms of energy (ΔE) = (Energy of HH-TT form) – (Energy of HT-HT form) with ΔE positive indicating that HT-HT form is more stable while a negative value indicates a more stable HH-TT form of the polymer.

Band structure plots for unsubstituted polythiophene with few of the highest occupied crystalline orbitals (HOCO) and lowest unoccupied crystalline orbitals (LUCO) energies are plotted in Figure 4.1. The band gap is found to be 2.04 eV for polythiophene which is in good agreement with experimental band gap of ~2.1 eV [24-26]. The HOCO and LUCO energy states in polythiophene are stabilized by about 1 eV when compared to the corresponding oligomeric systems [27].

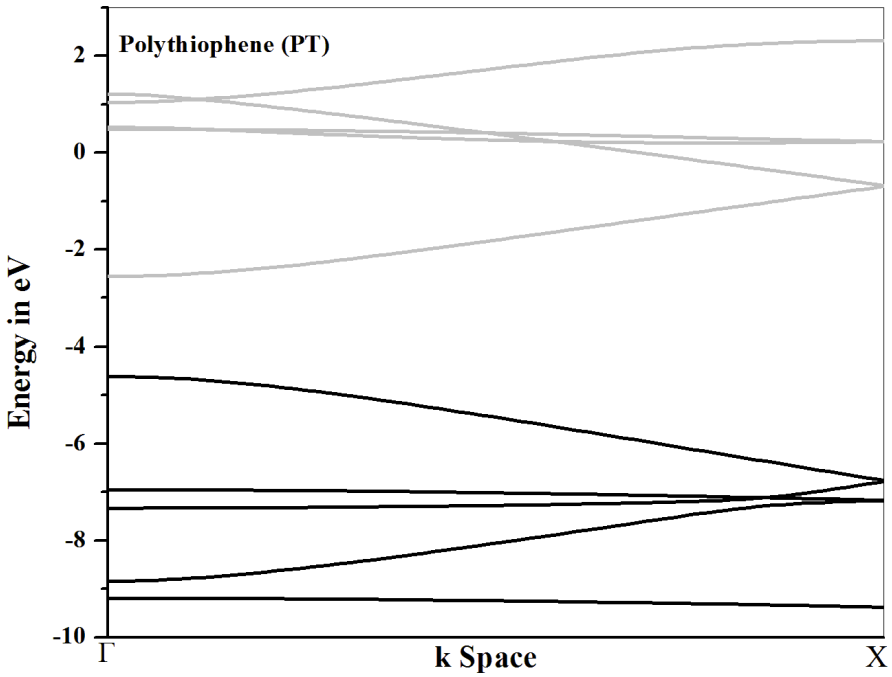

Figure 4.1. Band structure of unsubstituted polythiophene. Black lines represent the crystalline orbitals in valence band region and the gray lines indicate the crystalline orbitals in conduction band.

4.2. Substitution with alkyl Groups

Various alkyl groups like methyl, ethyl, and cyclohexyl are substituted in HT-HT form and HH-TT form and their stability, dihedral angles and band gaps are given in Table 4.1.

System	Band gap HT-HT (eV)	DDA HT-HT	Band gap HH-TT (eV)	DDA HH-TT	Stability* (kcal/mole)
Me-PT	1.99	0.21	2.02	0.03	5.5
Et-PT	2.15	16.61	1.97	0.02	2.07
CyH-PT	2.05	0.41	2.67	40.03	-4.35

Table 4.1. Band gaps, deviation in dihedral angles (DDA) of various alkyl substituted polythiophenes in HT-HT form and HH-TT form. *****Indicates stability of HH-TT form with respect to the corresponding HT-HT form.

In the case of methyl substitution, both HT-HT form and HH-TT form have shown similar band gaps and the dimers show almost the same structural properties with similar dihedral angles. An HT-HT form of methyl substituted polythiophene is slightly more stable compared to that of corresponding HH-TT form. Slight decrease in the band gap of methyl substituted polythiophene is observed compared to the unsubstituted polythiophene. This is due to electron releasing nature methyl group which increases the conjugation on polymer backbone by positive inductive effect. In the case of ethyl substituted polythiophene, HT-HT form is found to have a band gap of 2.15 eV more than that of polythiophene. This slight increase is attributed to the loss in planarity with deviation in dihedral angle of 16.79º. In HH-TT form, the dimeric forms assumed planarity with a slight decrease in the band gap of 1.97 eV compared to that of unsubstituted polythiophene. On substitution with cyclohexyl group, HT-HT form almost remained planar with a band gap of 2.05 and HH-TT form band gap increased by 2.67 eV with DDA of 40.03º. The stability of HH-TT form is found to be 4.35 kcal/mole more than that of the HT-HT form. This can be attributed to steric repulsions arising from close bulky groups in close proximity in the HH-TT form. Due to this effect polymer is found to deviate from planarity which is an important criteria for delocalization of electrons and for conductivity. Alkyl groups act as electron donating groups by positive inductive effect and in the cases where the planarity is maintained alkyl substitution resulted

in a slight decrease of the band gap (almost the same in the case of cyclohexyl). In the cases where the planarity is lost due to a loss in conjugation or lesser delocalization of π electrons band gap is found to increase significantly. As a whole, no significant decrease in the band gap of polythiophenes is observed on substitution with alkyl groups. Band structure graphs of ethyl and cyclohexyl substituted polythiophenes are shown in Figure 4.2 for comparison.

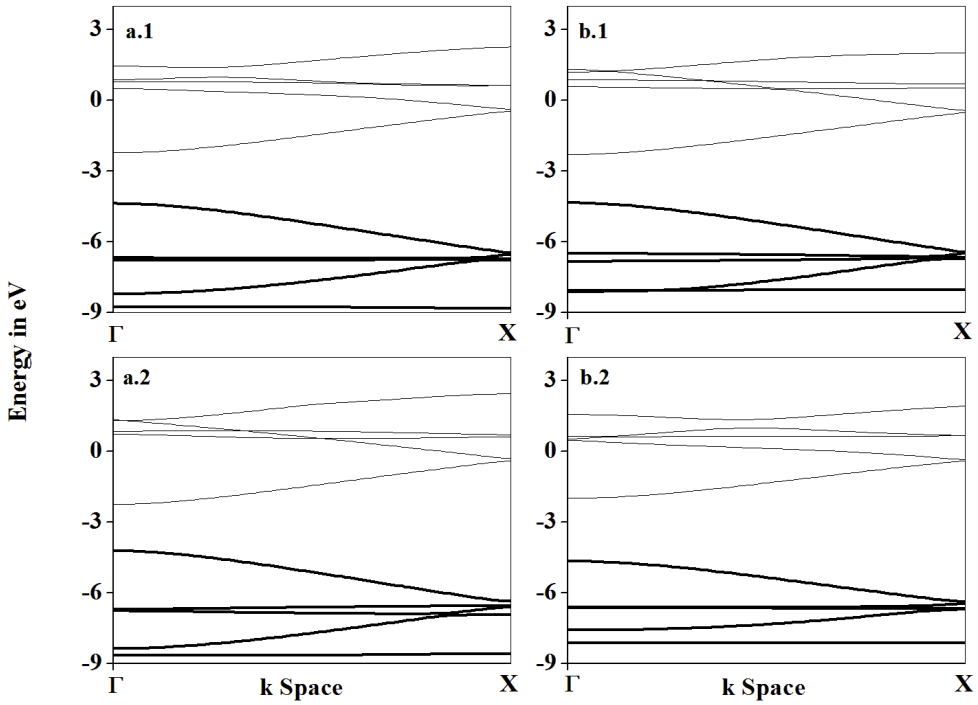

Figure 4.2. Band structure graphs of ethyl and cyclohexyl substituted polythiophenes. **a.1** Et-PT (HT-HT) **a.2** Et-PT (HH-TT), **b.1** CyH-PT (HT-HT), **b.2** CyH-PT (HH-TT). Black lines represent occupied crystalline orbitals and the gray lines represent unoccupied crystalline orbitals.

HOCO and LUCO energies for various alkyl substituted polythiophenes in various forms are plotted in Figure 4.3 to understand the changes in Fermi energy states upon substitution. From this, it is clear that in the case of methyl substitution, HOCO and LUCO energies are destabilized with respect to the unsubstituted polythiophene and the band gaps is found to be similar to that of unsubstituted polythiophene in both HH-TT and HT-HT forms. HOCO, LUCO energies in the case of ethyl substitution resulted in an increase in energy compared to that of unsubstituted polythiophene and the increase is found to be more profound in the case of HT-HT form which deviates from planarity. Similar findings are observed in the case of cyclohexyl substitution where the HOCO and LUCO energies are altered significantly in HH-TT form due to deviations from planarity.

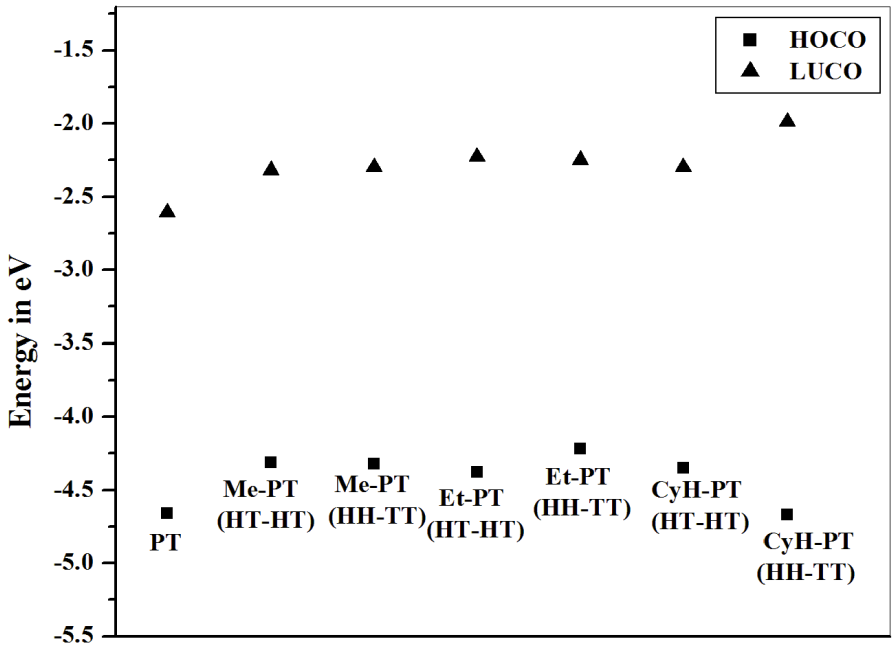

Figure 4.3. HOCO - LUCO energies of different alkyl substituted polythiophenes in HT-HT form and HH-TT form.

4.3. Substitution with halogens

On substitution with halogens the band gaps in both the forms remained the same as that of unsubstituted polythiophene with no deviations in dihedral angles are observed as shown in Table 4.2. Halogen substituted HT-HT forms and HH-TT forms are also found to be similar in energy. Band structure plots of Fluoro and Chloro polythiophenes in both forms are shown in Figure 4.4. Halogen atoms show impact neither on band gap nor on dihedral angle when they are substituted on polythiophene back bone.

System	Band gap HT-HT (eV)	DDA HT-HT	Band gap HH-TT (eV)	DDA HH-TT (eV)	Stability* (kcal/mole)
Fluoro-PT	2.02	0.00	2.0	0.00	0.32
Chloro-PT	2.13	0.00	2.15	0.00	1.50

Table 4.2. Band gaps, Deviation in dihedral angles (DDA) of halo substituted polythiophenes in HT-HT form and HH-TT form. *****Indicates stability of HH-TT form with respect to the corresponding HT-HT form.

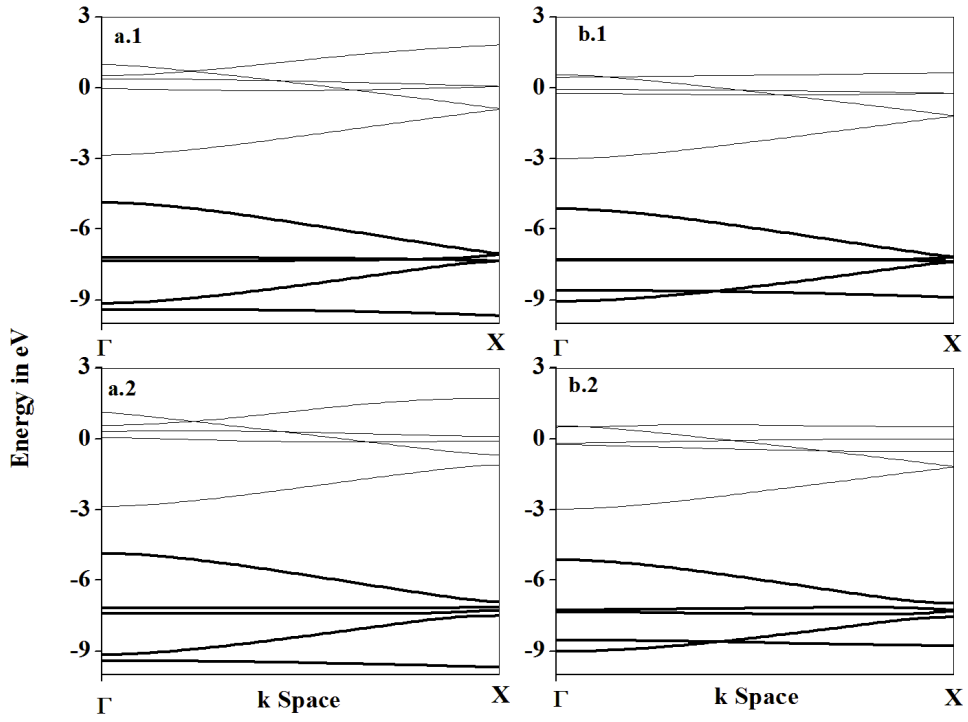

Figure 4.4. Band structure plots of halo substituted PTs in both the forms. **a.1** Fluoro-PT (HT-HT) **a.2** Fluoro-PT (HH-TT) **b.1** Chloro-PT (HT-HT) **b.2** Chloro-PT (HH-TT). Black lines represent occupied crystalline orbitals and gray lines represent unoccupied crystalline orbitals.

HOCO, LUCO energies plotted in Figure 4.5 indicate that on substitution with halogens, both HOCO and LUCO are stabilized compared to the unsubstituted polythiophene even though the band gaps remain unaffected. This indicates that these systems can be doped further. The decrease in HOCO and LUCO energies is more predominant in the case of chloro-substituted polythiophene with the energies lesser by about 0.5 eV for fluoro and about 1 eV for the chloro substituents. Both the forms HT-HT and HH-TT exhibit same dihedral angles and similar band gaps.

4.4. Substitution with Aromatic groups

Substitution with bulky phenyl group resulted in the loss of planarity of the polymer backbone and the deviation is found to be more profound in HH-TT form compared to that of the HT-HT form. The deviation of dihedral angle in the HT-HT form of phenyl substituted polythiophene from the planarity is around 6^0 which is a small deviation compared to the phenyl substituted oligothiophenes where the dihedral deviation is around 40^0. It indicates that dihedral angle deviations of a polymer are not same as in the oligomer.

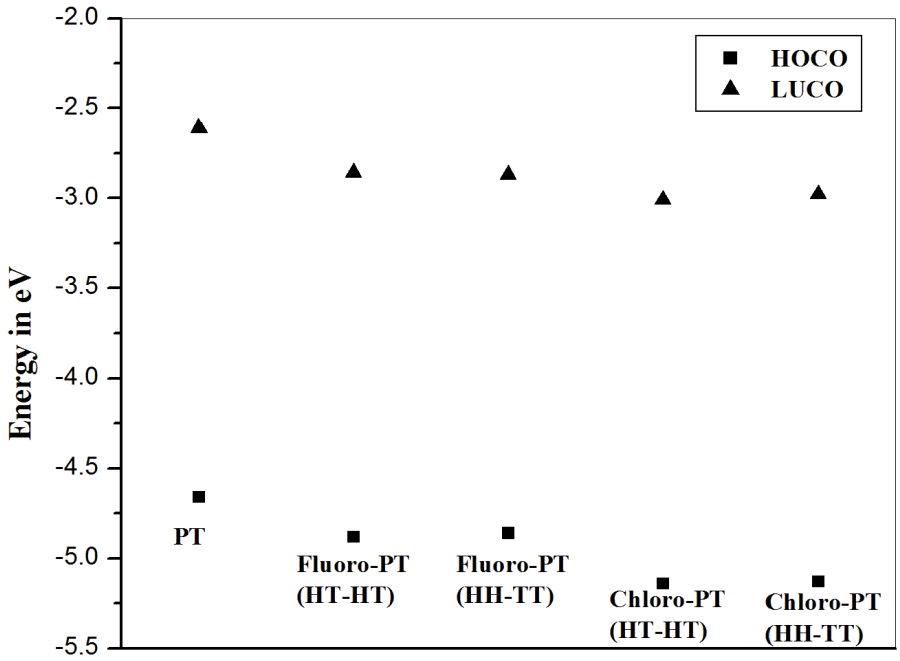

Figure 4.5. HOCO and LUCO energies of halo substituted polythiophene in both forms.

Band gaps are found to be increased from that of unsubstituted polythiophene since the deviation from planarity is comparatively more. On substitution with para methoxy phenyl, a similar trend in band gap is observed. Substitution of electron donating group at the para position of phenyl group did not alter the band gap due to loss of conjugation resulting from deviation of planarity of the backbone. On substitution with phenoxy group due to the presence of increased distance between thiophene unit and phenyl ring linked by an ether linkage, the steric repulsions between the polymer and substituent are minimized. Even though large structural changes are observed on substitution both the forms are found to show similar energies. Band gaps, dihedral angles, and stability for aromatic substituted polythiophenes are shown in Table 4.3 and the band structure plots of few aromatic systems are shown in Figure 4.6.

System	Band gap HT-HT (eV)	DDA HT-HT	Band gap HH-TT (eV)	DDA HH-TT (eV)	Stability* (kcal/mole)
Ph-PT	2.11	6.30	2.37	35.99	0.44
PMP-PT	2.06	11.78	2.33	35.57	0.39
PhO-PT	2.04	0.73	2.04	2.52	-0.48

Table 4.3. Band gaps, Deviation in dihedral angles (DDA) of various aromatic substituted polythiophenes in HT-HT form and HH-TT form. *Indicates stability of HH-TT form with respect to the corresponding HT-HT form.

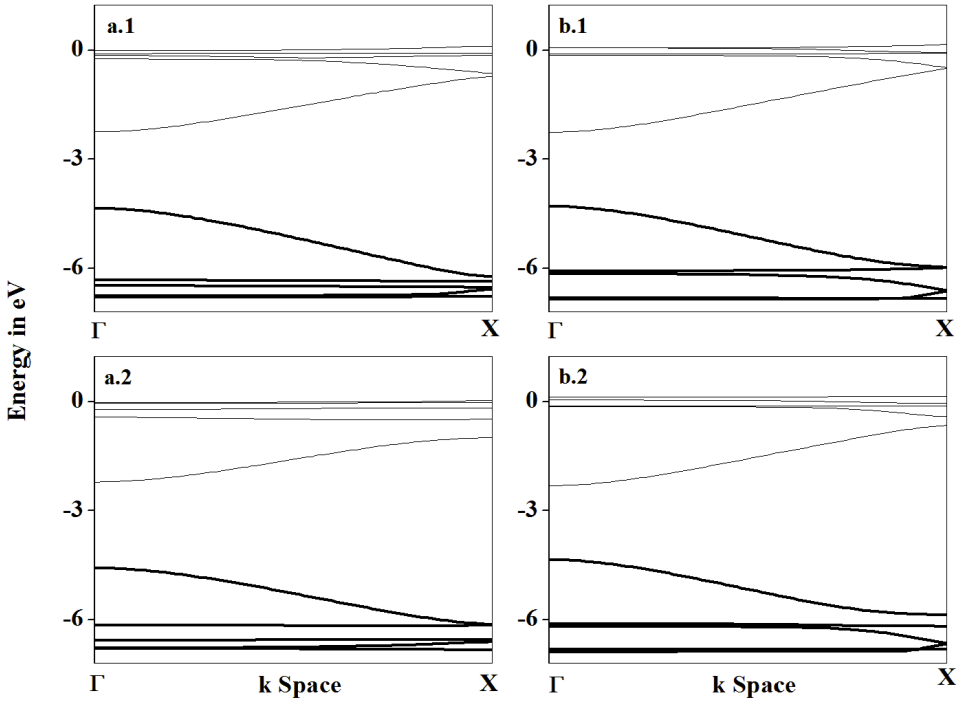

Figure 4.6. Band structure plots of polythiophene substituted with aromatic groups. **a.1** Ph-PT (HT-HT), **a.2** Ph-PT(HH-TT) **b.1** PhO-PT(HT-HT), **b.2** PhO-PT(HH-TT). Black lines represent occupied crystalline orbitals; Grey lines represent unoccupied crystalline orbitals.

HOCO, LUCO energies plotted in Figure 4.7 gives the energy changes associated with Fermi energy upon substitution of aromatic groups. All the aromatic substituents upon substitution resulted in an increase of HOCO and LUCO energies compared to that of unsubstituted polythiophene. The increase in energy is found to be more in the case of HT-HT form compared to that of their HH-TT counterparts. Band gaps are found to be slightly more than that of unsubstituted polythiophene. Band gaps of HH-TT form are more in aromatic substituted polythiophene compared to HT-HT form.

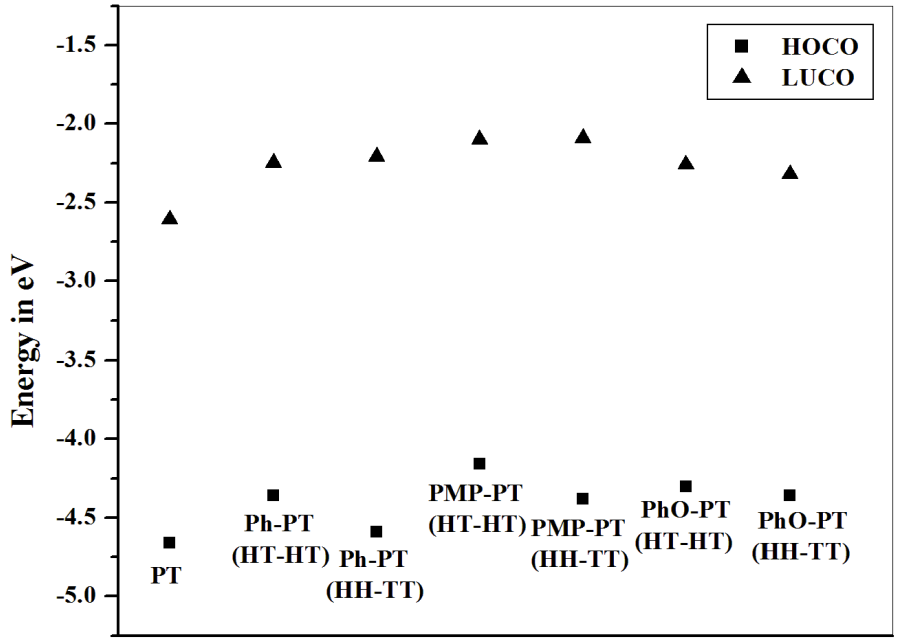

Figure 4.7. HOCO and LUCO energies of various aromatic substituted polythiophenes are shown in both HT-HT and HH-TT forms.

4.5. Substitution with Alkoxy groups

The band gaps are found to decrease significantly upon substitution with electron donating alkoxy groups as shown in Table 4.4. The decrease in band gaps is found to be slightly more in the case of HH-TT forms. Methoxy group is found to show a band gap of 1.74 eV and 1.64 eV in HT-HT and HH-TT forms. Ethoxy group has also shown similar band gaps as methoxy and no further decrease in band gap is observed. Methoxy and ethoxy groups have almost similar band gaps in both HT-HT and HH-TT form polymers as like methoxy and ethoxy substituted oligothiophenes where the band gaps of both the oligomers are also the same. Methoxy and ethoxy substituents show same behaviour on electronic structural properties whether it is oligomer or polymer [27].

Substituted dimeric systems retained planarity of the chain backbone on substitution with alkoxy groups in both the forms. Due to strong positive mesomeric effect and increase in delocalization of electrons along the polymer backbone, we observe a significant decrease in band gaps which is absent in other cases. In a recent study [27] of the alkoxy substituted oligomeric system similar trend of decreased band gaps is observed. The band structure plots of alkoxy substituted polythiophenes are presented in Figure 4.8.

System	Band gap HT-HT (eV)	DDA HT-HT	Band gap HH-TT (eV)	DDA HH-TT (eV)	Stability* (kcal/mole)
MeO-PT	1.74	0.07	1.64	0.00	1.20
EtO-PT	1.76	0.21	1.67	0.02	2.40

Table 4.4. Band gaps, Deviation in dihedral angles (DDA) of alkoxy substituted polythiophenes in HT-HT form and HH-TT forms. *Indicates stability of HT-HT form with respect to corresponding HH-TT form.

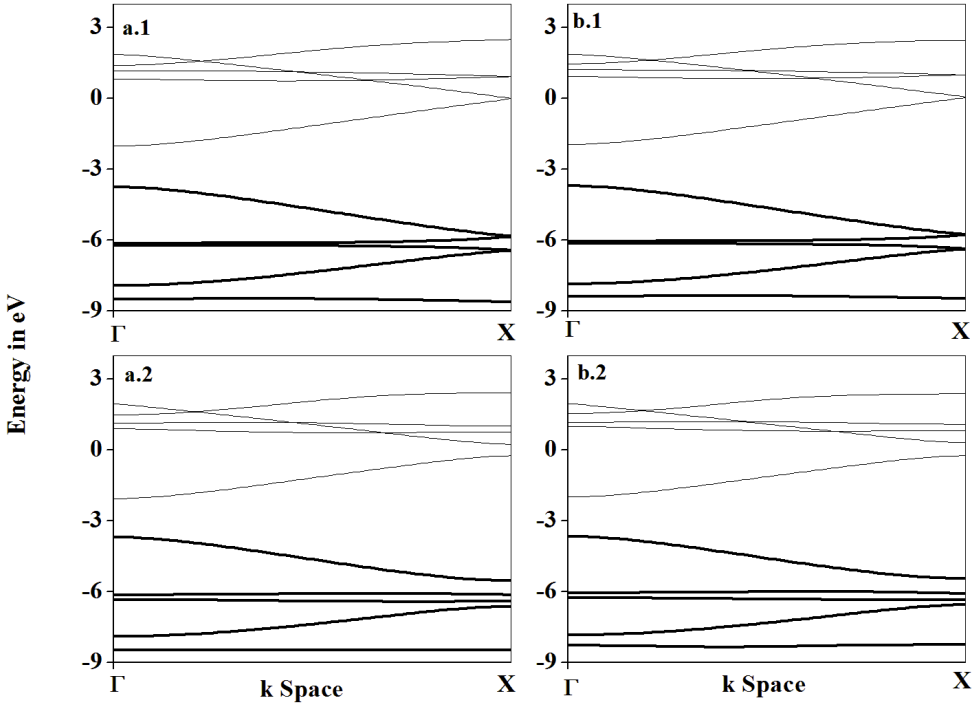

Figure 4.8. Band structure plots of alkoxy groups. **a.1** MeO-PT (HT-HT), **a.2** MeO-PT (HH-TT), **b.1** EtO-PT (HT-HT), **b.2** EtO-PT (HH-TT). Black lines represent occupied crystalline orbitals; Grey lines represent unoccupied crystalline orbitals.

It is seen in Figure 4.9 that there is a significant increase in HOCO energies compared to that of unsubstituted polythiophene whereas LUCO energies are slightly higher compared to that of unsubstituted polythiophene. The increase in HOCO is more compared to that of increase in LUCO which causes the band gap to decrease. It is noted in the recent work on oligomers [27] that the inverse relationship of '1/n' represented in Figure 4.10 holds for

oligomers because the length of the π-conjugated system and the number of electrons simultaneously increase as more monomer units are added.

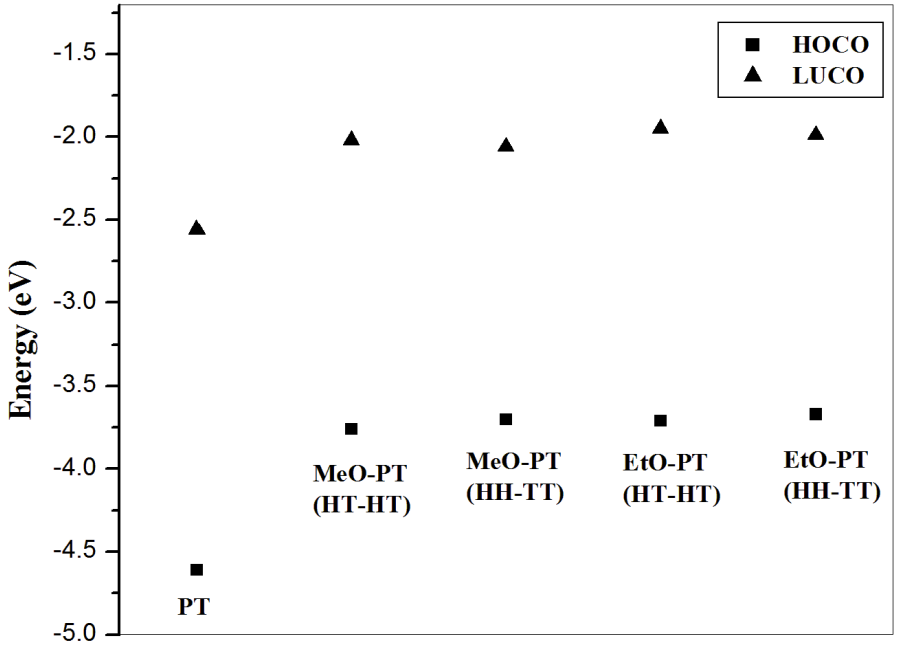

Figure 4.9. HOCO, LUCO energies of alkoxy substituted polythiophenes along with unsubstituted polythiophene.

As noted earlier [19], we also find that there is a serious limitation of simple oligomeric extrapolation approximation for the corresponding polymeric system. It is also clear from the DFT-PBC results below that the band gap of the corresponding polymers cannot be predicted from the simple extrapolation of the electronic structures of oligomers. The extrapolated values from Figure 4.10 and the values calculated for the infinite system using DFT periodic boundary condition (DFT-PBC) for the polymeric systems are listed in Table 4.5. The validity of our DFT-PBC calculations is checked with the available experimental results on unsubstituted polythiophene. It is seen that there is very good agreement with the experimental band gap of the polythiophene and the value calculated with DFT-PBC. In the case of unsubstituted polythiophene band gap obtained from the extrapolated graph of 1.78 eV is far less than the experimentally obtained band gap of 2.1eV whereas band gaps obtained from DFT-PBC calculation 2.05 eV is closer to the experimental band gaps. It can be observed that the band gaps predicted from extrapolation of oligomers will not give the accurate band gaps for the infinite polymeric systems and also underestimates the exact band gap of the polymers leading to erroneous conclusions.

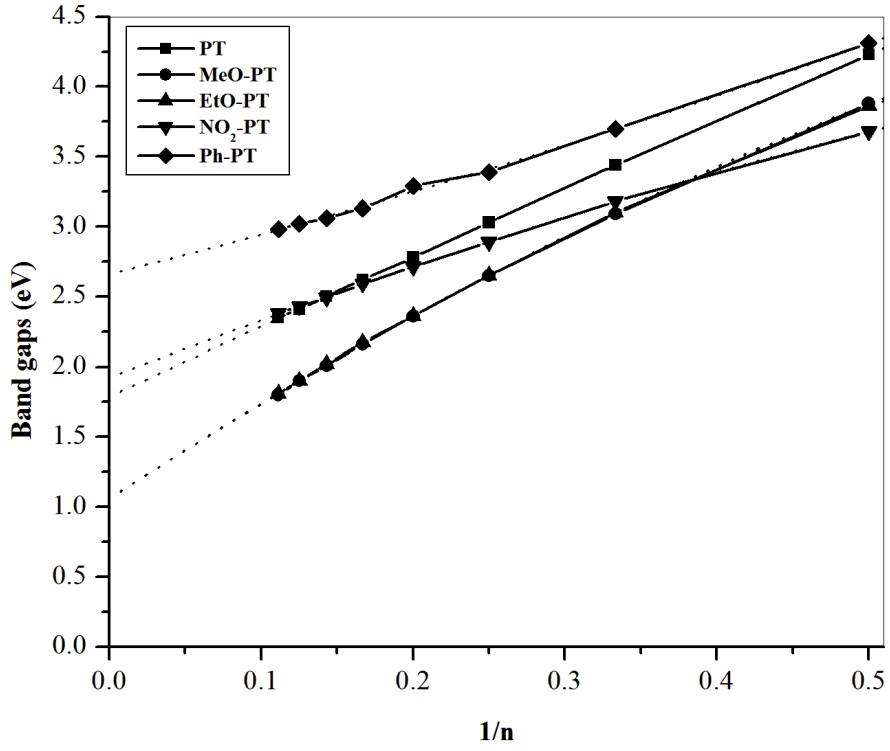

Figure 4.10. Calculated /B3LYP/6-31G(d) HOMO-LUMO gaps versus the reciprocal of the number of oligomer units 1/n for unsubstituted and substituted oligomers from n=2 to n=9. The experimental band gap of polythiophene is 2.1 eV. Substituted oligothiophenes are designated as R-nT, where R is –OMe, -OEt, -NO_2 and -Ph. Calculated oligomeric polynomial scaling is given in the inset. Extrapolated band gaps of polymers are calculated from the band gaps of oligomers.

For example, in the case of electron donating groups, the band gap was found to decrease to 1.74-1.76 eV for alkoxy groups from the PBC study whereas extrapolated band gaps suggest a band gap of 1.05 eV. With electron withdrawing groups nitro and phenyl substituted polythiophenes the band gaps are found to be 2.33 and 2.11 eV whereas the extrapolated band gaps give a band gap of 1.92 and 2.65 eV respectively. Overall the bandgaps obtained from extrapolated values of oligomers seems to underestimate the band gaps of the polymeric system except for the phenyl substituted system.

System	Band gaps (eV) (DFT-PBC)	Band gaps (eV) (Extrapolated)
PT (Unsubstituted)	2.05 (~ 2.1 *)	1.78

MeO-PT	1.74	1.05
EtO- PT	1.76	1.05
NO_2-PT	2.33	1.92
Ph-PT	2.11	2.65

Table 4.5. Band gaps calculated from PBC conditions and also by extrapolation from band gaps of oligomers. ***** refers to the experimental value

Similarly, for MeO-PT, we have 1.74eV calculated from the PBC whereas the extrapolated value of the oligomer is only 1.05 eV. Therefore the empirically extrapolated values of calculations with oligo system do not hold good for infinite polymer chains since it does not accurately describe the asymptotic behavior. Thus we also expect that the extrapolated band gaps for the substituted oligomeric systems may not describe the electronic properties of the corresponding polymeric systems correctly. This deviation can be understood as resulting from the increased degree of freedom and therefore the increased conformational entropy and flexibility as the chain length is increased which need additional calculations to establish. It should, therefore, be noted that electronic properties of polymeric systems are very much different from that of the corresponding oligomers mainly owing to the less conformational entropy of the oligomer.

There is a serious constraint of simple oligomeric extrapolation approximation for the corresponding polymeric system as proven earlier [28-30]. In our case also, we find that the extrapolated values of oligomeric systems differ appreciably from the DFT-PBC results. Extrapolated bandgaps of polymers are calculated from the bandgaps of oligomers, and the bandgaps calculated employing DFT-PBC calculations on the infinite system show considerable disagreement in their values. These values are represented in Figure 4.11.

The rationality of the DFT-PBC calculations is checked, comparing the computational value for the unsubstituted polymer with the available experimental bandgap of the same [15,16,31-33]. The great deal of correspondence between the calculated and experimental values indicates the importance of DFT-PBC method for the calculation of bandgaps. The experimental bandgap of polythiophene is 2.1 eV. The extrapolation in most cases leads to underestimated values of band gaps. With the electron donating substituents like alkoxy, we find low band gap of about 1.74 eV, whereas electron-withdrawing groups cause slight increment in the values.

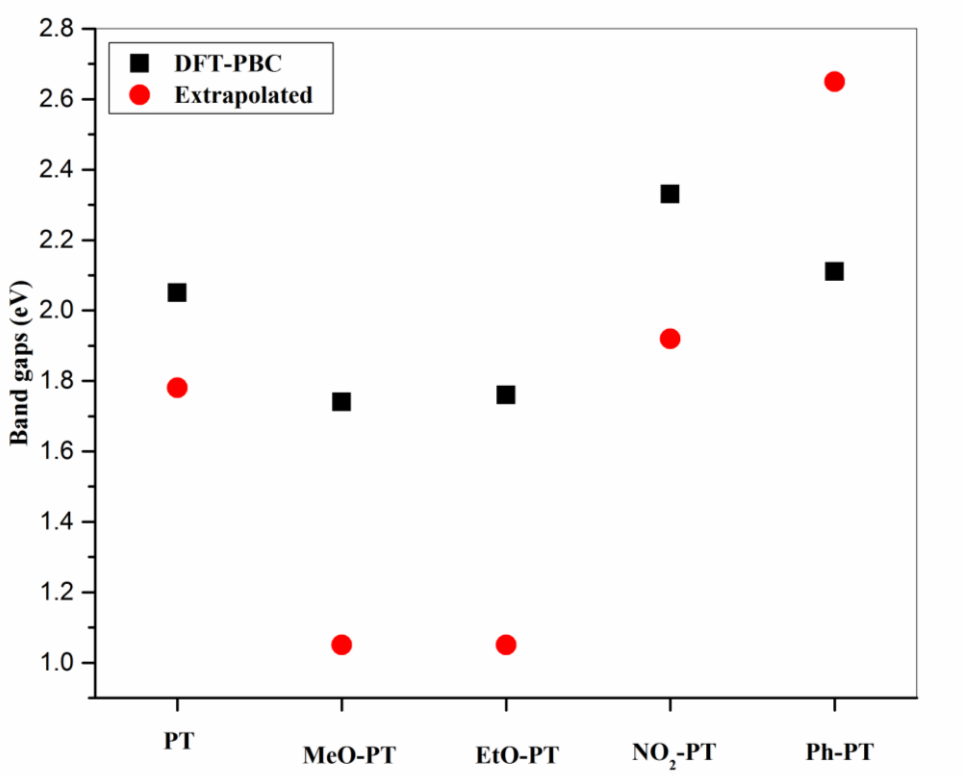

Figure 4.11. The comparison of the extrapolated values for bandgaps from oligomeric systems and the values calculated employing the periodic boundary condition. Substituted polythiophenes are designated as R-PT, where R is –OMe, –OEt, –NO_2, and –Ph.

4.6. Conclusion

Planarity of the backbone is found to play a critical role in determining the band gap of various substituted polymers. Substituted polythiophenes where the corresponding oligomer is found to deviate from the planarity on the oligomeric scale have shown an increase in band gap. Alkoxy groups which upon substitution retained planarity in dimeric and oligomeric systems reduced the band gaps appreciably compared to that of other substituents. This is due to the strong mesomeric effect by which alkoxy groups increase the electron density along the polymer back bone and thereby increasing the π delocalization. Alkyl groups and halogens which exhibit positive and negative inductive effects did not affect the band gaps indicating that the inductive effect do not alter the delocalization of electrons along the polymer backbone. Substitution with bulky aromatic groups once again emphasized the impact of planarity in determining the band gaps. On substitution with bulky aromatic groups like phenyl and para-methoxy phenyl, polythiophenes lost planarity even in short chain oligomers in both the forms which resulted in increase of band gaps. The band gap increase and deviation in planarity is found to be more in case of HH-TT form compared

to that of HT-HT form for aromatic substituents. On the other hand aromatic group linked to thiophene unit by ether linkage (PhO-) due to increase in distance of phenyl group and thiophene steric repulsions minimized and the polymer resumed planarity and the band gap is found to be similar to that of unsubstituted system.

It is also interesting to note that the empirically extrapolated values of calculations with oligo systems do not hold good for infinite polymer chains since it does not accurately describe the asymptotic behaviour. This deviation can be attributed to the increased degree of freedom and therefore the increased conformational entropy and flexibility of the polymer compared to the corresponding oligomers. It should therefore be noted that electronic properties of polymeric systems are very much different from that of the corresponding oligomers mainly owing to lesser conformational entropy of the oligomer.

4.7. References

[1] A Pron, P. Rannou, Prog. Polym. Sci., 2002, 27, 135.

[2] N. Somanathan, S. Radhakrishnan, Int. J. Mod. Phys. B, 2005, 19, 4645.

[3] S. Roth, M. Burghard, G. Leising, Curr. Opin. Solid State Mater. Sci., 1998, 3, 209.

[4] J. Alper, Science, 1989 246, 208.

[5] D. Fichou, *Handbook of Oligo- and Polythiophenes*, WILEY-VCH Verlag GmbH, 1999.

[6] L. Groenendaal, F. Jonas, D. Freitag, H. Pielartzik, J. R. Reynolds, Adv. Mater., 2000, 12, 481.

[7] G. Heywang, F. Jonas, Adv. Mater., 4, 116, 1992.

[8] D. M. Welsh, A. Kumar, E. W. Meijer, J. R. Reynolds, Adv. Mater., 1999, 11, 1379.

[9] F. Wang, M. S Wilson, R. D. Rauh, P. Scottland, B. C. Thompson, J. R. Reynolds, Macromolecules, 2000, 33, 2083.

[10] D. J. Pinner, R. H. Friend, N. Tessler, Appl. Phys. Lett., 2000, 76, 1137.

[11] L. Ding, M. Jonforsen, L. S. Roman, M. R. Andersson, O. Inganas, Synth. Met., 2000, 110, 113.

[12] P. Li, Y. Cui, C. Song, H. Zhang, J. Phys. Chem. C, 2016, 120, 14484.

[13] H. Guan, M. Cai, L. Chen, Y. Wang, Z. He, Luminescence, 2010, 25, 311.

[14] P. Sista, K. Ghosh, J. S. Martinez, and R. C. Rocha, J. Nanosci. Nanotechnol., 2014, 14, 250.

[15] A. R. Murphy , P. C. Chang , P. VanDyke, J. Liu, J. M. J. Fréchet, V. Subramanian, D. M. DeLongchamp, S. Sambasivan, D. A. Fischer, E. K. Lin, Chem. Mater., 2005, 17, 6033.

[16] L. Zhang, N. S. Colella, B. P. Cherniawski, S. C. B. Mannsfeld, A. L. Briseno, ACS Appl. Mater. Interfaces, 2014, 6, 5327.

[17] K. Y. Jen, G. G. Miller, R. L. Elsenbaumer, J. Chem. Soc. Chem. Commun., 1986, 1346.

[18] I. Osaka, R. McCullough, Acc. Chem. Res., 2008, 41, 1202.

[19] R. D. McCullogh, R. D. Lowe, M. Jayaraman, D. L. Andersson, J. Org. Chem., 1993,

58, 904.

[20] D. T. McQuade, A. E. Pullen, T. M. Swager, Chem. Rev., 2000, 100, 2537.

[21] P. S. Heeger, A. J. Heeger, Proc. Natl. Acad. Sci., 1999, 96, 12219.

[22] H. Usta, A. Facchetti, *Polymeric and Small-Molecule Semiconductors for Organic Field-Effect Transistors*, Edited by M. Caironi, Y-Y. Noh, Wiley-VCH Verlag GmbH & Co. GaA, 2015.

[23] G. Perepichka, D. F. Perepichka, H. Meng, F. Wudl, Adv. Mater., 2005, 17, 2281.

[24] G. Tourillon, F. Garnier, J. Electroanal. Chem., 1982, 135, 173.

[25] G. Tourillon, F. Garnier, J. Electroanal. Chem., 1984, 161, 407.

[26] F. Wudl, M. Kobayashi, N. Colaneri, M. Boysel, A. J. Heeger, Mol. Cryst. Liq. Cryst., 1985, 118, 199.

[27] T. Vikramaditya, M. Saisudhakar, K. Sumithra, J. Mol. Struct., 2015, 1081, 114.

[28] G. R. Hutchison, M. A. Ratner, T. J. Marks, J. Phys. Chem. A, 2002, 106, 10596.

[29] L. Bredas, J. Cornil, D. Beljonne, D. D. Santos, Z. G. Shuai, Acc. Chem. Res., 1999, 32, 267.

[30] S. S. Zade, N. Zamoschik, M. Bendikov, Acc. Chem. Res., 2011, 44, 14.

[31] Y. Pang, X. Li, G. Shi, L. Jin, Thin Solid Films, 2008, 516, 6512.

[32] F. Alakhras, R. Holze, J. Solid State Electrochem., 2008, 12, 81.

[33] D. Aradilla, J. Casanovas, F. Estrany, J. I. Iribarren, C. Alemán, Polym. Chem., 2012, 3, 436.

Chapter 5

Comprehensive evaluation of the effect of various exchange correlation functionals and basis sets on the optical properties of oligothiophenes

5.1. Introduction

Thiophene based molecules are building blocks in the design of various applications like displays, transistors and sensors etc. This is due to their photoactive and electroactive properties. Thiophene based molecules have attracted the concentration of researchers due to their ease of chemical modification and fine-tuning of their physical properties. The optical properties of oligothiophenes are one of the key factors which make these molecules as excellent materials in the applications of photovoltaics and light emitting diodes. This is because of their effective π-conjugation and co-planarity.

Theoretical calculations on optical properties like absorption, emission will assess the experimentalist and gives a conclusion before they perform the experiments. Time-dependent density functional theory is well established as the most widely used, effective approach to investigate the optical properties and excited state properties of organic molecules in gas phase, solution and also in complex environments [1-11]. The advantages of DFT and its time-dependent formalism are combined in TD-DFT [12-14] to make it well suited for an accurate description of structures, energies and electronic excitations over the past few years [15-20]. The accuracy of this TD-DFT is limited because of the adiabatic approximation and requires the appropriate exchange-correlation functional (XCF). Even though TD-DFT predicts molecular excited states correctly, long-range charge transfer effects are not accurately defined [21-24]. It is also known [21-26] that the use of conventional XCF drastically underestimates the charge transfer excitation energies and yields incorrect asymptotic potential energy surfaces. The selection of an appropriate XCF for modelling excited state properties has been the subject of several benchmarks performed on different systems over the past few years [24-27]. It is now well established in the literature that the conventional functionals fail for long-range charge transfer states and also for the correct prediction of optically excited states [28-31].

In this chapter, the optical properties of a series of α-oligothiophenes 2-7 with TD-DFT methodology are discussed. The most popular hybrid functional B3LYP, Meta hybrid functional M06, long-range corrected functionals ωB97XD, CAM-B3LYP are used to study

the absorption and emission properties with various levels of Pople basis sets such as 6-31G, including polarization functions (6-31G(d), 6-31G(d,p)), diffusion functions 6-31+G (d,p) and in few cases Hartree-Fock methods used with correlation consistent basis sets by including two solvent approaches, linear response (LR) and state specific (SS) approximations in Polarizable continuum model (PCM).

5.2. Absorption studies

The absorption and emission wavelengths of oligothiophenes in the 1,4-dioxane solvent are carried out employing two widely used methods, linear response and state-specific approaches with important representative functionals and basis sets. Basis sets level is increased in the level of hierarchy 6-31G, 6-31G(d), 6-31G(d,p) and 6-31+G(d,p) in order to account the role of polarization and diffusion functions in determining the accuracy of optical properties. Ground state optimizations are carried out with DFT employing various functionals B3LYP, M06, ωB97XD and CAM-B3LYP and the excited state calculations are performed with TD-DFT using the same functionals and basis sets. PCM solvent formalism is chosen to consider the effects of solvent with both SS and LR approaches.

5.2.1. 6-31G Basis set

The wavelength of absorption maximum**,** λ_{max}, with 6-31G basis set is given in Table 5.1 and (percentage of deviation with respect to experimental values are plotted in Figure 5.1 with various basis sets), employing various functionals with increasing chain length of oligothiophenes. From the Table 5.1, it is clear that range-separated hybrid functionals ωB97XD and CAM-B3LYP predict the λ_{max} values closer to the experiment. For shorter chain lengths (n=2) global and meta-hybrid functionals predict absorption maximum values closer to the experiments, but as the chain length increases the accuracy is found to decrease. Absorption studies carried out with hybrid functional B3LYP and meta-hybrid functional M06 are found to overestimate the λ_{max} values. As the chain length increases, we can observe an increase in deviation with respect to global and meta-hybrid functionals. The percentage of deviation is found to be more in the case of LR approach compared to the SS approach.

Chain Length	B3LYP	M06	ωB97XD	CAM-B3LYP	Expt.
2	311 (320)	312 (321)	286 (293)	287 (294)	303

3	387 (403)	384 (399)	339 (350)	343 (354)	354
4	448 (471)	439 (460)	375 (388)	382 (395)	392
5	499 (526)	484 (508)	401 (415)	410 (425)	417
6	543 (572)	520 (545)	419 (433)	431 (446)	436
7	579 (609)	550 (575)	433 (446)	447 (461)	441

Table 5.1. Absorption λ_{max} values (nm) of oligothiophenes of chain length(2-7) employing 6-31G basis set with SS and LR approaches (shown inside the parenthesis) with different functionals.

B3LYP functional exhibited a percentage deviation in the range of 2.6 to 31.3% in SS approach and 5.6 to 38.1% in LR approach. Although M06 exhibited a similar trend, the magnitude is found to be less in comparison with B3LYP. M06 has shown the deviation in the range 2.9 to 24.7% and 5.9 to 30.4% with SS and LR approaches respectively. Range separated Hybrid Functionals ωB97XD and CAM-B3LYP predicted the values much closer to the experimental results. ωB97XD functional underestimated the λ_{max} values of absorption in the range of -5.6 to 1.8%, -3.3 to 1.13% with SS and LR approaches (shown in Figure 5.1). CAM-B3LYP predicted the values closer to the experimental values with the percentage of deviation in the range of -5.3 to 1.4% and -2.9 to 4.5% employing SS and LR approaches respectively. It is seen that the RSH functionals show a marked improvement over the global and meta-hybrid functionals. The flexibility arising from two extra parameters α and β in the Eq. (2.21) seems to facilitate a better calculation of absorption properties and allow us to look at the importance of the HF exchange contribution for the short-range region and the DFT counterpart for the long range region for RSH functionals.

5.2.2. 6-31G(d) Basis set

6-31G(d) is one of the most widely used basis set in the literature. The inclusion of higher angular momentum functions in basis sets enables the molecular density to distort from the usual spherical symmetry of the atoms at the levels of DFT and HF and also serves in describing the electron correlation cusp for correlated calculations [59]. Absorption λ_{max} values are tabulated employing 6-31G(d) basis set shown in Table 5.2 and percentage of deviation with respect to experimental values are plotted in Figure 5.1.

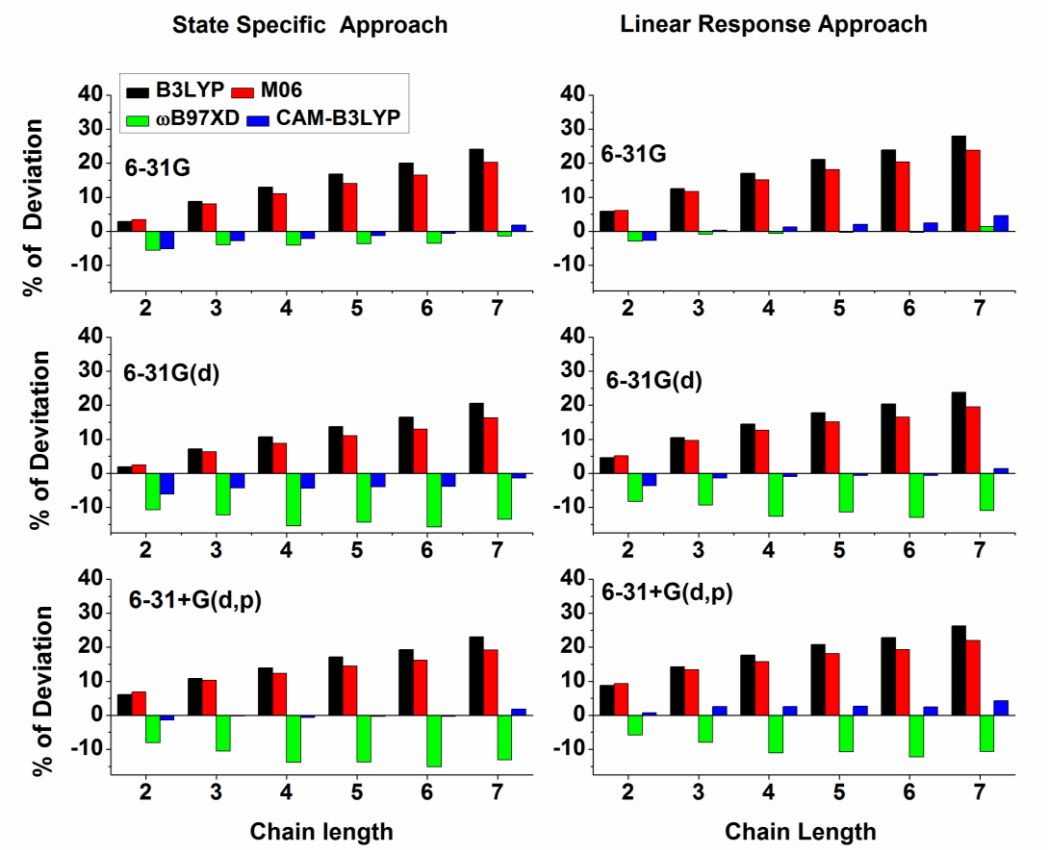

Figure 5.1. Deviation of λ_{max} values (absorption) of oligothiophenes of chain length 2-7, with various functionals B3LYP, M06, ωB97XD and CAM-B3LYP with basis sets, 6-31G, 6-31G(d), 631+G(d,p) basis sets with SS and LR approach in the PCM framework.

With the inclusion of higher angular momentum "d" functionals in the basis set improved the accuracy in calculating the optical properties with all the functionals. With SS approach, global hybrid functional B3LYP has shown a deviation in the range of 1.6 to 25.2%, and 4.3 to 30.83% with LR Approach. The lowest deviation is observed for chain length 2 and highest for 7. Meta hybrid functional M06 exhibited a deviation in the range of 2.3 to 19.0% with SS approach and 4.9-23.8% with LR approach.

Chain Length	B3LYP	M06	ωB97XD	CAM-B3LYP	Expt.
2	308 (317)	310 (318)	273 (279)	285 (292)	303
3	380 (395)	377 (391)	315 (323)	338 (348)	354
4	437 (457)	428 (446)	338 (347)	374 (387)	392

5	483 (506)	468 (489)	363 (373)	400 (413)	417
6	521 (546)	500 (521)	376 (385)	419 (432)	436
7	552 (577)	525 (546)	388 (396)	433 (445)	441

Table 5.2. Absorption λ_{max} values (nm) of oligothiophenes of chain length (2-7) employing 6-31G(d) basis set with SS and LR approaches (shown inside the parenthesis) with different functionals.

From Figure 5.1, it can be clearly observed that global and meta-hybrid functionals overestimate the λ_{max} values. RSH functionals, in contrast, have underestimated the absorption maxima values in most of the cases. ωB97XD has shown a deviation of 9.9% for n=2 and 13.76% for n=6 with SS approach. Similarly, with LR approach, it has shown a deviation of 7.9% for n=2 and 11.6% for n=6. With CAM-B3LYP, SS approach has shown a deviation of 5.9% for dimer and only a deviation of 1.8% for the chain length of n=7. With LR approach deviation is found to be in the range of 3.63 to 0.9% for n=2 and 7 respectively.

5.2.3. 6-31G(d,p) Basis set

The inclusion of polarization "p" functions in the basis set 6-31(d,p) exhibited almost no difference compared to 6-31 G(d) and the absorption λ_{max} wavelengths almost remained the same with respect to all the functionals employed using 631(d,p) basis set (λ_{max} values are given in Table 5.3). Thus it can be concluded that inclusion of lower angular momentum functions like "p" has no effect in altering the optical properties, unlike the "d" functions.

Chain Length	B3LYP	M06	ωB97XD	CAM-B3LYP	Expt.
2	308 (317)	310 (318)	273 (279)	285 (292)	303
3	380 (395)	377 (391)	315 (323)	338 (348)	354
4	437 (457)	428 (446)	338 (347)	374 (387)	392
5	483 (506)	468 (489)	363 (373)	400 (413)	417
6	521 (546)	500 (521)	376 (385)	419 (432)	436

7	552 (577)	525 (546)	387 (396)	433 (445)	441

Table 5.3. Absorption λ_{max} values (nm) of oligothiophenes of chain length(2-7) employing 6-31G(d,p) basis set with SS and LR approaches (shown inside the parenthesis) with different functionals.

The comparison of percentage of between the basis sets 6-31G(d) and 6-31G(d,p) is shown in the Figure 5.2. It is observed that the addition of polarization function like 'p' functions to the hydrogen atoms has no impact on the percentage of deviation of oligothiophene absorption (λ_{max}) values with respect to the all the functionals. The percentage of deviations is calculated with reference to the experimental values. Similar kind trend has been observed both in SS and LR approaches.

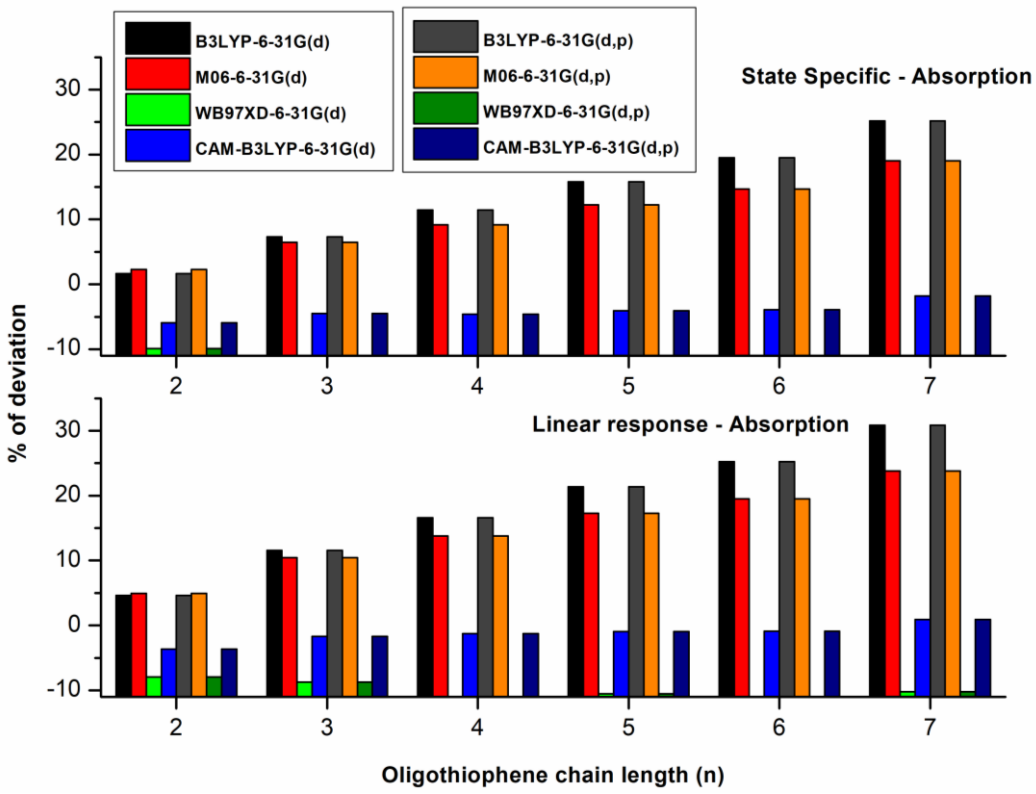

Figure 5.2. The comparison of absorption (λ_{max}) of oligothiophene between the basis set 6-31G(d) and 6-31G(d,p) basis set.

5.2.4. 6-31+G(d,p) Basis set

In order to understand the effect of diffused functions in basis set, absorption studies are carried out employing 6-31+G(d,p) basis set (shown in Table 5.4 and Figure 5.1). B3LYP functional with SS approach has shown an increase in deviation with the inclusion of

diffused functions in the basis set with a deviation in the range 6.3 to 29.3% and 9.2 to 34.9% with LR approach. Meta hybrid functional M06 has also shown an increase in deviation from the experimental values in the range of 6.9 to 23.1% with SS approach and 9.9 to 27.9% with LR approach. RSH functional ωB97XD has shown a deviation in the range of 7.9 to 13.3% with SS approach and 5.9 to 11.23% with LR approach. With the inclusion of diffused functions in the basis set, the accuracy of CAM-B3LYP functional increased with negligible deviations of the range 1.36 to 1.98% and 0.33 to 4.08% with SS and LR approaches respectively.

Chain Length	B3LYP	M06	ωB97XD	CAM-B3LYP	Expt.
2	322 (331)	324 (333)	279 (285)	297 (304)	303
3	396 (411)	394 (408)	319 (327)	352 (362)	354
4	454 (474)	446 (464)	343 (351)	388 (401)	392
5	501 (524)	486 (507)	366 (375)	414 (427)	417
6	538 (563)	518 (539)	378 (387)	433 (446)	436
7	570 (595)	543 (564)	388 (396)	447 (459)	441

Table 5.4. Absorption λ_{max} values (nm) of oligothiophenes with chain length (2-7) employing 6-31+G(d,p) basis set with SS and LR approaches (shown inside the parenthesis) with different functionals.

The inclusion of diffused functions in the basis set resulted in a deviation from experimental values more in the case of LR approach compared to SS approach with the functionals B3LYP and M06. ωB97XD consistently underestimated λ_{max} in most of the cases employing several basis sets although it performed better compared to B3LYP and M06. CAM-B3LYP consistently predicted absorption maxima values closer to the experiment. In the case of LR approach, CAMB3LYP with 6-31G (d) basis set and SS approach with 6-31G+G(d,p) basis set predicted absorption values closer to the experimental results.

The raw data of computed λ_{max} values together with the experimental values are plotted together in Figure 5.3, which gives a clear idea as to how the values differ with the

use of each functional. Above Figure gives a description of the accuracy of various functionals and basis sets with SS and LR solvent formalisms. With respect to global and meta-hybrid functionals, we do not observe a significant increase in the level of accuracies with increasing basis set with both SS and LR approaches. In the case of RSH functionals, ωB97XD functional consistently underestimated λ_{max} of absorption with both SS and LR approaches. CAM-B3LYP performed well in comparison with other functionals and consistently predicted absorption λ_{max} values closer to the experiment with various basis sets, for example, SS approach with 6-31+G(d,p) basis set and LR approach 6-31G(d) basis set.

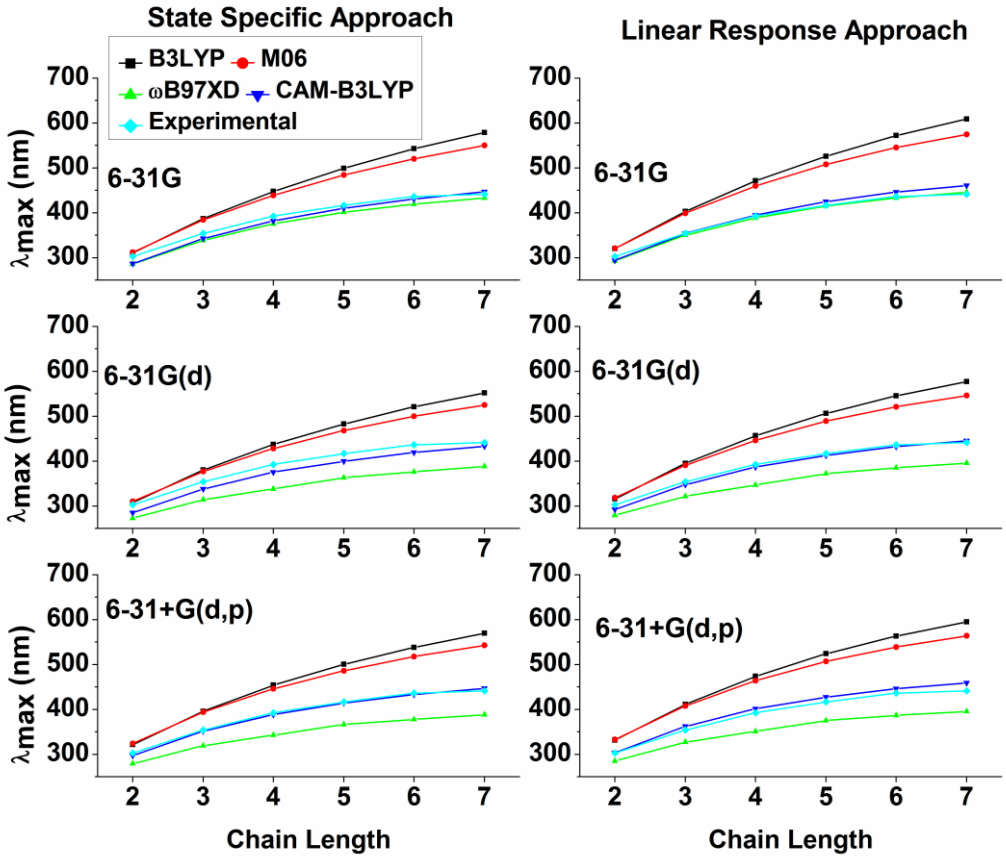

Figure 5.3. Comparison of absorption λ_{max} of Oligo[n]thiophenes (n=2-7) with various functionals and basis sets employing SS and LR approaches. Note that the experimental values and calculated values using CAM-B3LYP are coinciding for almost all cases.

5.3. Emission Studies

Similar studies for emission are carried out employing same functionals and basis sets with both SS and LR approaches. Fluorescence studies of oligothiophenes of various chain lengths (2-7) are carried out with 6-31G, 6-31G (d), 6-31G (d,p) and 6-31+G (d,p) basis sets with various functionals and are given in tables below.

5.3.1. 6-31G Basis set

Emission with 6-31G basis set with various functionals followed a similar trend to that of absorption. The accuracy is decreased with increase in chain length in both SS and LR approaches, for both B3LYP and M06 functionals. SS approach results are found to be accurate in comparison with LR approach. The results are found to be closer to the experimental results with the RSH functional, CAM-B3LYP. CAM-B3LYP predicted accurate results with the percentage of deviation around –3.87 to 1.25% with SS approach and 0.28 to 7.68% with LR approach. The deviation in emission λ_{max} values with various functionals and basis sets are shown in Figure 5.4.

Chain Length	B3LYP	M06	ωB97XD	CAM-B3LYP	Expt.
2	362 (378)	365 (382)	347 (362)	348 (363)	362
3	444 (474)	446 (475)	416 (440)	419 (444)	426
4	514 (556)	512 (552)	466 (496)	474 (505)	478
5	575 (626)	567 (615)	503 (536)	515 (550)	514
6	629 (686)	614 (667)	529 (562)	545 (582)	537
7	676 (737)	654 (708)	546 (578)	567 (603)	560

Table 5.5. Emission λ_{max} values (nm) of oligothiophenes with chain length (2-7) employing 6-31G basis set with SS and LR approaches (shown inside the parenthesis) with different functionals.

5.3.2. 6-31G(d) Basis set

Global hybrid functional B3LYP with 6-31G(d) basis set predicted the emission values (Table 5.6.) accurately for shorter chain lengths (n=2) and the deviation increased with the increase in chain length. The deviation from accuracy is found to be 1.1 to 15.36% in the case of SS approach and 3.3 to 24.64% with LR approach. Meta-hybrid functional also predicted a similar trend with a deviation in the range 0.55 to 11.96% and 4.97 to 20.18% with SS and LR approaches respectively. RSH functionals did not follow any specific trend of deviation with increasing chain length shown in Figure 5.3. With SS approach ωB97XD and CAMB3LYP predicted the deviation ranging between 4.42 to 6.25%

and 3.31 to 4.42% respectively. ωB97XD and CAM-B3LYP have shown lesser deviation from the experimental values with a deviation of 0.55 to 1.64% and 0.27 to 3.7% respectively with the LR approach.

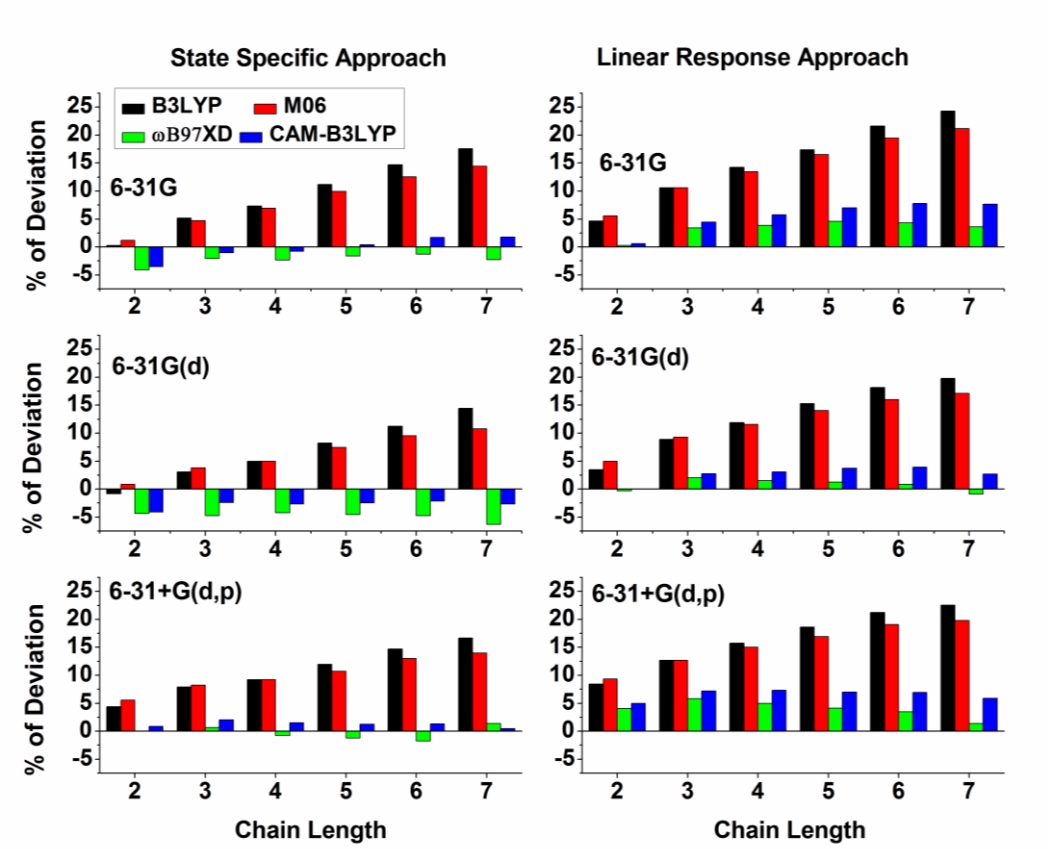

Figure 5.4. Deviation in λ_{max} values (Emission) of oligothiophenes of chain length 2-7, with various functionals B3LYP, M06, ωB97XD and CAM-B3LYP with basis sets 6-31G, 6-31G(d), 631+G(d,p) basis sets with SS and LR approach in the PCM framework.

Chain Length	B3LYP	M06	ωB97XD	CAM-B3LYP	Expt.
2	358 (374)	364 (380)	346 (360)	346 (361)	362
3	437 (465)	441 (468)	411 (433)	414 (437)	426
4	502 (540)	502 (538)	457 (484)	463 (492)	478
5	558 (603)	552 (594)	489 (519)	499 (531)	514
6	605 (655)	593 (638)	511 (541)	525 (557)	537

7	646 (698)	627 (673)	525 (553)	543 (575)	560

Table 5.6. Emission λ_{max} values (nm) of oligothiophenes with chain length (2-7) employing 6-31G (d) basis set with SS and LR approaches (shown inside the parenthesis) with different functionals.

5.3.3. 6-31G(d,p) Basis set

Inclusion of further polarization with "p" functions employing 6-31 G (d,p) basis set did not alter the emission values with any of the functionals using both SS and LR approaches. Results are found to be almost similar to that of 6-31G(d) basis set and are given in Table 5.7.

Chain Length	B3LYP	M06	ωB97XD	CAM-B3LYP	Expt.
2	359 (374)	364 (380)	346 (360)	347 (361)	362
3	438 (465)	441 (468)	411 (433)	414 (437)	426
4	503 (540)	502 (538)	457 (485)	464 (492)	478
5	559 (603)	552 (594)	490 (519)	500 (531)	514
6	606 (655)	593 (638)	512 (541)	526 (558)	537
7	647 (698)	627 (673)	525 (553)	544 (575)	560

Table 5.7. Emission λ_{max} values (nm) of oligothiophenes with chain length (2-7) employing 6-31G(d,p) basis set with SS and LR approaches (shown inside the parenthesis) with different functionals.

The comparison of percentage deviation of oligothiophene emission (λ_{max}) values is shown in the Figure 5.5 between 6-31G(d) and 6-31G(d,p) basis set using all the functionals. From Figure 5.5, we can observe that the percentage deviation calculated using 6-31G(d,p) is follows the similar kind of trend as 6-31G(d) basis set in SS as well as LR approaches. Inclusion of smaller functions like 'p' do not influence the optical properties of conjugated oligothiophenes.

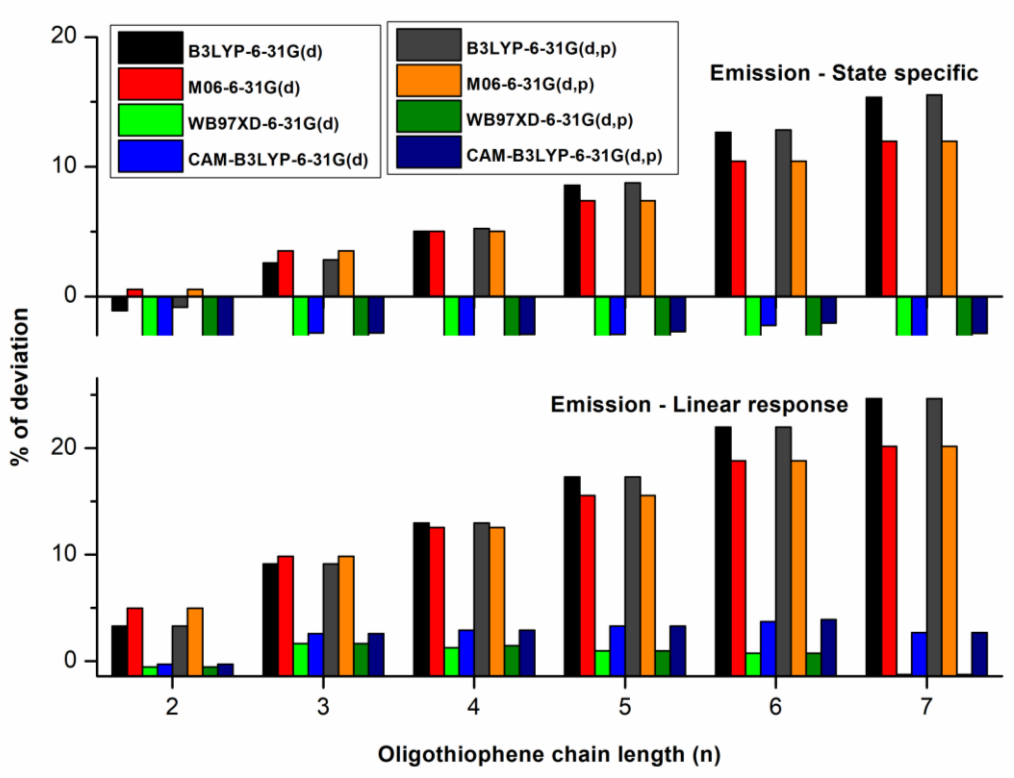

Figure 5.5. Comparison of percentage of deviation from experimental emission values (λ_{max}) between the basis sets 6-31G(d) and 6-31G(d,p)

5.3.4. 6-31G+(d,p) Basis set

Inclusion of diffused functions by employing 6-31+G (d,p) basis set is found to result in a variation of emission values with all the functionals, with both the approaches (shown in Table 5.8). The accuracy decreased with of global and meta-hybrid functionals B3LYP and M06, with deviations in the range 4.14 to 19.46% and 5.52 to 15.7% respectively, with SS approach. Deviations are found to increase with the increase in chain lengths. Accuracy further decreases with LR approach with deviations 8.84 to 28.93% and 10.22 to 24.11% with B3LYP and M06 respectively.

Chain Length	B3LYP	M06	ωB97XD	CAM-B3LYP	Expt.
2	377 (394)	382 (399)	361 (376)	364 (380)	362
3	459 (488)	463 (490)	427 (450)	434 (457)	426
4	525 (565)	525 (562)	473 (501)	483 (513)	478
5	581 (628)	575 (618)	505 (535)	519 (551)	514

6	629 (680)	616 (662)	526 (556)	544 (577)	537
7	669 (722)	648 (695)	538 (566)	561 (593)	560

Table 5.8. Emission λ_{max} values (nm) of oligothiophenes with chain length (2-7) employing 6-31+G(d,p) basis set with SS and LR approaches (shown inside the parenthesis) with different functionals.

In contrast to the global and meta-hybrid functionals, RSH functionals show an exactly opposite trend of increase in accuracy in predicting the emission values with the inclusion of diffused functions in the basis set. ωB97XD has shown deviations in the range of 0.27 to 3.93% and CAM-B3LYP showed excellent accuracy with small deviations in the range of 0.55 to 1.80% with SS approach. With LR approach the deviations are observed to be more, in the range of 1.07 to 5.63% and 4.97 to 5.89% with ωB97XD and CAM-B3LYP functionals respectively.

Figure 5.6 depicts an overview of emission values with respect to various functionals and basis sets. Global and meta-hybrid functionals exhibited a similar trend as in absorption. CAM-B3LYP functional yielded emission λ_{max} values closer to the experiment with SS and LR approaches. From the calculated values of absorption and emission, it is clear that no definite trend of increase or decrease in accuracy (or as a matter of fact no trend) is followed with increasing basis sets level which is the major drawback of Pople type of basis sets.

This can be analyzed by the fact that, different primitive GTOs are employed in the basis sets which are lacking sufficient higher angular momentum basis functions. So, we have calculated the absorption and emission λ_{max} values employing a very large basis set 631+G(3df,3pd) using the best functional CAM-B3LYP (among the functionals studied here) for a dimer. From the Figure 5.7, it is clear that no specific trend of increase or decrease in accuracy is obtained even with increasing the Pople basis sets in the order of hierarchy.

A similar study of absorption and emission are carried out employing Hartree-Fock method employing correlation- consistent polarized (ccp) valence double zeta (VDZ) and valence triple zeta (VTZ) basis sets shown in Table 5.9.

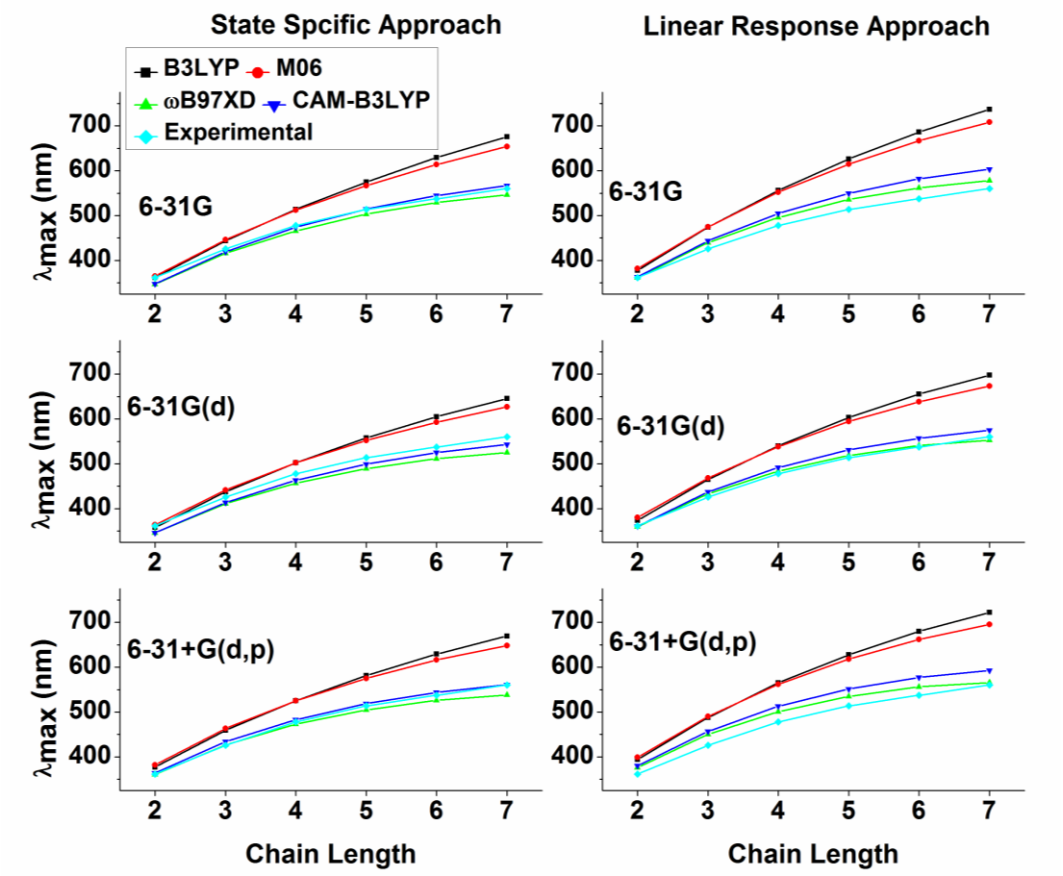

Figure 5.6. Comparison of emission λ_{max} of Oligo[n]thiophenes (n=2-7) with various functionals and basis sets employing SS and LR approaches.

Chain Length	CCP-VDZ (nm)	CCP-VTZ (nm)	Experimental (nm)
2 (A)	266 (272)	269 (275)	303
3 (A)	306 (313)	308 (315)	354
2 (E)	353 (369)	363 (379)	362
3 (E)	417 (441)	427 (452)	426

Table 5.9. Absorption (A) and emission (E) λ_{max} values (nm) of dimer and trimer oligothiophenes with ccp basis sets with HF method along with the experimental values.

From the Table 5.9, we observe that there is a trend of increase in accuracy with the increase in the level of basis sets employing HF method. But CAM-B3LYP results with Pople basis sets are very much nearer to the experimental values making DFT formalisms attractive. Unlike correlation consistent basis sets which converge towards the basis set limit by increasing the level of basis set in a systematic fashion, the same does not hold true with Pople basis sets with DFT functionals.

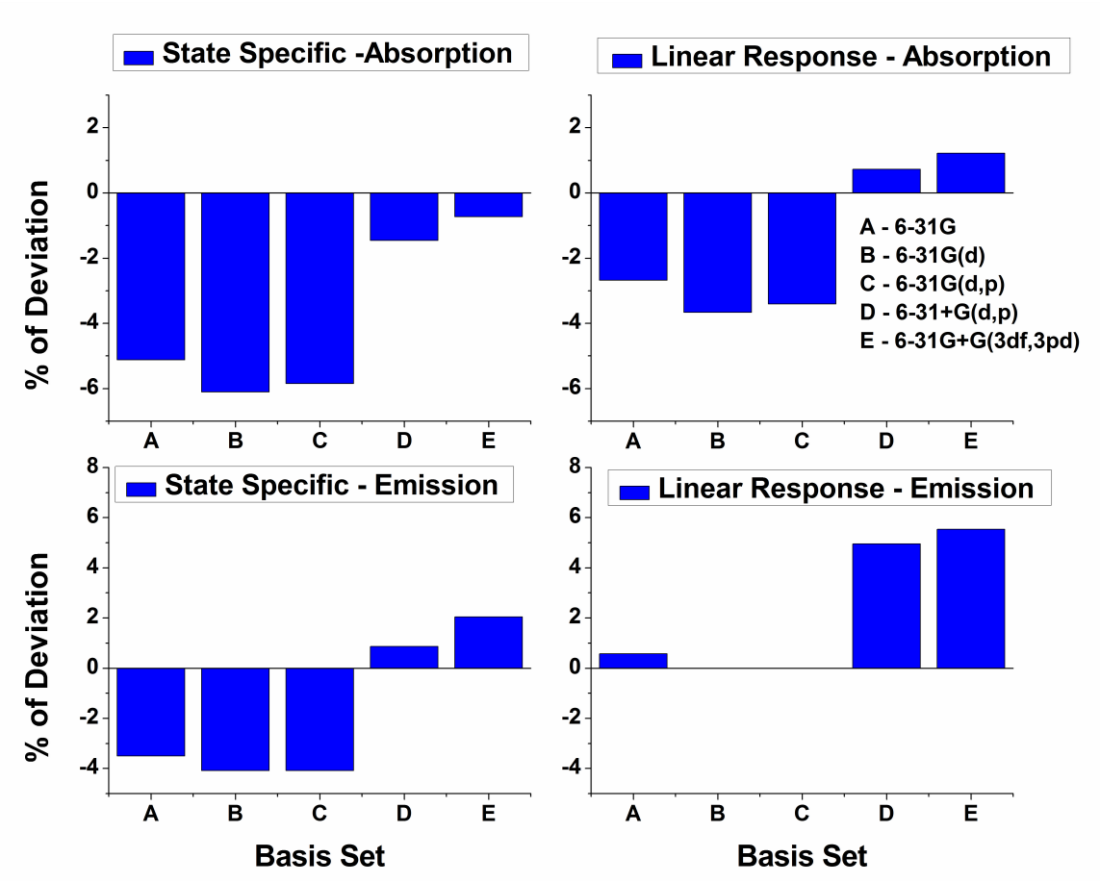

Figure 5.7. Percentage deviation of absorption and emission energies of dimer employing CAM-B3LYP functional with various basis sets in both SS and LR approaches in the PCM framework.

Exchange-correlation functionals used in DFT are developed adopting two strategies, either the functional should be self-interaction free, density should become constant in the case of the uniform electron gas, and few other constrains [32] or by fitting the parameters to reproduce the experimental results. Empirical functionals which are tested here contain a large number of parameters which are fitted to a training set to produce accurate experimental data and they give accurate results for the systems and properties contained in the training set [33]. The same is evident from examining the optical properties with various basis sets. When we increase the hierarchy of basis sets, we do not observe any specific trend being followed with respect to various exchange-correlation functionals, unlike non-empirical functionals which contain few or no fitted parameters and usually exhibit a trend. The inaccuracies in DFT formalisms arises basically due to lack of functional which exactly gives accurate exchange correlation energy and also due to insufficient basis set. A proper combination of functional and basis set which probably cancels out the error arising due to each other would give values closer to the experiments.

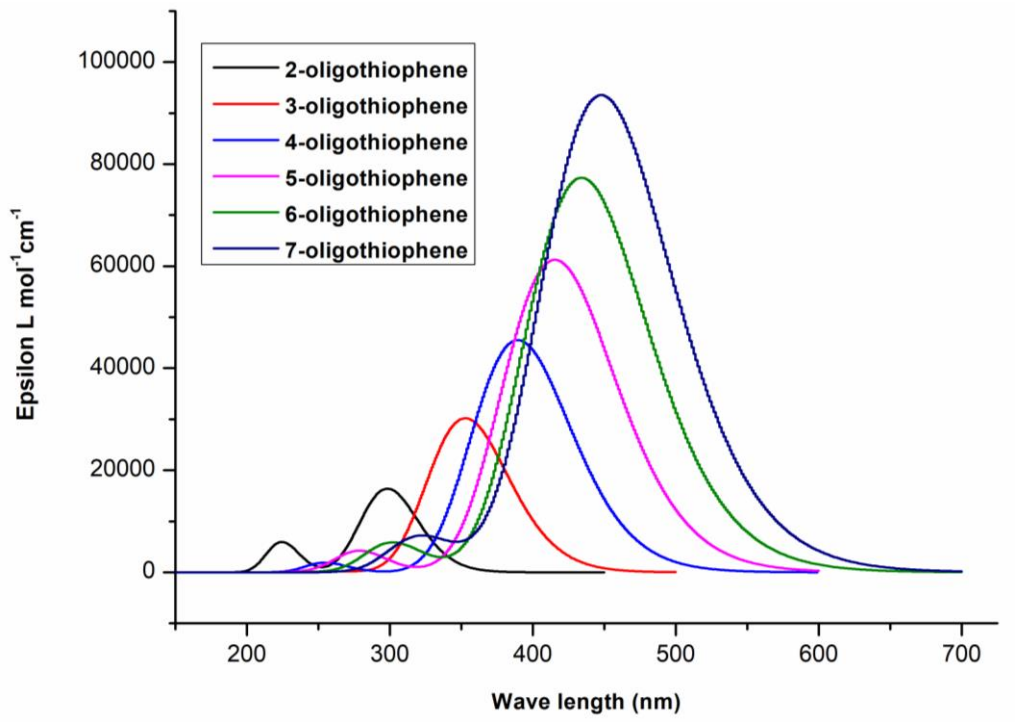

Figure 5.8. The calculated absporption spectra of oligothiophenes (2-7) with CAM-B3LYP functional and 6-31+G(d,p) in 1,4-Dioxane solvent.

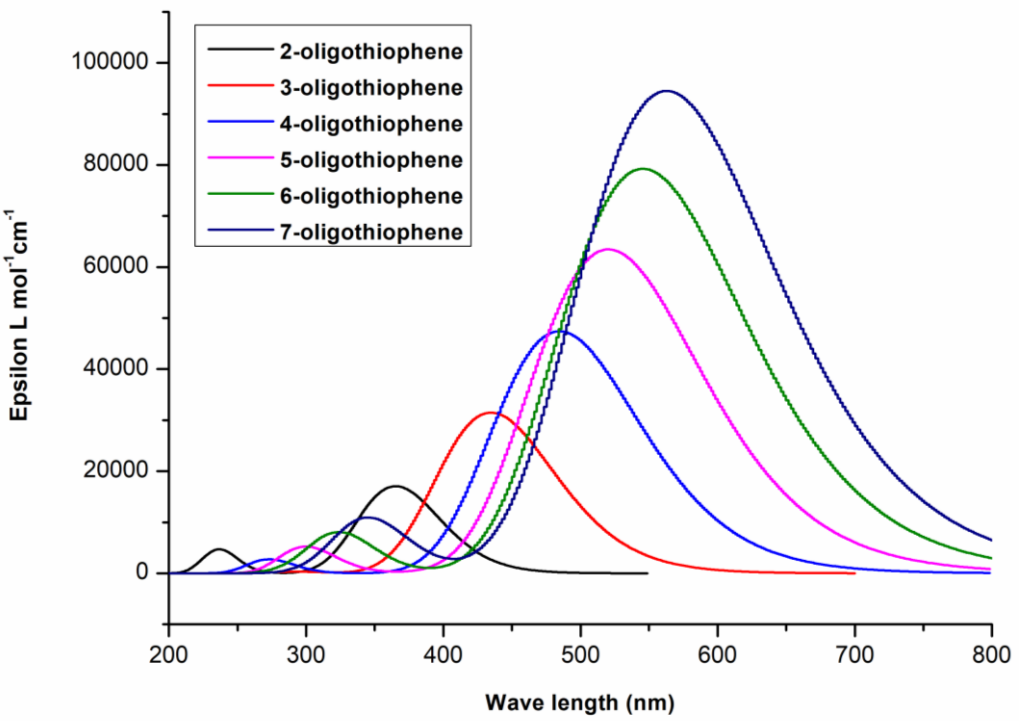

Figure 5.9. The calculated emission spectra of oligothiophenes (2-7) with CAM-B3LYP functional and 6-31+G(d,p) in 1,4-Dioxane solvent.

Among the tested functionals, CAM-B3LYP is found to give values closer to the experiments with various basis sets and solvent formalisms chosen. The absorption and emission spectra of all the oligothiophenes (2-7) calculated with the CAM-B3LYP functional and 6-31+G(d,p) basis set in SS approach are plotted in the Figures 5.8 and 5.9. From Figure 5.8 and 5.9, we observed that as the conjugation increases with the chain length, red shift is observed in the absorption and emission spectra of oligothiophenes.

5.4. Conclusions

The role of functional, solvent formalisms and basis set effects in determining optical properties is investigated for a series α-oligothiophenes. Among the various functionals tested, range-separated hybrid functional, CAM-B3LYP gave the results closer to the experiment when compared to the Global and Meta hybrid functionals. The accuracy of hybrid and meta-hybrid functionals decreased with increase in chain length and the addition of diffusion functions whereas the inclusion of "d" functions in the basis set improved results. On the other hand inclusion of "p" functions in the basis set with all the functionals and solvent, formalisms had no effect in varying the optical properties. Among the four functionals studied, the long-range corrected CAM-B3LYP produced accurate results and ωB97XD functional consistently underestimated the wavelength maxima values. SS approach in combination with CAM-B3LYP functional employing 6-31+G(d,p) provided better results, which can be attributed to a proper description of short and long range effects in the functional, proper description of molecular orbitals through the basis set and a better description of solute-solvent effects.

The most significant aspect which is often not highlighted in the literature is the fact that the accuracy of DFT methodologies with proper choice of basis set can also be due to the cancellation of errors. DFT methodologies employ empirical parameters based on comparison with experimental data using a specified basis set where DFT parameters absorbing the errors arise due to the incompleteness of basis sets. We did not observe any specific trend in the accuracy of optical properties with the increase of level of the basis sets using all the functionals. Hence, it need not be assumed that employing a very large basis set assures the accuracy in DFT formalism with functionals fitted with various empirical parameters. Thus we have shown how the accuracy of different functionals varies depending upon the basis set chosen and solvent formalism employed in determining the optical absorption and emission of an important π-conjugated system.

5.5. References

[1] C. Adamo, D. Jacquemin, Chem. Soc. Rev., 2013, 42, 845.

[2] B. Mennucci, Phys. Chem. Chem. Phys., 2013, 15, 6583.

[3] A. Pedone, G. Proampolini, S. Monti, V. Barone, Phys. Chem. Chem. Phys., 2011, 13, 16689.

[4] A. Pedone, V. Barone, Phys. Chem. Chem. Phys., 2010, 12, 2722.

[5] A. Pedone, J. Bloino, V. Barone, J. Phys. Chem. C, 2012, 116, 17807.

[6] A. Pedone, J. Bloino, S. Monti, G. Prampolini, V. Barone, Phys. Chem. Chem. Phys., 2010, 12, 1000.

[7] A. Pedone, G. Prampolini, S. Monti, V. Barone, Chem Mater., 2011, 23, 5016.

[8] D. Jacquemin, A. Planchat, C. Adamo, B. Mennucci, J. Chem. Theory Comput., 2012, 8, 2359.

[9] F. Labat, I. Ciofini, H. P. Hratchian, M. J. Frisch, K. Raghavachari, C. Adamo, J. Am. Chem. Soc., 2009, 131, 14290.

[10] A. Pedone, J. Chem. Theory Comput., 2013, 9, 4087.

[11] S. Chibani, A. D. Laurent, A. Blondel, B. Mennucci, D. Jacquemin, J. Chem. Theory Comput., 2014, 10, 1848.

[12] E. Runge, E. K. U. Gross, Phys. Rev. Lett., 1984, 52, 997.

[13] M. Petersilka, U. J. Grossmann, E. K. U. Gross, Phys. Rev. Lett., 1996, 76, 1212.

[14] M. A. L. Marques, E. K. U. Gross, Annu. Rev. Phys. Chem., 2004, 55, 427.

[15] M. E. Casida, *Recent Advances in Density Functional Methods*, World Scientific: Singapore, 1995.

[16] E. U. K. Gross, J. F. Dobson, M. Petersilka, *Density Functional Theory II*,

Springer: Heidelberg, 1996.

[17] R. Bauernschmitt, R. Ahlrichs, Chem. Phys. Lett., 1996, 256, 454.

[18] F. Furche, J. Chem. Phys., 2001, 114, 5982.

[19] J. Fabian, Theor. Chem. Acc., 2001, 106, 199.

[20] W. Meeto, S. Suramitr, S. Vannarat, S. Hannonbua, Chem. Phys., 2008, 349, 1.

[21] C. Jamorski, J. B. Foresman, C. Thilgen, H. P. Lüthi, J. Chem. Phys., 2002, 116, 8761.

[22] A. Dreuw, J. L. Weisman, M. HeadGordon, J. Chem. Phys., 2003, 119, 2943.

[23] A. Dreuw, M. Head-Gordon, J. Am. Chem. Soc., 2004, 126, 4007.

[24] D. J. Tozer, J. Chem. Phys., 2003, 119, 12697.

[25] A. L. Sobolewski, W. Domcke, Chem. Phys., 2003, 294, 73.

[26] S. Grimme, M. Parac, Chem. Phys. Chem., 2003, 4, 292.

[27] Y. Kurashinge, T. Nakajima, S. Kurashinge, K. Hirao, Y. Nishikitani, J. Phys. Chem. A, 2007, 111, 5544.

[28] B. M. Wong, J. G. Cordaro, J. Chem. Phys., 2008, 129, 214703.

[29] B. M. Wong, J. Phys. Chem. C, 2009, 113, 21921.

[30] B. M. Wong, M. Piacenza, F. D. Sala, Phys. Chem. Chem. Phys., 2009, 11, 4498.

[31] C. E. A. Azzam, A. Planchat, B. Mennucci, C. Adamo, D. Jacquemin, J. Chem. Theory Comput., 2013, 9, 2749.

[32] F. Jensen, *Introduction to computational chemistry*, 2nd edition, John Wiley & Sons Ltd, England, 2007.

[33] J. Tao, J. P. Perdew, V. N. Staroverov G. E. Scuseria, Phys. Rev. Lett., 2003, d91, 146401.

Chapter 6

Electronic structure calculations of linear and cyclic isothianaphthenes

6.1. Introduction

Thiophene based oligomers and polymers are one among the most frequently studied organic π-conjugated systems in organo-electronics due to their chemical stability, synthetic availability and tunable electronic properties. These are extensively used in the bulk heterojuction solarcells, polymer based organic thin films transistors, organic light emitting diodes etc [1-3]. Cyclothiophenes are new family of thiophenes and have advantages over their linear counterparts with respect to the stability in redox states, processability and lack of end-perturbing effects [4,5]. The HOMO-LUMO gap of oligomer with chain length n = 10 is almost close to the band gap of polymer. This indicates cyclothiophenes behave like a polythiophene as they move on to the higher oligomer n = 10 [6]. Cyclothiophenes could afford tunable cavities of known dimension in the nanometer range, so they can be useful for in molecular recognition and host-guest chemistry [7-10]. Self-assembly of such macro cyclic systems can lead to the formation of nanotubes which may find applications in the area of biological and material science [7-10]. Cyclothiophenes are also used as building blocks for complex structures such as catenanes and knots [11]. Higher membered cyclothiophenes are more flexible due to availability of more degree of freedom from additional double bonds and larger spatial arrangement, resulting in less effective π-overlap throughout the rings due to the changes in planarity [12].

Oligothiophenes where thiophene rings are fused with benzene rings are called as isothianaphthenes (ITNs) [13]. Polyisothianapthene is a low band gap conducting polymer where the monomer is a thiophene unit with a benzene ring built onto it [13]. The aromatic nature of the six-membered benzene ring is expected to affect the electronic structure of the polymer in two ways. Various resonance structures are expected to lead to higher stability and more nearly equal bond lengths along the pseudo polyene backbone. Similarly the polarizability of the benzene ring would tend to reduce the repulsive electron-electron interactions between two π-electrons on the same ring or on neighboring carbons along the backbone. Due to these peculiar properties, isothianaphthenes exhibit higher stabilities and lower band gaps than the corresponding thiophenes. We have investigated a detail account of structural and conductivity properties of cyclic and linear systems of isothianaphthenes and their relationship in altering the band gaps employing DFT.

In this chapter, we discuss the structural and electronic properties of both cyclic and linear isothianaphthenes of chain length n= 6, 8, 10, 12 and 14, using B3LYP functional and 6-31G(d) basis set and linear polyisothianaphthenes are also studied both in syn and anti-forms employing periodic boundary condition in Gaussian 09 software. The optical properties of cyclic isothianaphthenes are studied using B3LYP [14,15] and CAM-B3LYP [16,17] functionals.

6.2. Linear Isothianaphthenes

Linear isothianaphthenes of both syn and anti-conformations are presented in the schematic representation shown in Scheme 6.1. In order to find the most stable conformation, geometry optimizations are performed without any symmetrical constraints. A comparison of stability between both the forms is calculated by subtracting the energy of anti-form from that of syn form. Negative sign indicates stability of syn-form with respect to the corresponding anti-form.

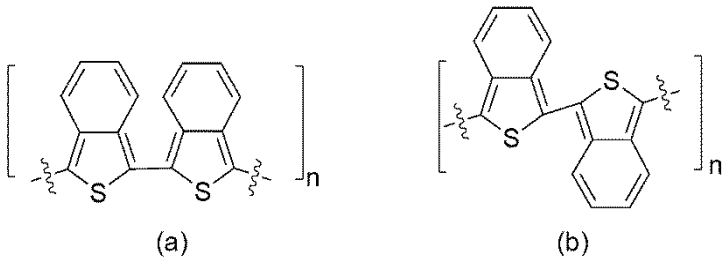

Scheme 6.1. Syn and anti-conformations of isothianaphthenes.

The syn and anti-forms of linear isothianaphthenes are found to be of almost equal energy. The optimized orientations of linear syn and anti-systems are shown in Figures 6.1 and 6.2 respectively. In order to understand the structural properties of linear isothianaphthenes in both the forms, dihedral angles of sulphur atoms between adjacent thiophene units of both syn and anti-forms in a dimeric unit are noted and found that the changes are similar for both forms, as tabulated in Tables 6.1 and 6.2 respectively.

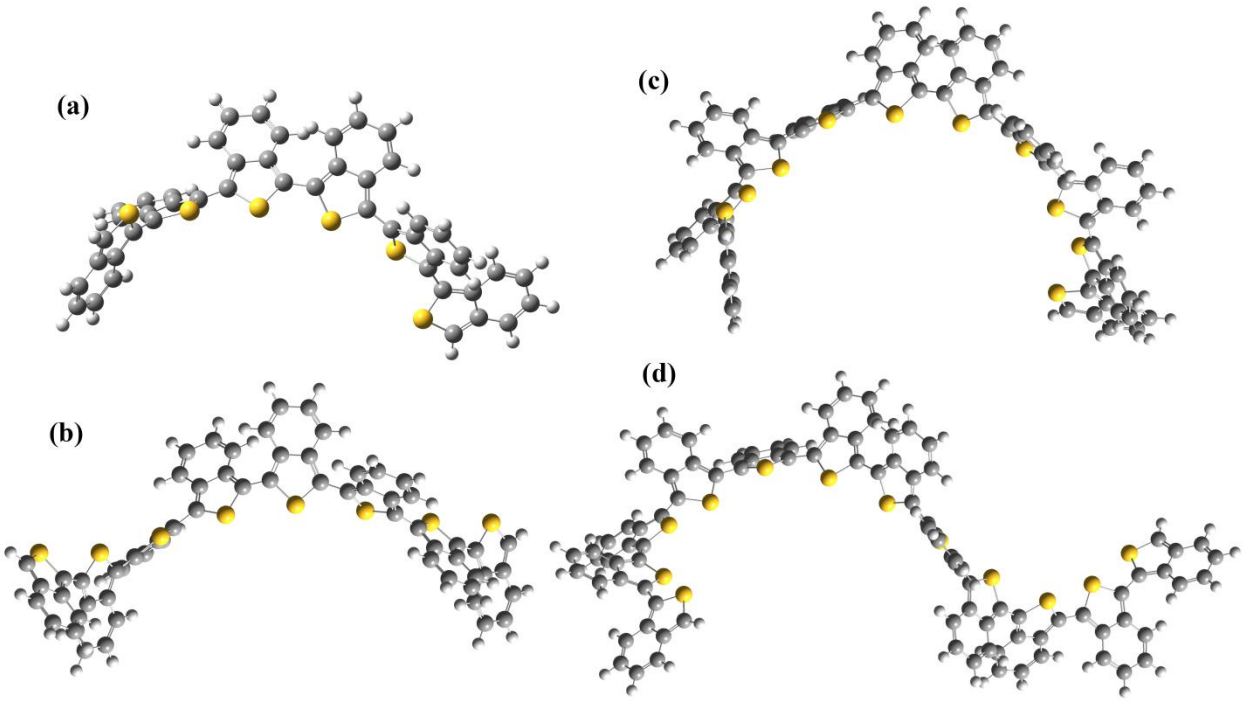

Figure 6.1. Geometry optimized structure of linear syn-isothianaphthenes (n=6, 8 10 and 12).

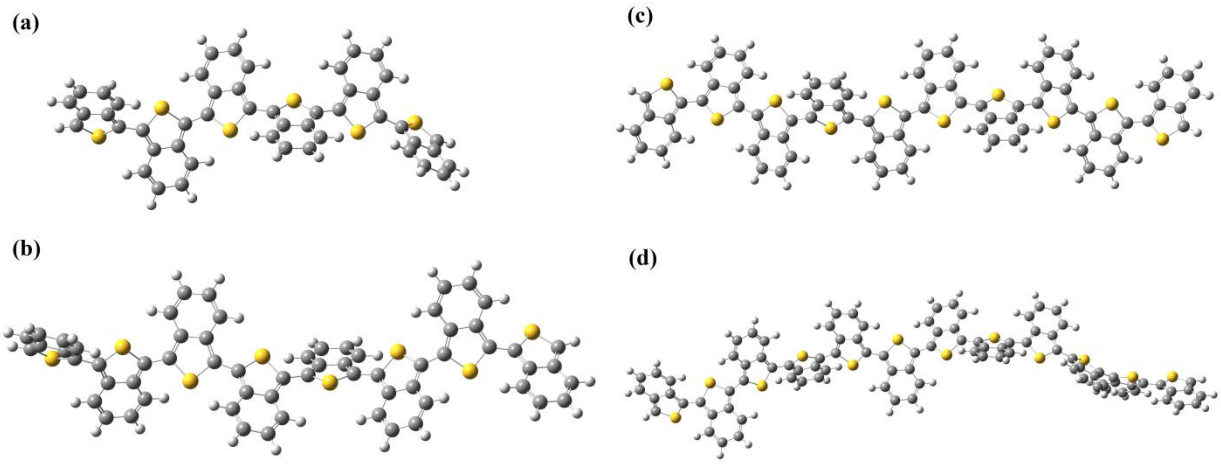

Figure 6.2. Optimized structure of Linear anti-isothianaphthenes (n=6,8,10,12).

From Table 6.1, and the optimized orientations shown in the above figures, it can be concluded that linear syn isothianaphthenes do not exhibit planarity and the dihedral angles indicate that the adjacent thiophene units are twisted in order to avoid steric repulsions between the adjacent benzene units fused with thiophene.

Dihedral Angles	LS-6- ITN	LS-8-ITN	LS-10-ITN	LS-12-ITN	LS-14-ITN
1	50.07	50.15	49.29	49.50	51.87
2	40.02	48.22	48.12	47.60	47.81
3	47.96	48.74	47.52	47.90	48.94
4	48.36	49.19	47.66	47.01	45.54
5	49.64	48.64	47.12	47.80	53.60
6		48.32	47.61	47.31	46.10
7		50.12	47.33	47.32	53.80
8			48.58	48.20	49.74
9			50.31	48.62	49.92
10				47.17	55.28
11				49.75	55.04
12					50.88
13					49.34

Table 6.1. Dihedral angles of Linear syn[n] ITN for n=6,8,10,12,14.

In order to understand the effect much better, we have considered a dimer unit, which is planar as shown in Figure 6.3(a). If planarity is to be maintained, it would result in closer distances of adjacent hydrogens of neighbouring benzene rings on isothianaphthene units. In order to avoid the steric repulsions arising from hydrogen atoms of benzene rings on adjacent monomers, the dihedral angles are twisted to give a stable geometry obtained after optimizations. The magnitude of this twist in linear syn isothianaphthene units of various chain lengths are given in Table 6.1. The twist which results in decreasing the steric repulsions of adjacent isothianaphthene units can be seen in Figure 6.3(b).

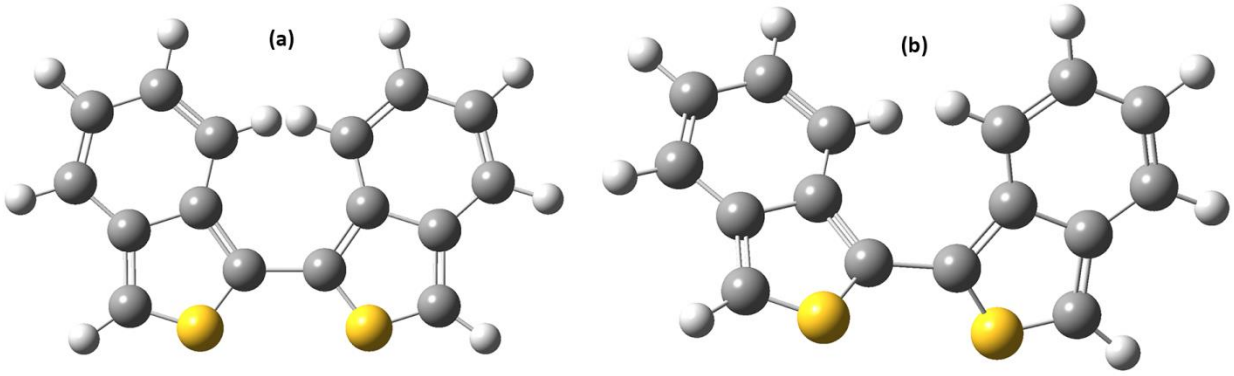

Figure 6.3. Linear syn isothianaphthenes (a). Syn form with planar orientation with dihedral angle 0^0 (b) Optimized Syn form with twist in dihedral angle of 51.95^0 from 0^0.

Even though these kind of steric repulsions are not directly envisaged in linear anti-form of isothianaphthenes as two isothianaphthenes are opposite to each other (Figure 6.4(a)), we observe that there is twist of the dihedral angles of adjacent sulphur atoms of isothianaphthene units which results in deviation from planarity as given in Table 6.2.

Dihedral angles	LA-6- ITN	LA-8-ITN	LA-10-ITN	LA-12-ITN	LA-14-ITN
1	133.87	134.02	133.69	133.84	133.49
2	136.67	137.29	136.97	136.07	136.47
3	136.07	138.06	136.74	136.73	137.00
4	135.88	138.18	138.05	137.10	137.88
5	132.96	137.54	140.66	137.15	137.28
6		136.29	138.06	139.03	137.28
7		133.41	136.73	138.61	137.44
8			136.96	137.32	136.70
9			133.68	137.47	137.46
10				136.80	137.52

11				132.48	136.90
12					136.12
13					133.29

Table 6.2. Dihedral angles of Linear Anti[n] ITN (LA[n]ITN) where n=6,8,10,12,14.

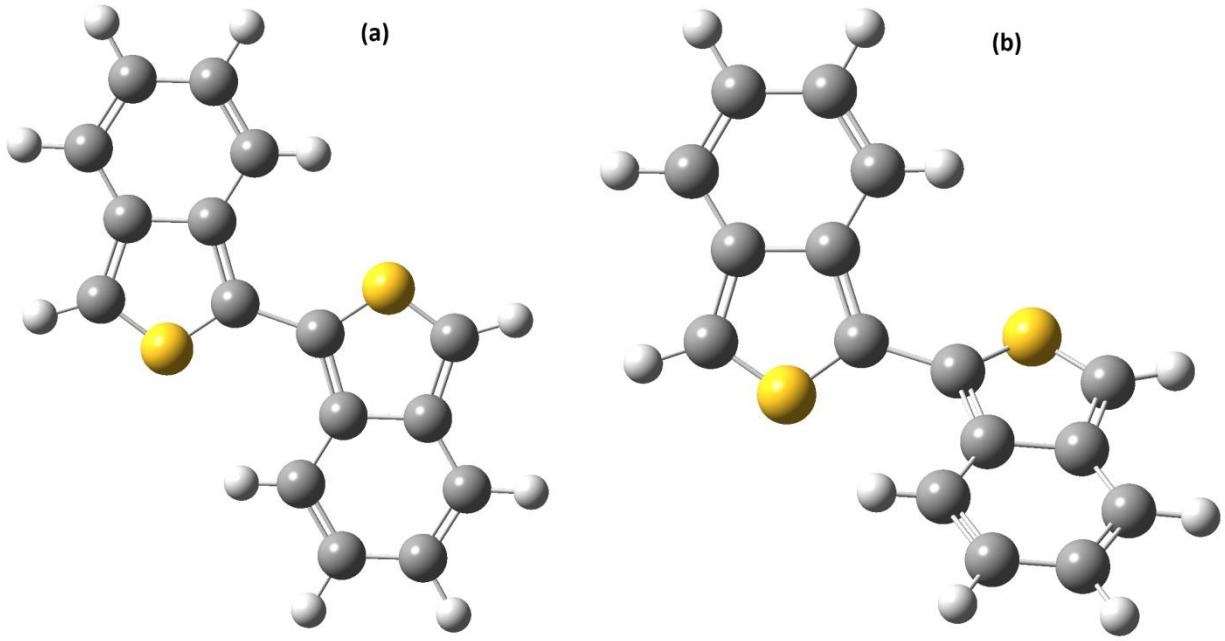

Figure 6.4. Linear anti ITNs (a). Anti-form with planar orientation with dihedral angle 180^0 (b) Anti-form with twist in dihedral angle 130.23^0 from 180^0.

If the adjacent isothianaphthene units assume the planarity, the distance between the sulphur atom and nearest hydrogen of fused benzene unit, on the adjacent isothanapthene unit would be around 2.2 Å, slight twist of around $40\text{-}50^0$ from the standard 180^0 which results in increase of sulphur to hydrogen distance to 2.7 Å thus relieving the strain in the molecule. Therefore the twisted architecture is slightly more stable than the planar forms of linear isothianaphthenes in both syn and anti-forms.

6.2.1. Bond length alterations (BLA)

One of the methods to alter the band gaps is by substitution on thiophene rings with various groups which can give rise to intermolecular charge transfer along the oligomer or polymer chain. Introduction of quinoid-type entity in the polymer backbone is found out to be a useful methodology from theoretical considerations. Bredas and co-workers have shown

that as quinoid structure is introduced into polythiophene geometry, band gap decreases linearly with increasing quinoid character [18]. Benzenoid and quinoid forms are shown in Figure 6.5. Bond length alterations (BLA) plots are drawn in order to understand the Aromaticity of ITNs.

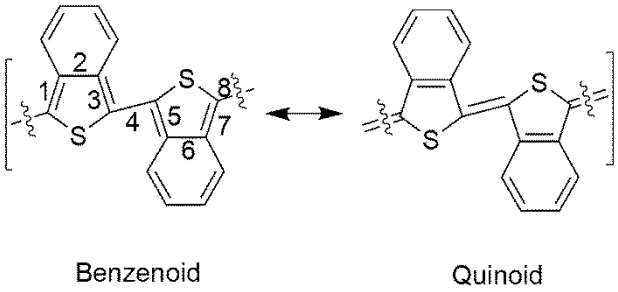

Figure 6.5. Benzenoid and quinoid forms of isothianapthenes.

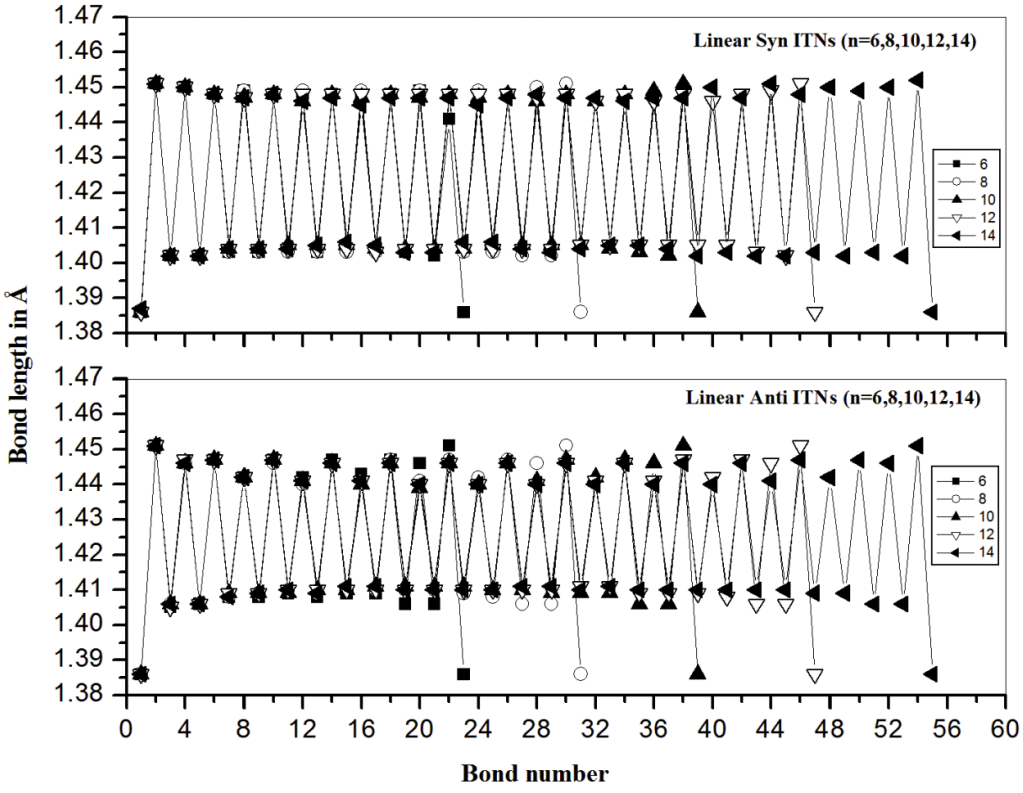

Figure 6.6. Bond length alterations of linear (n) isothianapthenes (both syn and anti-forms, n=6,8,10,12,14).

Increasing the chain lengths did not result in any change in variations of bond lengths in the linear systems. Due to the end effects, we observe that the terminal bonds at the edges of linear systems being reduced to a bond length of 1.38 Å in both the conformations. Linear

anti- isothianaphthenes exhibited lesser band gap due to the predominance of quinoid form compared to that of syn form. The inter-connecting bond between the two rings is found to be around 1.45Å for linear syn isothianaphthenes where as it is around 1.44 Å for anti isothianaphthenes. In essence, we conclude that linear isothianaphthenes assume a benzenoid form with bond lengths around 1.44 to 1.45 Å.

6.2.2. HOMO LUMO Energies and band gaps

To understand the electronic properties we have calculated frontier orbital energies and band gaps of linear syn and anti isothianaphthenes and tabulated in Table 6.3 and 6.4 respectively. From Table 6.3, it is clear that the band gaps of linear syn isothianaphthenes decrease with increase in number of units till n=14 and is not appreciably varying for n=10 to 14 systems. The oligomeric syn isothianaphthene is found to have a band gap comparable to polythiophene (2.05 eV). In contrast to linear syn-isothianaphthenes, anti isothianaphthenes have shown comparatively lesser band gaps (Table. 6.5) and are found to decrease drastically with the increase in chain length. This can be understood by examining the optimized orientations of syn and anti-conformations of linear isothianaphthenes shown in Figures 6.1 and 6.2. Compared to anti-forms linear syn-isothianaphthenes are found to be more strained and distorted in geometry due to the steric effects of fused benzene on the thiophene unit. This is attributed to the slightly larger band gaps of linear syn-isothianaphthenes when compared to the anti-forms.

No. of units	HOMO (eV)	LUMO (eV)	Band gap (eV)
6	-4.62	-2.27	2.35
8	-4.65	-2.31	2.34
10	-4.46	-2.41	2.05
12	-4.45	-2.42	2.03
14	-4.39	-2.43	1.96

Table 6.3. HOMO, LUMO energies and band gaps of linear syn-ITNs.

No. of units	HOMO (eV)	LUMO (eV)	Band gap (eV)
6	-4.39	-2.45	1.94
8	-4.32	-2.57	1.75
10	-4.25	-2.64	1.61
12	-4.24	-2.66	1.58
14	-4.18	-2.69	1.49

Table 6.4. HOMO, LUMO energies and band gaps of linear anti-ITNs.

6.3. Cyclic Isothianapthenes

Cyclic isothianaphthenes are peculiar in their geometry and different from linear isothianaphthenes in that they exhibit different strain effects. Following geometrical optimizations, stability of syn forms are calculated (Table 6.5) with respect to anti-forms employing a formula similar to that applied in the case of linear forms. In addition to that strain energies are also calculated (Table 6.6). Stability of syn cyclic isothianaphthenes found to decrease with increase in ring size where an exceptional stability is exhibited by the n=10 cyclic syn system.

No. of units	Stability (kcal/mole)
6	+16.94
8	+20.08
10	+53.34
12	+27.61
14	+47.69

Table 6.5. Stability of syn cyclo-ITNs with respect to anti-forms.

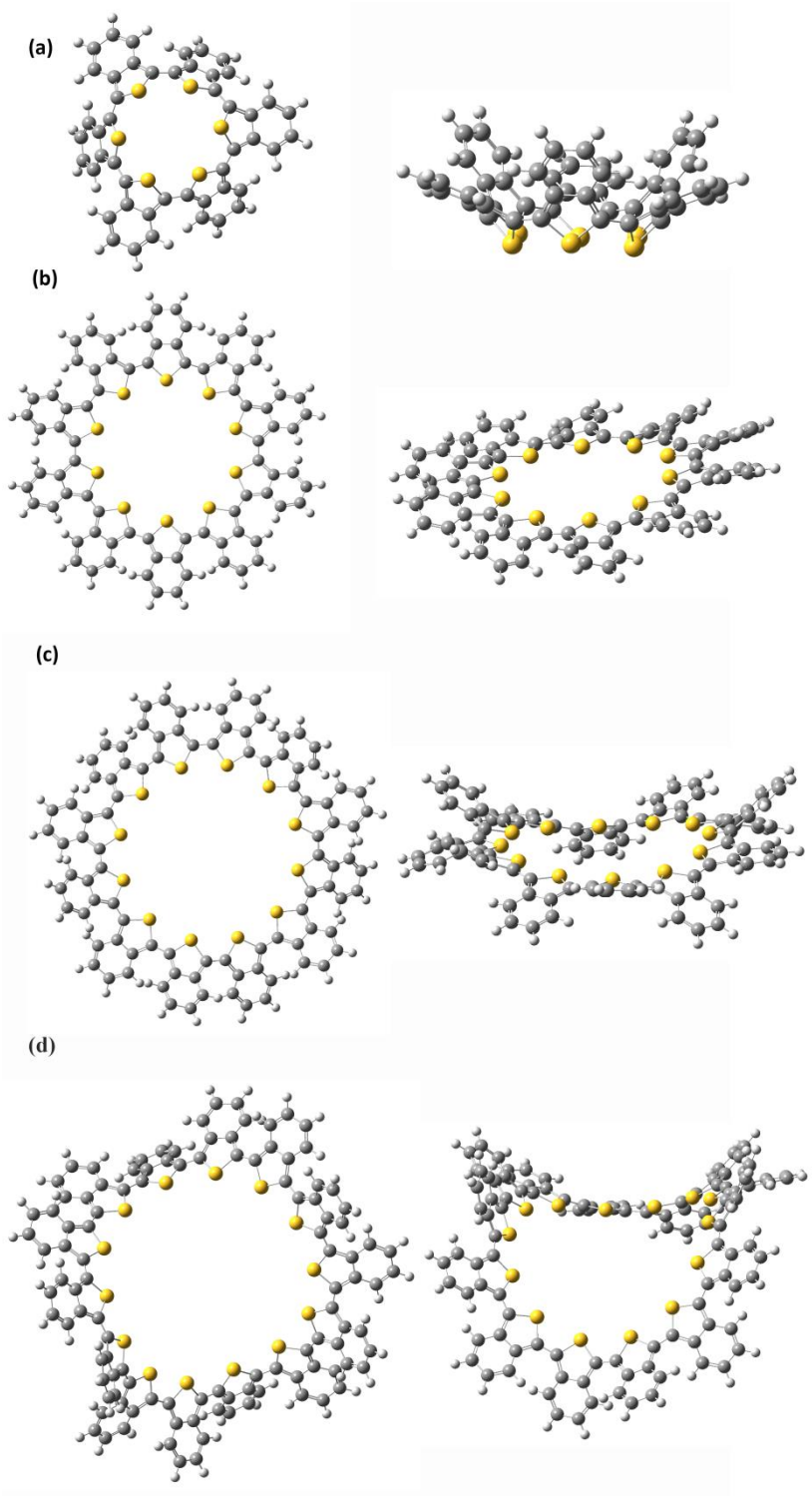

Figure 6.7. Optimized orientations of cyclic syn ITNs (n=6, 10, 12, 14) with top and side views respectively.

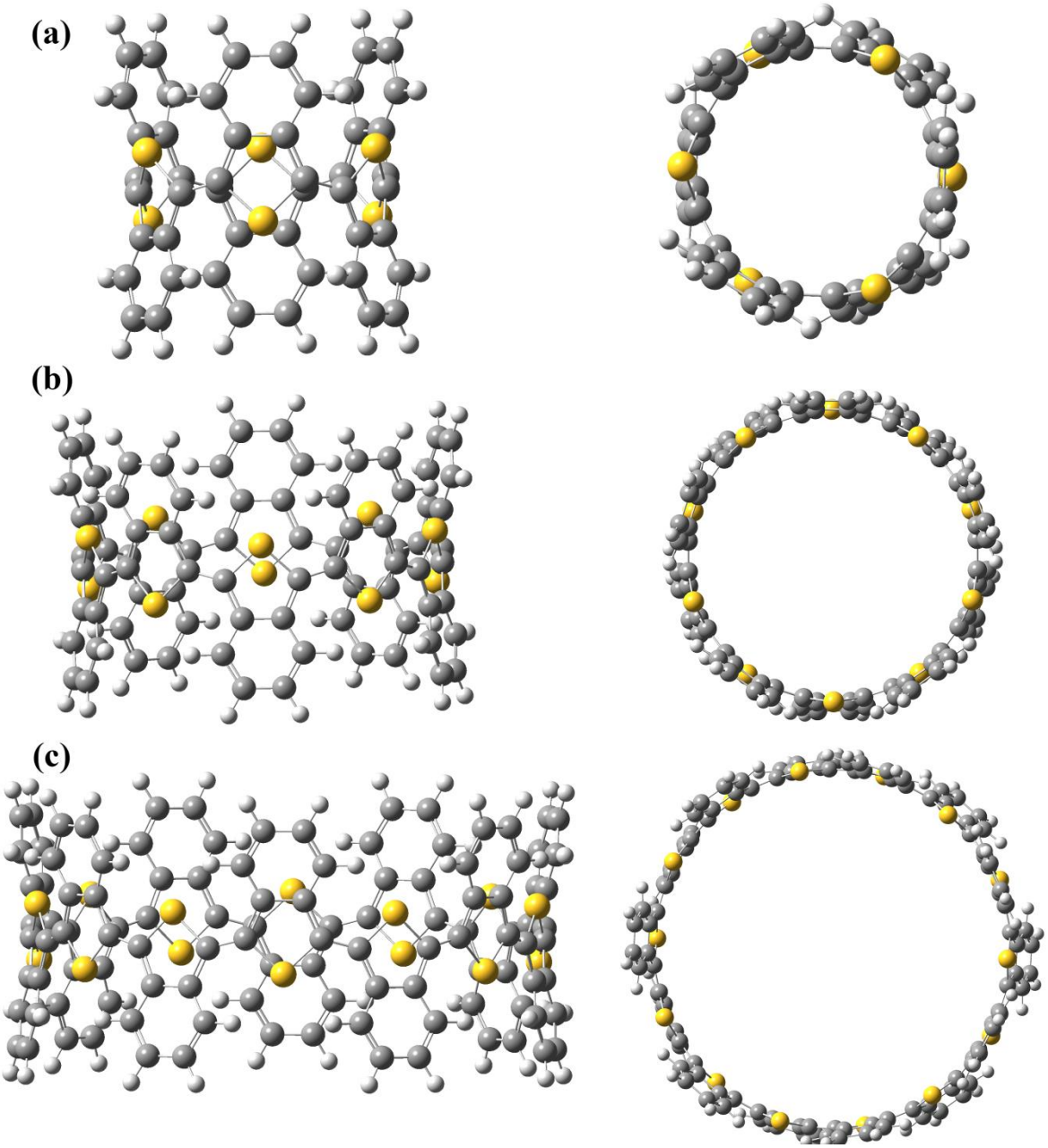

Figure 6.8. Optimized orientations of cyclic anti ITNs (n=6, 10, 14) with side and top views respectively.

From the optimized orientations, it is clear that syn-cyclic isothianaphthenes adopted crown shaped geometry whereas anti-forms adopted a cylindrical geometry shown in Figure 6.7 and 6.8 respectively. There is an exceptional instability associated with syn-isothianaphthene of size n=10, in order to understand this exceptional behaviour strain energies are calculated for cyclic systems.

6.3.1 Strain energies of the cyclic isothianaphthenes

Compared to the linear isothianaphthenes, cyclic isothianaphthenes have strain energies due to their curvature. Strain energy per monomer unit for cyclic systems are calculated in order to understand the anomaly associated with stability, where we observe no definite change in pattern of stability (Table 6.5) with the increase in value of n. Strain energy E_n is calculated in comparison with the linear polymeric system using the following equation [6],

$$En = (E_{(Cyclic\ nITN)} - nE_{(PITN)})/n \qquad (1)$$

(Absolute energy per ITNs unit $E_{(PITN)}$ is obtained from PBC calculation of isothianaphthenes at the same level of basis set and functional. Two isothianaphthene units were used as the unit cell, and the absolute energy of the unit cell was divided by 2 and energies of syn and anti-forms are calculated separately. Strain energies of cyclic systems are shown in Table 6.6.

No of units	Cyclic syn ITN (Strain energy Kcal/mole)	Cyclic anti ITN (Strain energy Kcal/mole)
6	8.51	5.23
8	4.94	2.00
10	6.46	0.74
12	2.86	0.14
14	3.69	-0.14

Table 6.6. Strain energies of cyclic syn and anti ITNs.

Cyclic syn-isothianaphthenes strain energy found to decrease from 8.51 kcal/monomer to 4.94 kcal for n=6 and 8 and there is an increase in strain energy for n=10, where the strain energy is 6.49 kcal. Zang and co-workers, discussed the peculiar molecular and electronic properties of syn cylco[10]thiophene. They found that this system exhibited unusual optoelectronic properties due to the ring strain. The unusual strain energy of cyclic isothianaphthenes (n=10) would be responsible for low stabilities. There is a decrease in strain energy for n=12 and a slight increase for n=14 system. For all the anti-systems we find

a decrease in strain energy with the increase in ring size showing a general trend. The strain energy variations provide us with an insight into the trend of stability of the systems. Comparison of strain energies of both syn and anti-cyclic isothianaphthenes are shown in Figure 6.9.

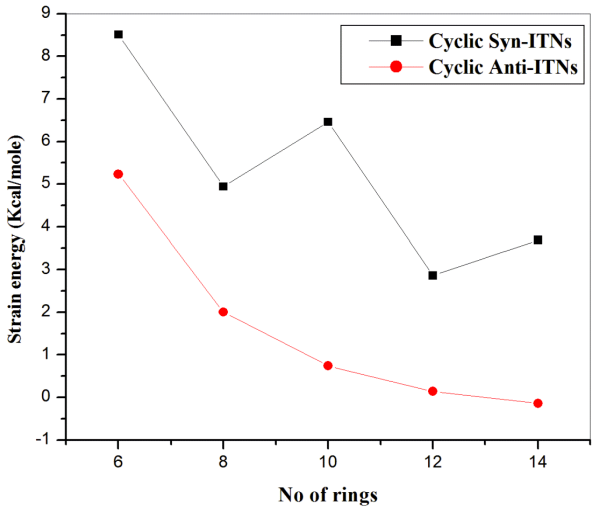

Figure 6.9. Strain energies of syn and anti-cyclic ITNs (n=6,8,10,12,14).

Anti-forms are found to exhibit lower strain energies compared to the syn cyclic isothianaphthenes correlating well with the stabilities. Cyclic syn- isothianaphthene system with n=10 found to show an exceptional instability due to the high strain energy associated with it. For anti-systems we can observe from n=14, the strain energy is -0.14 indicating that strain energy decreases as the n number increase in anti-systems. Lower strain energy also gives us the insight that anti-form is more stable than the syn-counterparts.

6.3.2. Bond length alterations (BLA)

Employing bond length alteration calculations, we found that in the case of cyclic isothianaphthenes the qunioid form is found to be predominant compared to that of benzenoid form, with inter-connecting bonds between the adjacent rings around 1.36 to 1.37 Å (shown in Figure 6.10). Compared to the cyclic syn isothianaphthenes the bond length (around 1.365 Å) of inter-connecting bond in anti isothianaphthenes was found to be lower (around 1.355 Å) indicating that cyclic anti isothianaphthenes have more quinoid character compared to cyclic syn isothianaphthenes. On the other hand the band gap of cyclic syn isothianaphthenes found to be lesser than that of cyclic anti isothianaphthenes.

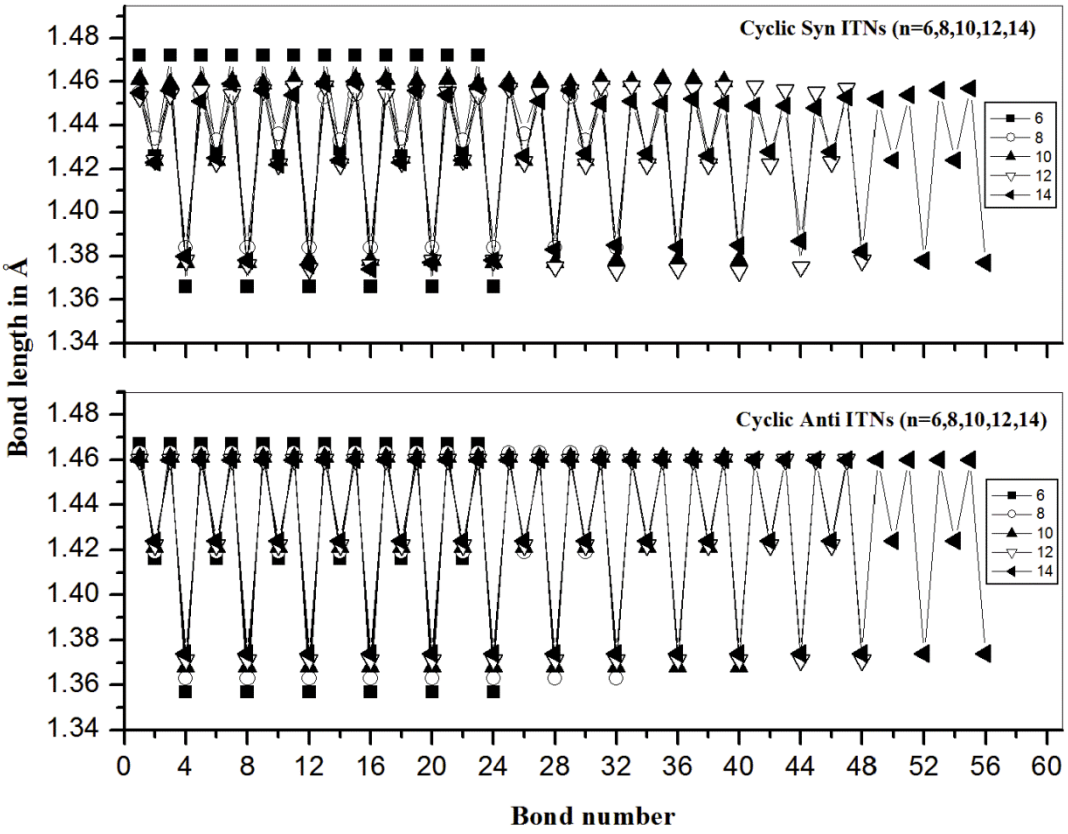

Figure 6.10. Bond length alterations of cyclic ITNs in both syn and anti-forms are shown.

6.3.3. HOMO, LUMO energies and band gaps

Analysing Table 6.7 and 6.8 it is clear that the cyclic syn-isothianaphthenes exhibit lower band gaps compared to the anti-forms. It is important to see that among the optimized orientations of both the forms, syn-cyclic isothianaphthenes adopt an almost planar crown form whereas anti-forms are in the cylindrical form. In the case of cyclic syn-isothianaphthenes, there is a decrease in band gap from n=6 to 8 and then a sharp increase in band gap for n=10 and again a decrease in band gap from n=12. The higher strain energy of cyclic syn-isothianaphthene (n=10) leads to decrease in HOMO energy thus increasing the band gap. Although not exactly, it almost coincides with the strain energies where we observe a decrease in strain energy from n=6 to 8 with a sharp increase for n=10 followed by decrease. Figure 6.11 plotted between number of rings and strain energy/band gap shows a good correlation of band gap and strain energy.

No. of units	HOMO (eV)	LUMO(eV)	Band gap(eV)
6	-4.69	-2.16	2.53

8	-4.04	-2.81	1.23
10	-4.16	-2.67	1.49
12	-3.98	-2.69	1.29
14	-3.90	-2.79	1.11

Table 6.7. HOMO, LUMO energies and band gaps of cyclic syn ITNs.

No. of units	HOMO (eV)	LUMO(eV)	Band gap(eV)
6	-4.62	-1.87	2.75
8	-4.38	-2.15	2.23
10	-4.26	-2.32	1.94
12	-4.20	-2.44	1.76
14	-4.16	-2.51	1.65

Table 6.8. HOMO, LUMO energies and band gaps of cyclic anti-ITNs.

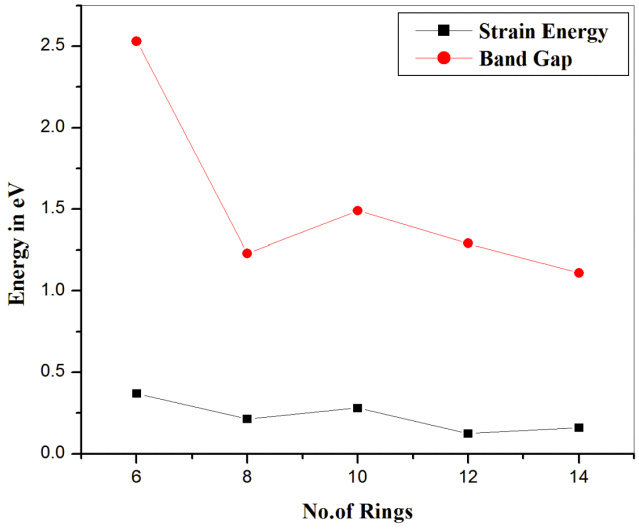

Figure 6.11. Strain energies and Band gaps of cyclic syn ITNs (n=6,8,10,12,14).

Thus it is clear that the increase in band gap would be due to the increase in strain energy. In case of anti-systems the correlation between band gap and strain energy is almost

exact where we observe the decrease in band gap with increasing chain length. HOMO and LUMOs of linear isothianaphthenes and cyclic isothianaphthenes have shown in the Figures 6.13 and 6.14 respectively. Due to non-planarity and distortion linear syn-isothianaphthenes HOMOs and LUMOs are not uniformly confined throughout the ring. In the case of linear anti isothianaphthenes as the chain length increases we observe that HOMOs, LUMOs contribution at the edges decreases. Unlike its linear counterparts, we observe that the HOMOs, LUMOs in the cyclic systems are confined throughout the ring due to the regular structures. As the chain length increases, the contribution of benzene ring of isothianaphthene unit decreases in both syn and anti-conformations.

6.3.4. Electrostatic potential surfaces of cyclic isothianaphthenes

Electrostatic potential (ESP) mapped surface is measure of charge distribution in a molecule three dimensionally, which allows us to visualize variably charged regions of a molecule, using colour codes [19]. The electrostatic charge of cyclic isothianaphthenes are computed by DFT has been superimposed on an electron isodensity surface. The red region indicate the higher negative electrostatic potential which is favourable to interact with electron density acceptors and the highest positive potential is represented by blue color indicates the electron deficient region, which is favourable to interact with electron rich species. The positive and negative regions of the molecule show where polar reactions might be more or less likely.

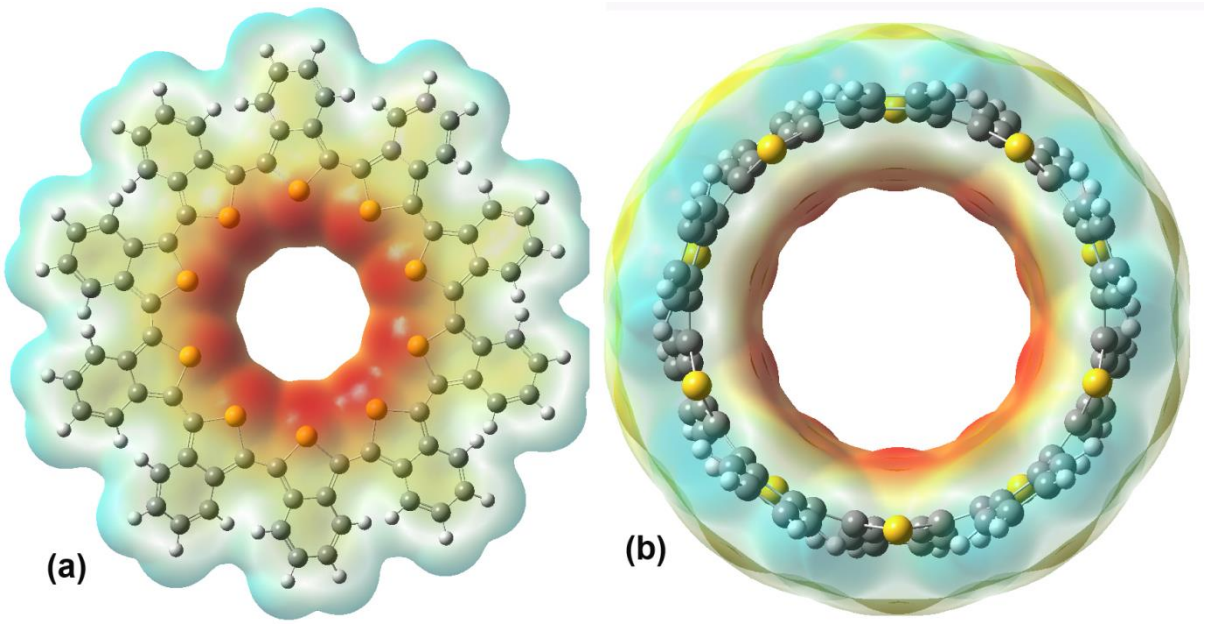

Figure 6.12. Electrostatic mapped potential of cyclic-syn [10]-ITN (a) and cyclic-anti-[10] ITN.

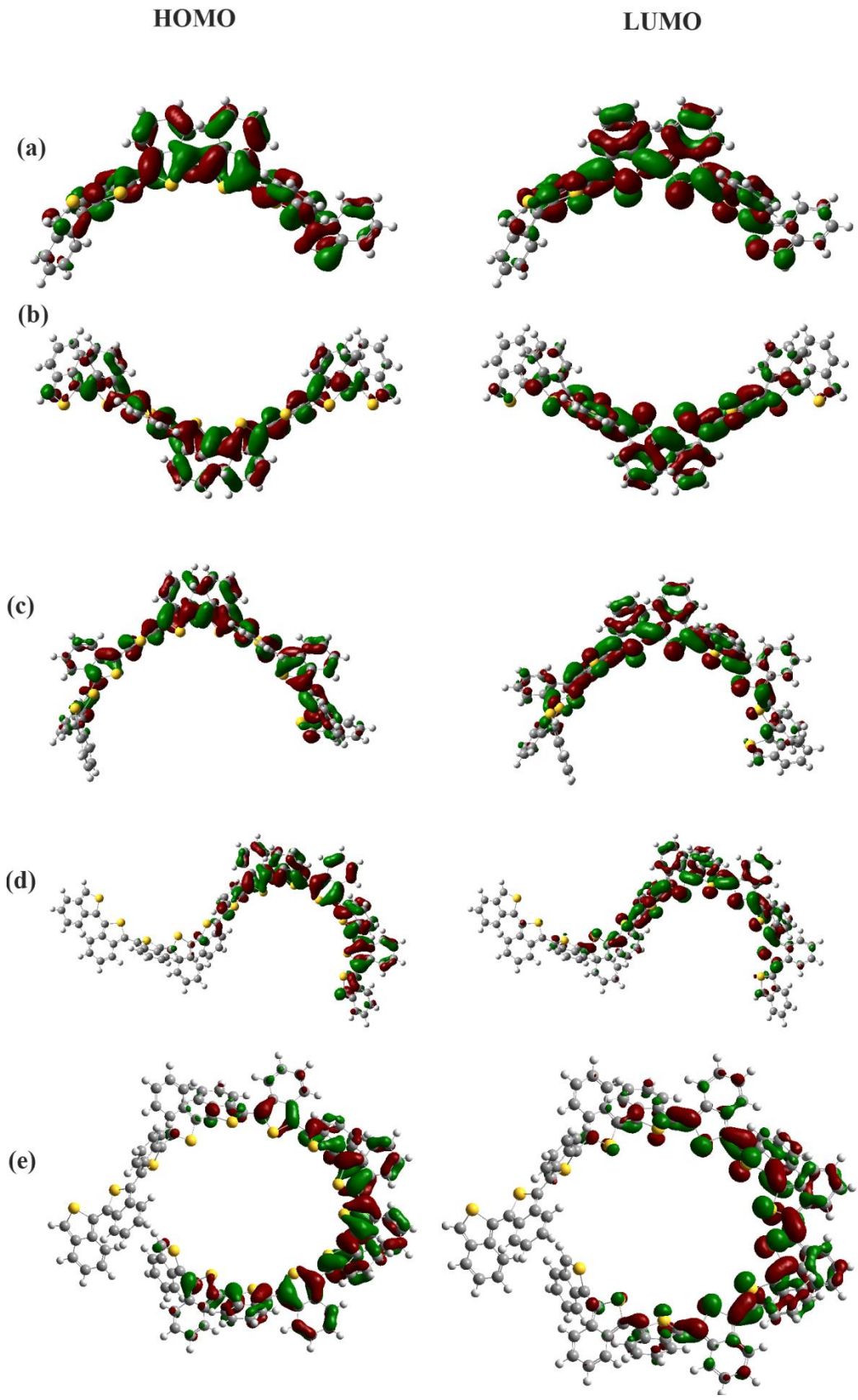

Figure 6.13. (a) HOMO and LUMO of Lin-Syn-[n]-ITN and (b) HOMO and LUMO of Lin-Anti-[n]-INT.

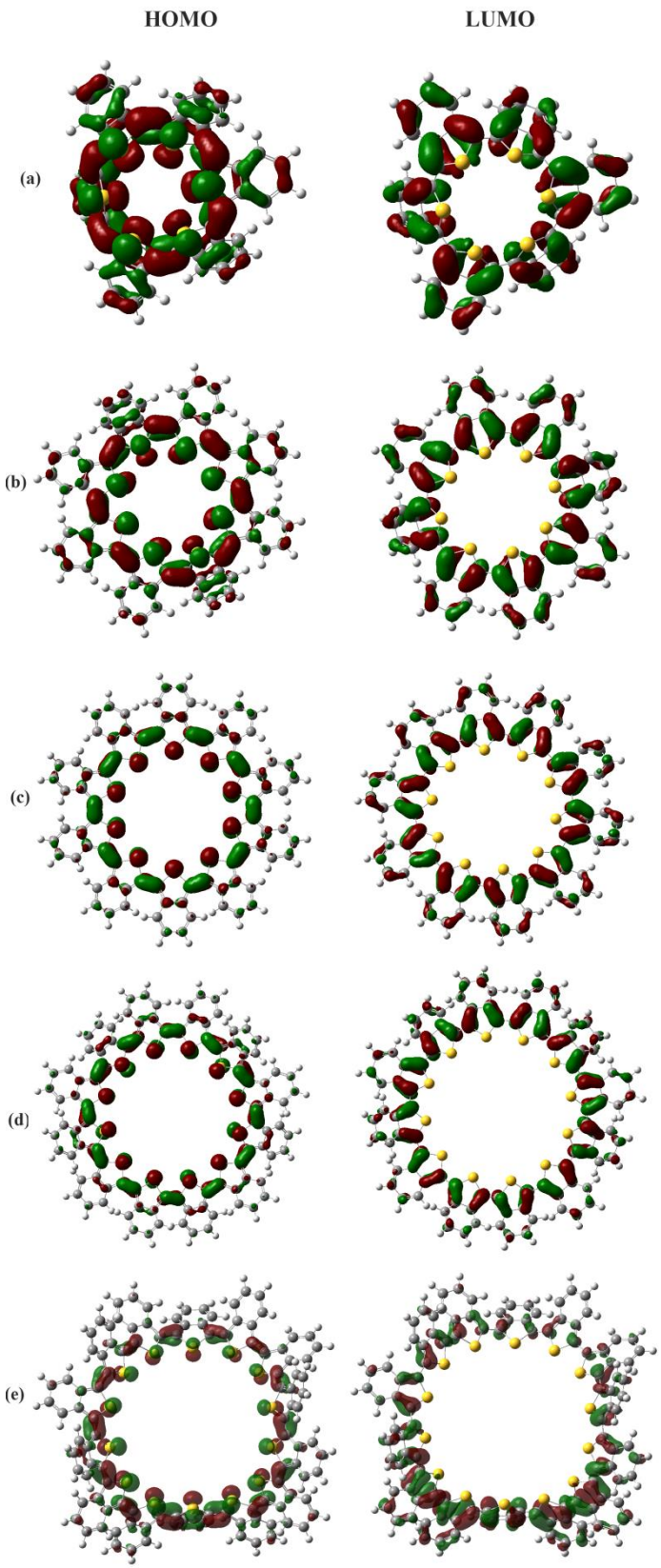

Figure 6.14. (a) HOMO and LUMO of Cyc-Syn-[n]-ITN and (b) HOMO and LUMO of Cyc-Anti-[n]-ITN.

From Figure 6.12, we can observe that the electron density (red colour) is concentrated more at the centre of the cyclic systems in both syn and anti isothianaphthenes. This suggests that these type of cyclic molecules with cavities attract cations may find application in host-guest chemistry as like crown ethers [20,21]. The diameters of the cyclic systems are also calculated for all the syn and cyclic isothianaphthenes and are shown in the Table 6.9 Cylic anti isothianaphthenes possess more diameter compared to the corresponding cylic syn isothianaphthenes.

No. of ITN units	Diameter (A^0)	
	Cyclic Syn ITNs	Cyclic Anti ITNs
6	6.14	8.15
8	7.66	10.24
10	9.67	12.83
12	12.42	15.09
14	13.78	17.70

Table 6.9. Calculated diameters of cyclic ITNs in both syn and anti forms.

6.3.5. Optical properties of cyclic isothianaphthenes

The optical properties of cyclic isothianaphthenes are studied in both syn and anti-forms using TD-DFT formalism with hybrid functional B3LYP and long-range corrected CAM-B3LYP functional in gas phase. Even though there are many theoretical and experimental studies on thiophene based cyclic systems [1-12] there are no studies on the optical properties of cyclic isothianaphthenes in the literature. It is now established that the hybrid functional B3LYP is inadequate to explain the charge transfer phenomena at long ranges and often deviate from the experimental values [22-24]. The long-range corrected functional CAM-B3LYP describes the charge transfer phenomena at short and long-ranges and produces a good correlation with experimental values [25].

As the chain length of the cyclic isothianaphthenes increases, the absorption value moves towards the lower energy/higher wave length region (infrared region). The absorption spectra of cyclic syn-[n]-ITNs as shown in the Figure 6.15 and intense transitions and molecular orbital contributions in electronic transitions between the occupied and unoccupied orbitals are tabulated in Table 6.10. As the chain length increases, the contribution from HOMO-1(H-1) $\rightarrow$ LUMO (L) increases till 10-monomer then again decreases till14-

monomer of cyclic syn isothianaphthene. The electronic transition from HOMO (H) → LUMO+1(L+1) contribution in the intense absorption transition is decreased. The systematic redshift is not observed with increase of chain length in the absorption spectra of cyclic syn isothianaphthenes calculated with both CAM-B3LYP and B3LYP functional.

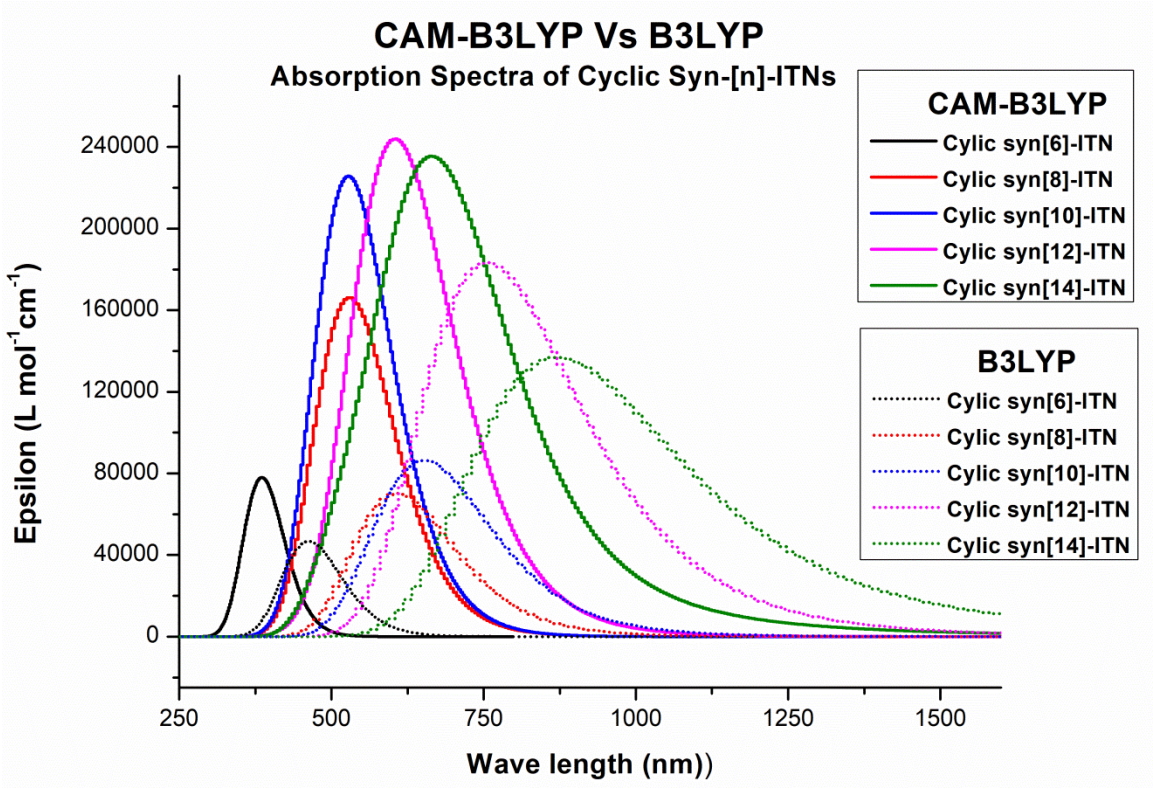

Figure 6.15. The calculated absorption spectra of cyclic syn-[n]-ITNs using B3LYP and CAM-B3LYP functionals.

Cyclic ITNs chain length	Absorption of Cyclic Syn ITNs			
	B3LYP		CAM- B3LYP	
	Intense absorption wave length (nm)	Major electronic transitions	Intense absorption wave length (nm)	Major electronic transitions
6	459	H-1→LUMO (65%), HOMO→L+1 (23%)	385	H-1→LUMO (30%), HOMO→L+1 (57%)
8	601	H-2→LUMO (64%), HOMO→L+2 (38%)	535	H-1→LUMO (43%), HOMO→L+1 (53%)

10	647	H-1→LUMO (58%), HOMO->L+1 (44%)	530	H-1→LUMO (42%), HOMO→L+1 (50%)
12	747	H-1→LUMO (63%), HOMO→L+1 (39%)	606	H-1→LUMO (38%), HOMO→L+1 (50%)
14	858	H-2→LUMO (43%), HOMO→L+1 (18%), HOMO→L+2 (26%)	674	H-1→LUMO (25%), HOMO→L+1 (42%)

Table 6.10. Intense absorption wave length (nm) and major electronic transitions of cyclic syn-[n]-ITNs calculated with B3LYP and CAM-B3LYP.

From the Figure 6.16, we observed that the absorption of cyclic anti-[n]-ITNs increases linearly with the increase of 'n' value with respect to both the functionals B3LYP and CAM-B3LYP. Computational studies of Kim and co-workers on absorption properties of organic sensitizers suggest that the long-range corrected CAM-B3LYP functional results in accurate results which describe long-range and short range interactions accurately [24].

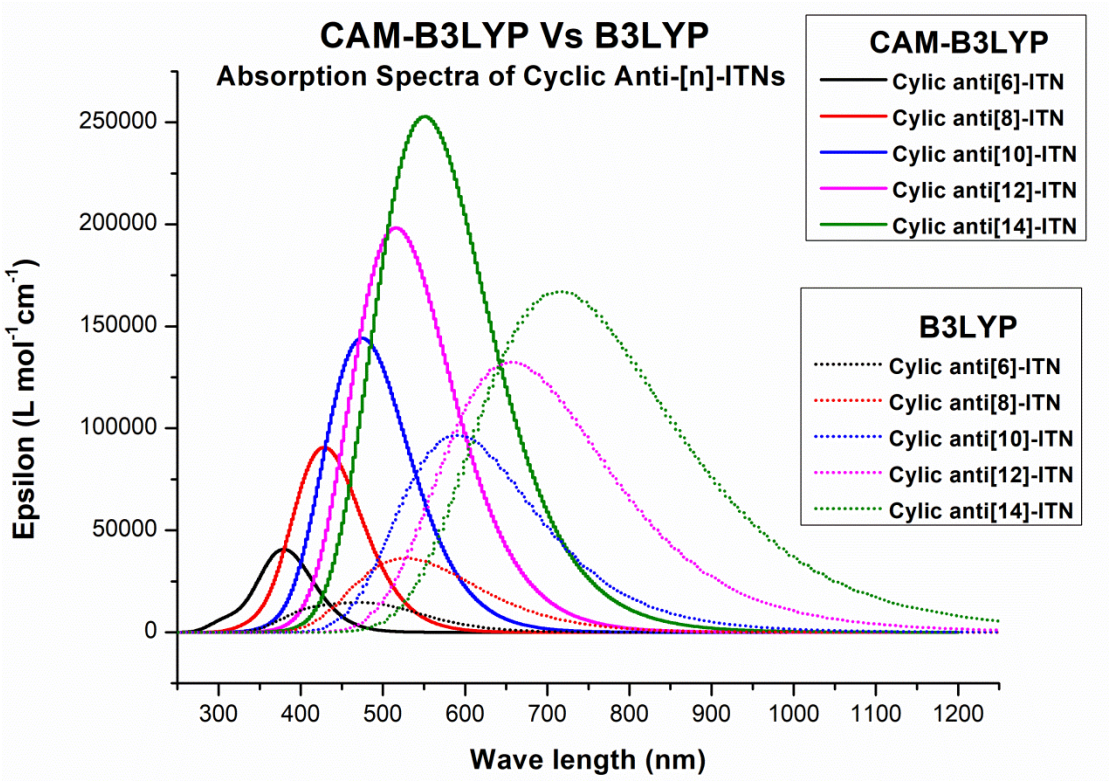

Figure 6.16. The calculated absorption spectra of cyclic anti-[n]-ITNs using B3LYP and CAM-B3LYP functionals.

Cyclic ITNs chain length	Absorption of Cyclic Anti ITNs			
	B3LYP		CAM- B3LYP	
	Intense absorption wave length (nm)	Major electronic transitions	Intense absorption wave length (nm)	Major electronic transitions
6	408	H-2→LUMO (26%), H-1→LUMO (69%)	379	H-1→LUMO (10%), HOMO→L+1 (78%)
8	499	H-2→LUMO (27%), H-1→LUMO (67%)	427	H-2→LUMO (11%), H-1→LUMO (11%), HOMO→L+1 (24%), HOMO→L+2 (42%)
10	577	H-1→LUMO (88%), H-2→LUMO (2%)	473	H-1→LUMO (23%), HOMO→L+1 (38%), HOMO→L+2 (19%)
12	645	H-2→LUMO (87%), HOMO→L+2 (13%)	514	H-2→LUMO (33%), HOMO→L+2 (50%)
14	705	H-2→LUMO (85%), HOMO->L+2 (13%	549	H-1→LUMO(34%), HOMO→L+1 (45%)

Table 6.11. Intense absorption wave length (nm) and major electronic transitions of cyclic anti-[n]-ITNs calculated with B3LYP and CAM-B3LYP.

The absorption spectra of all the cyclic isothianaphthenes (syn and trans) appear in UV-Visible region for shorter isothianaphthenes. As the chain length increases red shift is observed in absorption spectra. Because of their optical properties and extended conjugation, these cyclic systems may be useful in LED and photovoltaic applications. We have compared the absorption wave lengths of cyclic sy isothianaphthenes with earlier studies of Fabian and co-workers [26], Bäurle and co-workers on cyclothiophenes [7]. Cyclic syn isothianaphthenes show higher absorption wave lengths and more intense transitions than the corresponding syn cyclothiophenes studied. This can attributed to their higher conjugation in cyclic syn isothianaphthenes.

6.4. Conclusion

Structural and electronic properties of linear and cyclic isothianaphthenes in both syn and anti-conformations have been carried out. Linear isothianaphthenes are found to be twisted form rather than being in planar form to avoid the steric interactions. Both syn and anti-forms of linear isothianaphthenes are found to be almost equally stable. Stability of syn conformations are comparable to that of anti-forms although the magnitude of stability is found to be negligible. Band gaps of anti linear isothianaphthenes are found to be less compared to the corresponding syn forms and this could be due to less steric repulsions of anti-forms. Band gaps of linear anti-isothianaphthenes are found to be lower than that of syn-isothianaphthenes due to high distortion in geometry.

In the case of cyclic isothianaphthenes, anti-forms are found to be more stable compared to that of syn forms. Cyclic syn forms exhibited crown shaped geometry and anti-form exhibited a cylindrical geometry. Band gaps of cyclic isothianaphthenes in syn forms are found to be low compared to the anti-forms. Syn forms exhibited lower band gaps than anti-forms, which can be attributed to the geometrical nature of both the forms. Cyclic syn-isothianaphthenes exhibited higher strain energy than the of anti-forms. Cyclic isothianaphthene (n=10) found to show peculiar properties due to higher ring strain associated with curvature the effects of ring.

6.5. References

[1] D. Fichou, J. Mater. Chem., 2000, 10, 571.

[2] W. Ma, C. Yang, X. Gong, K. Lee, A. J. Heeger, Adv. Funct. Mater., 2005, 15, 1617.

[3] B. S. Ong, Y. Wu, Y. Li, P. Liu, H. Pan, Chem. Eur. J., 2008, 14, 4766.

[4] G. Fuhrmann, T. Debaerdemaeker, P. Bäuerle, Chem. Commun., 2003, 948.

[5] J. Krömer, I. Rios-Carreras, G. Fuhrmann, C. Musch, M. Wunderlin, T. Dabaerdemaeker, E. Mena-Osteritz, P. Bäuerle, Angew. Chem., Int. Ed. 2000, 39, 3481.

[6] S. S. Zade, M. Bendikov, J. Org. Chem., 2006, 71, 2972.

[7] M. Bednarz, P. Rwineker, E. Mena-Osteritz, P. Bäuerle, J. Lumin., 2004, 110, 225.

[8] E. Mena-Osteritz, P. Bäuerle, Adv. Mater., 2001, 13, 243.

[9] E. Mena-Osteritz, Adv. Mater., 2002, 14, 609.

[10] J. Casado, V. Hernández, R. P. Ortiz, M. C. R. Delgado, J. T. L. Navarrete, G. Fuhrmann, P. Bäuerle, J. Raman Spectrosc., 2004, 35, 592.

[11] S. Foumine, P. Guadarrama, J. Phys. Chem. A, 2006, 110, 10098.

[12] W-H. Michele, A. Bhaskar, G. Ramakrishna, T. Goodson, M. Imamura, A. Mawatari, K. Nakao, H. Enozawa, T. Nishinaga, M. Iyoda, J. Am. Chem. Soc., 2008, 130, 3252.

[13] M. Kobayashi, N. Colaneri, M. Boysel, F. Wudl, A. J. Heeger, J. Chem. Phys., 1985, 82, 5717.

[14] A. D. Becke, J. Chem. Phys., 1993, 98, 5648.

[15] A. Lee, W. Yang, R. G. Parr, Phys. Rev. B, 1988, 37, 785.

[16] Y. Tawada, T. Tsuneda, S. Yanagisawa, T. Yanai, K. Hirao, J. Chem. Phys., 2004, 120, 8425.

[17] T. Yanai, D. P. Tew, N. C. Handy, Chem. Phys. Lett., 2004, 393, 51.

[18] J. L. Bredas, J. Cornil, D. Beljonne, D. D. Santos, Z. G. Shuai, Acc. Chem. Res., 1999, 32, 267.

[19] J. S. Murray and K. Sen (Ed.), *Molecular Electrostatic Potential, Concepts and*

Application, *Elsevier Science*, Amsterdam, 1996, 3, 371.

[20] C. J. Pedersen, J. Am. Chem. Soc., 1967, 89, 2495.

[21] C. J. Pedersen, J. Am. Chem. Soc., 1967, 89, 7017.

[22] M. Wykes, B. Milian-Medina, J. Gierschner, Front. Chem., 2013, 1, 135.

[23] J. Gierschner, J. Cornil, H.-J. Eglehaaf, Adv. Mater., 2007, 19, 173.

[24] A. Karolewski, T. Stein, R. Baer, S. Kümmel, J. Chem. Phys., 2011, 134, 151101.

[25] M. P. Balanay, D. H. Kim, J. Phys. Chem. C, 2011, 115, 19424.

[26] J. Fabian, H. Hartmann, J. Phys. Org. Chem., 2007, 20, 554.

Chapter 7

Computational modelling of thiophene based donor-acceptor molecules towards photovoltaic applications

7.1. Introduction

Thiophene based oligomers have received much attention because of their light harvesting efficiency (LHE), versatile structure and intrinsic charge transport behaviour [1]. The conjugated oligomers possess some critical advantages over their polymeric counterparts, such as well-defined molecular structures, synthetic reproducibility, high device performance, etc. In addition, crystalline features of oligomers favour the long-range interactions in solid state to enhance the charge transport properties, and devices can be easily fabricated [1]. Oligothiophene based molecules are among the most promising materials due to their structural versatility due to which tailor made materials can be made for tuning the device performances [2,3]. These molecules are used in the applications of solar cells, light emitting diodes etc. due to their planar geometry and tunable electronic and optical properties [4,5]. These oligothiophenes can be modified to get the desired properties which can be used in solar cells by coupling with donor-acceptor moieties at both the ends. The donor-acceptor moieties on conjugated oligomers serve as excellent components in solar cells due to their well-defined structure which enlarges the light absorbing region at higher wave lengths and also due to their strong inter molecular interactions [6].

In this chapter, we have discussed the electronic and optical properties of thiophene based triphenylamine (TPA) donor - cyanoacrylic acid (CAA) acceptor molecules (shown in Scheme 7.1) with different π-spacer length (n = 2-4) towards photovoltaic applications. Electronic properties of these molecules are studied with density functional methodology using B3LYP [7,8] functional and 6-31G(d) basis set. The optical properties like absorption, oscillator strength, Gibbs free energy change, excited state lifetime etc. are studied with TD-DFT formalism with long-range corrected functional CAM-B3LYP [9,10] and 6-31G(d) basis set in tetrahydrofuran solvent. The optimized structures of some of these molecules (1a) and (3a) are shown in Figure 7.1. Dihedral angles between donor and thiophene ring in π-spacer between sulphur atoms of adjacent thiophene units π-spacer and acceptor show that all the molecules exhibit non- planarity in their geometry. The details of dihedral angles are provided in Table 7.1.

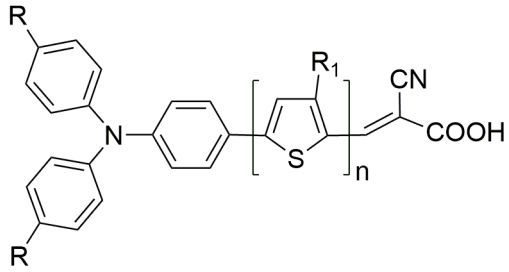

R=H R1 = H n= 2 (**1a**) R= CH_3 R1 = H n= 2 (**2a**)
R=H R1 = H n= 3 (**1b**) R= CH_3 R1 = H n= 3 (**2b**)
R=H R1 = H n= 4 (**1c**) R=CH_3 R1 = H n= 4 (**2c**)

R=CH_3O R1 = H n= 2 (**3a**) R=CH_3O R1 = CN n= 2 (**4a**)
R=CH_3O R1 = H n= 3 (**3b**) R= CH_3O R1 = CN n= 3 (**4b**)
R=CH_3O R1 = H n= 4 (**3c**) R= CH_3O R1 = CN n= 4 (**4c**)

Scheme 7.1. Thiophene based triphenylamine donor – cynoacrylic acid acceptor molecules.

System	Dihedral angles		
	Donor-spacer	between thiophene units	Spacer-acceptor
1a	20°	175°	0°
1b	22°	172° 178°	0°
1c	22°	171° 175° 179°	0°
2a	20°	176°	0°
2b	22°	172° 178°	0°
2c	21°	172° 176° 179°	0°
3a	18°	175°	0°
3b	21°	175° 179°	0°
3c	21	170° 178° 179°	0°
4a	20	168	0
4b	21	171 172	0

4c	22	166 165 163	0

Table 7.1 Dihedral angles between donor, spacer and acceptor. D, S and A indicate donor, π-spacer and acceptor respectively.

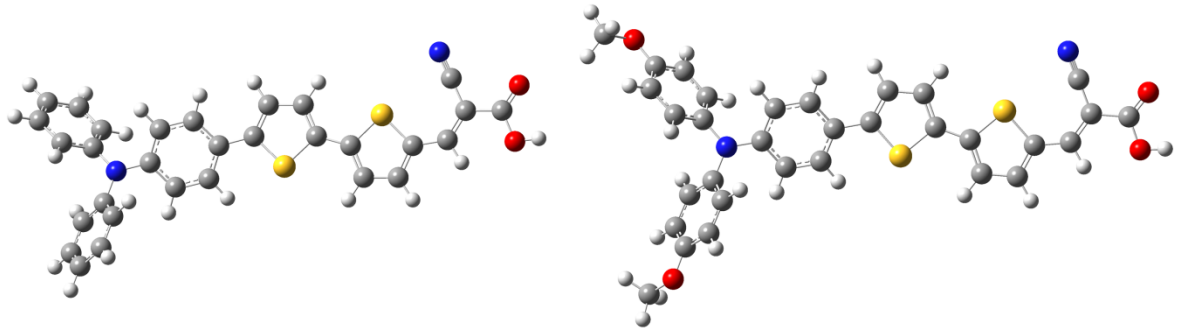

Figure 7.1. Optimized geometry of thiophene based donor-acceptor molecules (1(a) and3(a)).

The dihedral angle between donor and π-spacer is around 20^{o} in every molecule. The non-planarity in these molecules inhibits the dye aggregation and recombination which may improve the power conversion efficiency. In all these molecules π-spacer maintains the planarity which helps electron transfer from triphenylamine donor moiety to the cyanoacrylic acid acceptor. The CAA acid acceptor is completely in planar with the thiophene π-spacer.

7.2. Electronic properties of tripehenylamine donor- thiophene π-spacer – cyanoacrylic acid acceptor

Band gap is the one of the important factor in diciding the efficiency in dye sensitized solar cells (DSSCs). In dyes having smaller energy gaps, electron excitation takes place readily, which is beneficiary for absorption of dyes in the longer (red) wavelength region [11]. The band gaps of the dyes decrease when the donor group abilities results in increased are more effective conjugation length. The band gaps of all the four set of molecules are shown in the Table 7.2.

Oligothiophene chain length	TPA-nT	Me-TPA-nT	MeO-TPA-nT	MeO-TPA-nT(CN)
2	2.24 (2.20e)	2.21 (2.31e)	2.07 (2.27e)	1.65
3	2.11 (2.17e)	2.03	1.94	1.47
4	2.00	1.93	1.84	1.40

Table 7.2. Band gaps calculated with B3LYP functional, 6-31G(d) basis set in THF solvent. e refer to the experimental values [12,13]

Design of a DSSC requires a variety of factors, such as structural parameters like dihedral angles, stability, electronic levels, and absorption of the DSSC etc. Dye molecule absorbs the solar light energy through the pores of semiconducting material and excites its electron from occupied levels to unoccupied levels. Electron injection takes place from the LUMO level of the dye to the conduction band (CB) of semiconductor, which generates the electricity by reaching the electrodes. Dye should follow some criteria to convert the solar energy into electricity, such as, (i) dye must possess the band gap of less than 2eV. (ii) LUMO level should be higher in energy than that of CB edge of the semiconductor (iii) HOMO of the dye should be lower in energy than that of electrolyte and (iv) absorption of dye should be in visible region range. Schematic representation of electron flow mechanism in solar cells is shown in Figure 7.2.

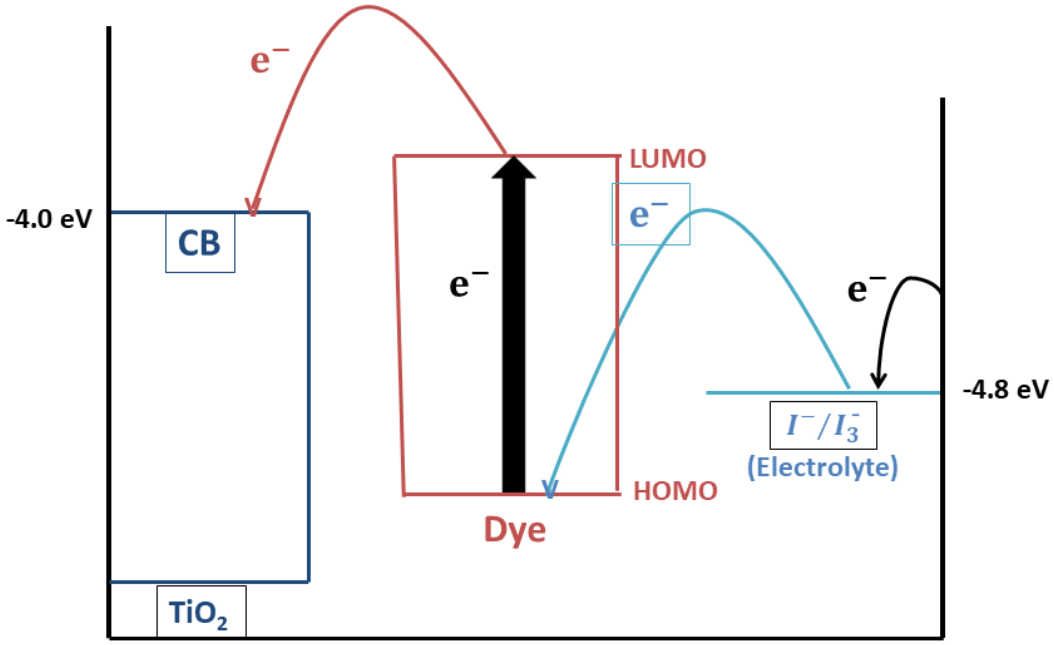

Figure 7.2. Schematic representation of electron flow mechanism in dye sensitized solar cell.

One of the factors for favourable electron transfer from the dye to semiconductor is that the LUMO level of dye should lie higher in energy than the conduction band (4.0 eV) of the semiconductor i.e, TiO_2 [14]. After absorption of solar energy, dye will be oxidized by exciting its electron to LUMO level and this oxidized dye can be reduced by taking electron from idodide/triiodide (I^-/I_3^-)electrolyte. For favourable electron transfer from electrolyte

to dye molecule, the HOMO level of dye should be lower in energy than the HOMO of the electrolyte (4.80 eV) [15]. Increase in chain length lowers the band gap and methyl, methoxy substitutions on triphenylamine moiety further lowers the band gap. HOMO and LUMO levels of all the molecules are as shown in Figure 7.3.

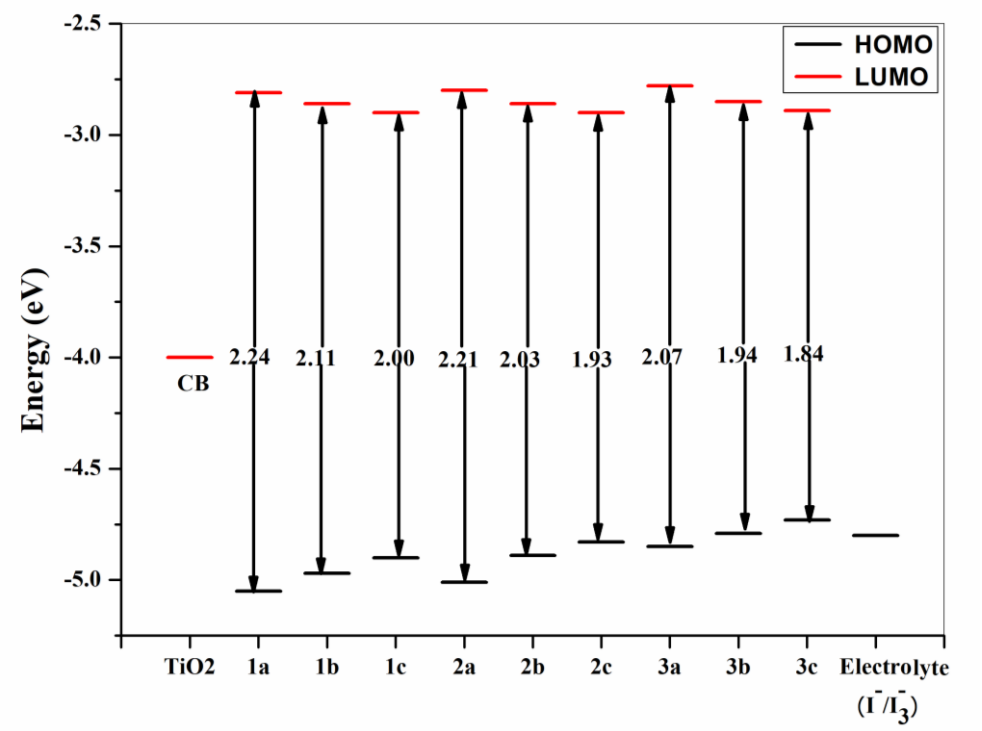

Figure 7.3. HOMO, LUMO and band gaps in eV of dyes of thiophene based dyes with H, Me and MeO substitutions on triphenylamine donor moiety.

From Figure 7.3, we conclude that all the LUMOs of dyes lie above the conduction band and therefore favourable electron transfer takes place from LUMO to conduction band of the TiO_2 semiconductor and all the HOMOs of the molecules are placed below the HOMO of the electrolyte so that they can be reduced by the electrolyte except for 3b (4.79 eV) and 3c (4.73 eV) for which HOMO levels are lie above the HOMO of the electrolyte. Increase in chain length as well as increase in the strength of electron donating group increases the HOMO energy level which is not favourable for dye regeneration from the electrolyte. In all three sets -H, -Me and -OMe substitution on triphenylamine moiety shows linear increase in HOMO and decrease in LUMO is observed. In order to lower the HOMO level for favourable reduction of the dye from electrolyte, these molecules can be substituted with strong electron withdrawing cyano (-CN) group [16], which may favour the dye reduction

from the electrolyte. The HOMO and LUMO levels of cyano substituted π-spacer are depicted in the Figure 7.4.

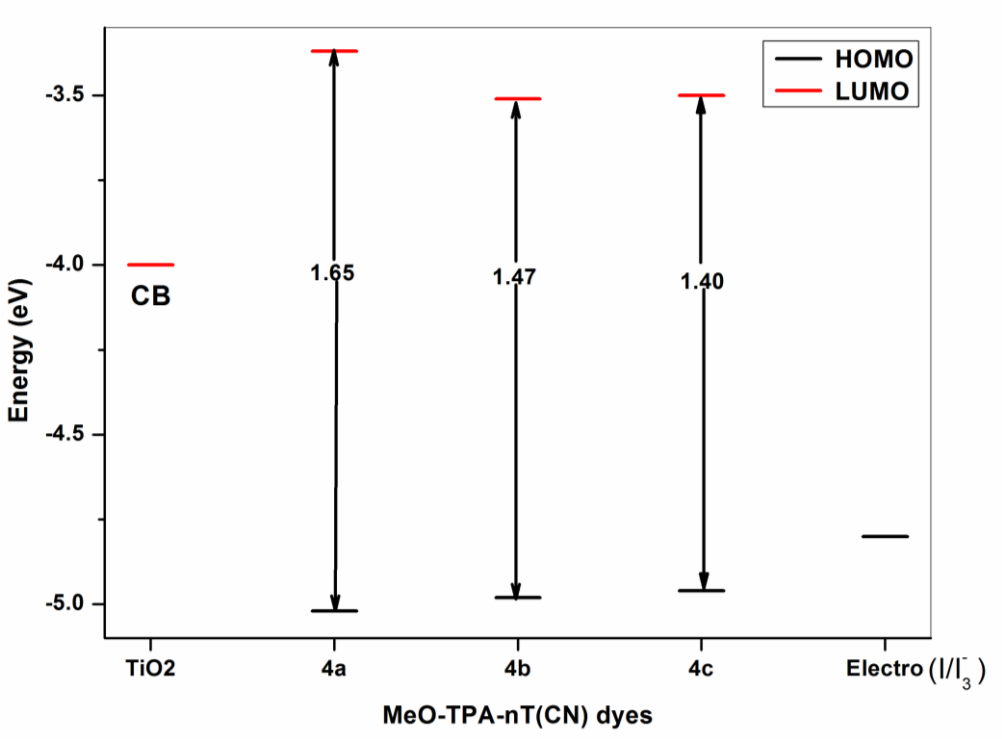

Figure 7.4. HOMO, LUMO levels and band gaps of CN substitution on π-spacer thiophene moiety (4a-4c).

As per Shockley-Queisser effect, theoretical ideal band gap for maximum efficiency of a p-n junction solar cell is 1.4 eV that gives the power conversion efficiency of 30% [17]. One of our molecules substituted with electron withdrawing -CN group on thiophene rings falls into this category without compromising the HOMO and LUMO levels for electron transfer.

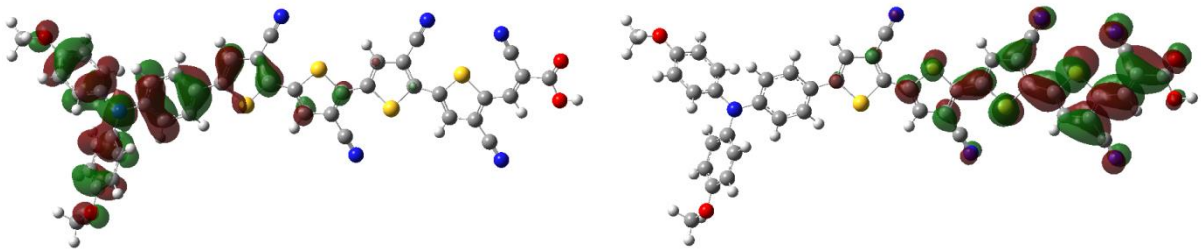

Figure 7.5. HOMO and LUMO of 4c molecule.

As can be seen in Figure 7.5, the electron densities of HOMOs are majorly concentrated on donor and slightly on the π-spacer and LUMOs are concentrated more on

acceptor moiety, so electronic transitions from HOMO to LUMO could lead to the intramolecular charge transfer from donor to acceptor through planar π-spacer. The LUMO of all these dyes is concentrated on the anchoring group –COOH of cyanoacrylic acid which indicates the strong electron coupling between the dye and semiconductor.

Other electron withdrawing groups like nitro (-NO_2) and fluoro (-F) substitutions on each thiophene unit of the π-spacer are studied. Fluorine substitution on thiophene π-spacer of donor-acceptor moiety, maintains the planarity but the HOMO (-4.76 eV) energy level lies above the HOMO of the I^-/I_3^- electrolyte which is not favourable for reduction of oxidized dye whereas nitro substituted HOMO and LUMO levels fall at favourable height for electron reduction by electrolyte and electron injection on to the semiconductor TiO_2. Nitro substitution on thiophene π-spacer disturbs the planarity of the π-spacer which is not favourable for transfer for electron density from triphenylamine donor moiety to cynoacrylic acid acceptor.

7.3. Optical properties of the thiophene based donor-acceptor molecules

Optical properties like absorption, oscillator strength and Gibbs free energy change etc. also play vital role in the determination of power conversion efficiency of a solar cell. Intense and broad absorption spectrum of a dye in visible and near infrared region lead to increased short circuit current (J_{SC}) [18]. Traditional exchange functionals like B3LYP, M06, and B3PW91 overestimate the optical properties. Therefore TD-DFT calculations are employed for the calculation of optical properties of dye molecules in tetrahydrofuran solvent using polarizable continuum model with long range corrected CAM-B3LYP functional.

The absorption band of λ_{max} for all the dyes are in visible region with highest oscillator strength. The absorption λ_{max} (intramolecular charge transfer band) values, oscillator strengths, major orbital contributions in the lowest energy transitions of all the dyes are mentioned in the Table 7.3. HOMO to LUMO and HOMO-1 to LUMO are majorly contributing to the lowest energy transition of all the molecules. As the length of the π-spacer increases the contribution from HOMO-1 to LUMO is increased and HOMO to LUMO is decreased. Small red shift has been observed upon substitution of methyl and methoxy substitutions on the triphenylamine moiety. Absorption spectra of all the dyes as shown in the Figure 7.6. Ground and excited state properties of methoxy substitution on donor triphenylamine based dyes have been studied theoretically with PBE based functionals. The excitation energy of the molecule (3a) calculated with CAM-B3LYP (2.81eV) is found

to be close to the experimental (2.84eV) [19] value than the Climent co-workers best value calculated with LRC-ωPBE (3.03eV) functional [20]. From Figure 7.6, we observe that the most of the absorption spectrum of all the molecules is in visible region which is favourable for solar cells. Slight red shift is observed in the absorption spectra as the strength of donor increases whereas upon cyano substitution on π-spacer, significant redshift of 0.3-0.4 eV is observed.

System	E_{Opt} (eV)	λ_{max} (nm)	Oscillator strength (f)	Major orbital contributions
1a	2.84	436 (448e)	1.61	H-1→LUMO (29%), HOMO→LUMO (62%)
1b	2.78	445 (459e)	2.04	H-1→LUMO (38%), HOMO→LUMO (48%)
1c	2.72	455	2.23	H-1→LUMO (41%), HOMO→LUMO (37%)
2a	2.81	441 (429e)	1.62	H-1→LUMO (30%), HOMO→LUMO (61%)
2b	2.77	448	2.05	H-1→LUMO (41%), HOMO→LUMO (45%)
2c	2.71	457	2.27	H-1→LUMO (45%), HOMO→LUMO (32%)
3a	2.78	445 (437e)	1.62	H-1→LUMO (30%), HOMO→LUMO (61%)
3b	2.74	452	2.06	H-1→LUMO (42%), HOMO→LUMO (43%)
3c	2.70	458	2.28	H-1→LUMO (47%), HOMO→LUMO (29%)
4a	2.40	516	1.22	H-1→LUMO (21%), HOMO→LUMO (71%)
4b	2.40	516	1.56	H-1→LUMO (30%), HOMO→LUMO (53%)
4c	2.47	502	1.90	H-1→LUMO (34%), HOMO→LUMO (34%)

Table 7.3. Absorption values, oscillator strength and orbital contributions of dyes using CAM-B3LYP and 6-31G(d) values are in THF solvent, 'e' indicates experimental values [15].

There are majorly three molecular orbitals HOMO, HOMO-1 and LUMO are involved in the electronic transitions of all these molecules. We have calculated the contribution of each moiety i.e., for triphenylamine unit, thiophene π-spacer and for anchoring group cyanoacrylic acid in these molecular orbitals as shown in the Table 7.4. In all these dyes, π-spacer (52-62%) and cyanoacrylic acid (around 40%) have the major contributions towards the LUMO and in HOMO and HOMO-1 triphenylamine (55-87, 30-45) and π-spacer (17-43%, 51-61 %) has the major contribution. This indicates that all the molecules will have better coupling with the TiO_2 semicondcuctor.

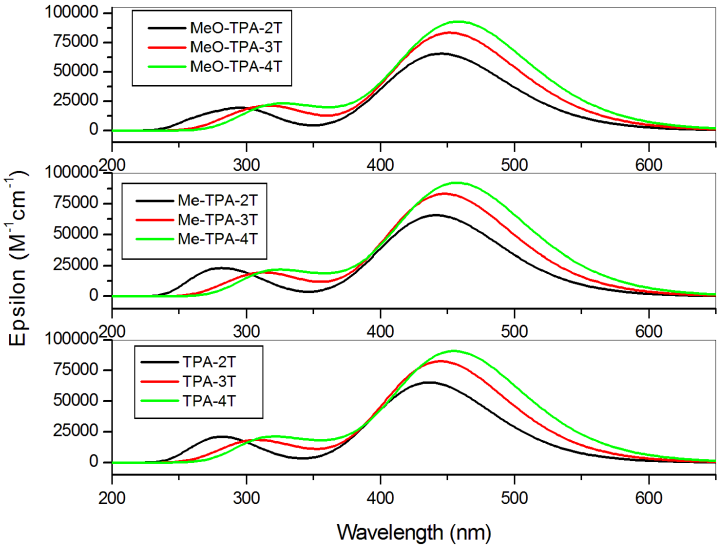

Figure 7.6. The absorption spectra of thiophene based triphenylamine donor and cyanoacrylic acid acceptor.

System	Molecular Orbital	% contribution		
		TPA	Π-spacer (thiophene)	CAA
1a	LUMO	6	52	42
	HOMO	74	22	4
	HOMO-1	33	52	15

1b	LUMO	2	61	37
	HOMO	64	33	3
	HOMO-1	35	55	10
1c	LUMO	1	62	37
	HOMO	55	43	2
	HOMO-1	39	55	6
2a	LUMO	6	52	42
	HOMO	77	19	4
	HOMO-1	32	53	15
2b	LUMO	3	60	37
	HOMO	70	28	2
	HOMO-1	32	58	10
2c	LUMO	1	62	37
	HOMO	62	37	1
	HOMO-1	34	60	6
3a	LUMO	6	52	42
	HOMO	80	17	3
	HOMO-1	35	51	14
3b	LUMO	3	60	37
	HOMO	75	23	2
	HOMO-1	30	61	9
3c	LUMO	1	62	37
	HOMO	69	30	1
	HOMO-1	30	64	6
4a	LUMO	4	56	40
	HOMO	87	11	2
	HOMO-1	45	46	9
4b	LUMO	2	63	35
	HOMO	87	13	1

	HOMO-1	34	60	6
4c	LUMO	1	64	35
	HOMO	87	13	0
	HOMO-1	28	69	3

Table 7.4. Percentage of contribution of each moiety in the molecular orbitals LUMO, HOMO and HOMO-1.

Increase in light harvesting efficiency leads to higher photo current generation from solar cell or dye. Comparison of light harvesting efficiencies of the substitution on triphenylamine moiety as well as cyano group on π-spacer is shown in the Figure 7.7. LHE of unsubstituted/substituted thiophene-dimer (π-spacer) is found to be 97.5%. As the π-spacer increases light harvesting efficiency values are also increased from 99-99.5%.

The calculated ΔG_{Inject} values, open circuit voltage (V_{OC}) values for all the molecules tabulated in Table 7.5 are exergonic and favourable for electron injection on to the semiconductor. As the chain length increases the ΔG_{Inject} value decreases, which shows that increase in chain length decreases the favourability of electron injection into semiconductor TiO_2. ΔG_{Inject} is also calculated for all the dyes 1-3 (ΔG_{Inject} = -3.64 to -3.84 eV) series of molecules are more favourable for electron injection, whereas ΔG_{Inject} is decrease upon cyano substitution on π-spacer. No significant change is observed in the open circuit voltage values of these molecules even after substitution of methyl and methoxy groups on triphenylamine donor unit. In addition open circuit voltage values of these molecules decrease with the increase in chain length of the π-spacer. Open circuit voltage values also decrease upon substitution of cyano groups on the linker moiety which inhibits the power conversion efficiency. The cyano substitution on π-linker is found to reduce all these values.

The excited state lifetime is one of the important factors of DSSC, which can be useful to estimate the efficiency of electron injection to the semiconductor TiO_2. Solar cells should have lesser excited life time for faster electron injection to avoid recombination and maximum V_{OC} value for maximum efficiency. Electron injection from the excited of DSSC molecule to the semiconductor occurs within 100 fs. This fast injection means that increasing concentration of acceptor species on the TiO_2 surface, leading to electron recombination, which results in a short electron lifetime.

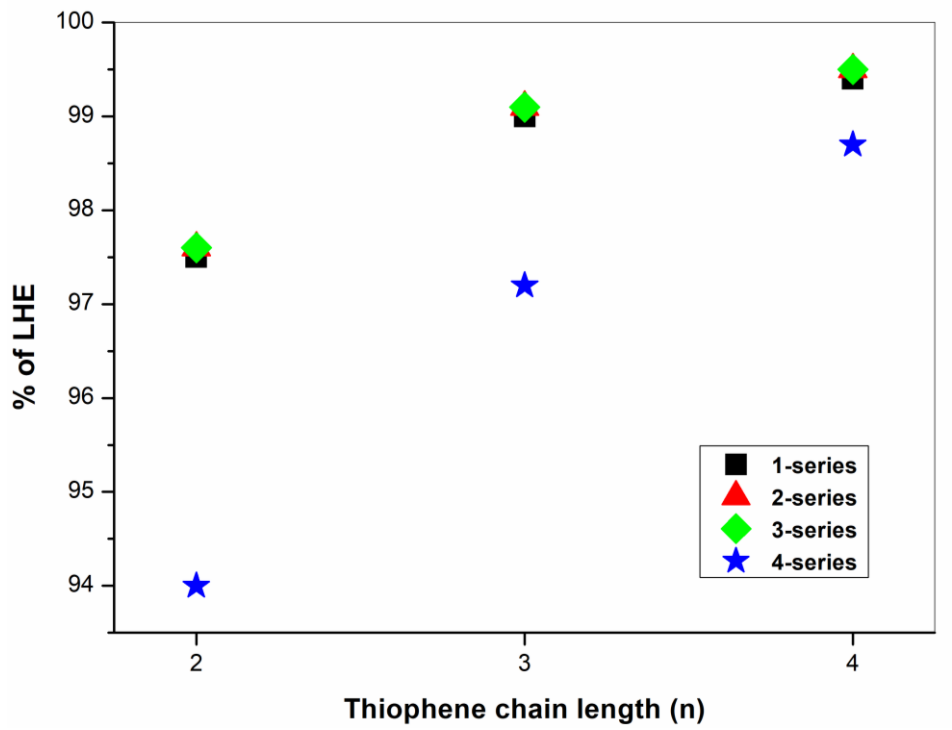

Figure 7.7. Calculated LHE values of TPA based dyes with substitution H, Me, and MeO on triphenylamine moiety.

This lowers the photovoltage and reduces the efficiency of charge collection, decreasing the short circuit photocurrent density and photocurrent efficiency. In order to avoid the electron recombination, excited state electron life time has to be increased.

System	ΔG_{Inject} (eV)	V_{OC}	τ(ns)	E_b
1a	-3.84	1.19	2.81	0.60
1b	-3.74	1.14	2.69	0.67
1c	-3.67	1.10	2.68	0.72
2a	-3.83	1.20	2.82	0.60
2b	-3.73	1.14	2.72	0.74
2c	-3.67	1.10	2.67	0.78
3a	-3.83	1.22	2.91	0.71
3b	-3.72	1.15	2.73	0.80

3c	-3.64	1.11	2.71	0.86
4a	-2.85	0.49	4.08	0.75
4b	-2.72	0.63	3.57	0.93
4c	-2.73	0.44	3.03	1.07

Table 7.5. Calculated values of ΔG_{Inject}, open circuit voltage and excited state life time (τ).

The excited state life times and exciton binding energies are calculated for the first excited state and lowest excitation energy and its corresponding oscillator strength are considered. The calculated excited state life time of dyes is presented in the Table 7.5. Excited state life times are found to be decreased with increase in chain length of the π-spacer which increases the power conversion efficiency. On substitution of electron donating groups, methyl and methoxy groupds on triphenylamine donor moiety of the dye molecules, the excited state life time is found to be increased. This increase in excited state life time enhances the the charge recombination thereby decreasing the power conversion efficiency. First three series of dyes (1a-c,2a-c, 3a-c) have excited state lifetime of 2.67-2.81 nano seconds (ns) whereas upon substitution of cyano group on thiophene linker, excited state lifetimes have been increased to 3.03-4.08 ns.

7.4. Nonlinear optical properties:

Polarization in the molecule behaves as an internal electric field which causes the charge carrier separation and reduces the charge recombination. Larger the nonlinear optical (NLO) properties, polarizability, hyperpolarizability, the larger is the efficiency in the separation of charges. NLO properties are used to describe the efficiency of electron charge transfer which influences the short circuit current and power conversion efficiency. A list of NLO properties such as polarizability (α), polarizability anisotropy (Δα) and hyperpolarizabilities (β) are calculated using B3LYP functional. As observed from the Table 7.6, we can see that the magnitudes of nonlinear coefficients are found to increase with increase of π-spacer chain length and the strength of the electron donating triphenylamine group. Hyperpolarizability of molecules labelled 1(a), 1(b), 1(c) are $17.601.10^4$, $26.069.10^4$ and $34.797.10^4$ atomic units respectively. This indicates that hypepolarizability is chain length dependent and increase with the increase of conjugated π-spacer chain length. Upon substitution with methyl ($20.748.10^4$ - $39.693.10^4$) and methoxy ($24.908.10^4$ - $47.188.10^4$)

groups on triphenylamine, hyperpolarizabilities are increased. By increasing the strength of the electron donating group by substitution of methyl and methoxy groups on triphenylamine moiety the NLO properties also is found to increase but this increase is comparitively lesser than the increase in NLO properties when the π-spacer chain length is increased.

Polarizability 'α' is the measure of electrons response to the electric field. Larger value of α indicates the ease with which electrons move from the donor to acceptor moiety. Polarizability/polarizability anisotropy follows the same trend as like hyperpolarizabilty. Polarizability and polarizability anisotropy is of the range $7.24.10^2$ - $10.86.10^2$ au and 10.67-18.35 for TPA-nT series respectively. These values have been increased with increase of bridge chain length and upon methyl ($\alpha = 7.77.10^2$ - $11.38.10^2$, $\Delta\alpha=11.23.10^2 – 18.87.10^2$ au **)** and methoxy ($\alpha = 8.08.10^2$ - $11.71.10^2$, $\Delta\alpha =11.91.10^2 – 19.63.10^2$ au) substitutions.

System	α (10^2 au)	Δα (10^2 au)	β_{tot} (10^4 au)
1a	7.24	10.67	17.601
1b	9.17	14.94	26.069
1c	10.86	18.35	34.797
2a	7.77	11.23	20.748
2b	9.69	15.49	30.329
2c	11.38	18.87	39.693
3a	8.08	11.91	24.908
3b	10.04	16.28	36.686
3c	11.71	19.63	47.188

Table 7.6. Polarizabilities, polarizability anisotropy, and hyperpolarizabilities

Nonlinear optical properties (α, Δα and β) properties describe the tendency on the delocalization of intramolecular charge in donor-acceptor molecules. The NLO properties increases with the increase of chain length which can modify the electronic properties and can affect the nature of the interaction between dye molecule and semiconductor TiO_2. This increase in NLO properties result in higher charge separation and therefore enhance the power conversion efficiency of solar cells. The NLO properties are improved with increase of donor strength by substituting triphenylamine with methyl and methoxy groups.

7.5. Conclusion

The structural, electronic and optical properties of thiophene based donor-acceptor molecules have studied with B3LYP hybrid functional and 6-31G(d) basis set including solvent formalism polarizable continuum model in tetrahydrofuran solvent and found that the calculated electronic band gaps are closer to the experimental values. The optical absorption properties are calculated with CAM-B3LYP functional, employing TD-DFT and found excellent accordance with the experimental values. The negative ΔG_{Inject} values favour the electron transfer from excited state of the dyes to conduction band of the semiconductor. Substitution of electron donating groups methyl and methoxy substitution on triphenylamine showed positive results such as less band gap, increase in oscillator strength and consequently increase in light harvesting efficiency, excited state life time etc. Substitution of strong electron withdrawing cyano group brings the band gap of 1.4 eV (4c) which falls in the Shockley-Queisser theoretical limit but other parameters like ΔG_{Inject}, open circuit voltage, light harvesting efficiency, excited state life time etc. are diminished.

7.6 References

[1] F. Zhang, D. Wu, Y. Xu, X. Feng, J. Mater. Chem., 2011, 21, 17590.

[2] N. Noma, T. Tsuzuki, Y. Shirota, Adv. Matter., 1995, 7, 647.

[3] A. Mishra, C. Q. Ma, P. Bäurle, Chem. Rev., 2009, 109, 1141.

[4] N Noma, T Tsuzuki, Y. Shirota, Adv. Mater., 7, 1995, 647.

[5] M. Piacenza, M. Zambianchi, G. Barbarella, G. Gigli, F. D. Sala, Phys. Chem. Chem. Phys., 2008, 10, 5363.

[6] N. Koumura, Z-S Wang, S. Mori, M. Miyashita, E. Suzuki, K. Hara, J. Am. Chem. Soc., 2006, 128, 14256; Q. Feng, Q. Zhang, X. Lu, H. Wang, G. Zhou, Z-S Wang, ACS Appl. Mater. Interfaces, 2013, 5, 8982.

[7] A. D. Becke, J. Chem. Phys., 1993, 98, 5648.

[8] A. Lee, W. Yang, R. G. Parr, Phys. Rev. B, 1988, 37, 785.

[9] Y. Tawada, T. Tsuneda, S. Yanagisawa, T. Yanai, K. Hirao, J. Chem. Phys., 2004, 120, 8425.

[10] T. Yanai, D. P. Tew, N. C. Handy, Chem. Phys. Lett., 2004, 393, 51.

[11] S. Sharma and M. Bendikov, Chem. Eur. J., 2013, 19, 13127.

[12] N. Somanathan, S. Radhakrishnan, Int. J. Mod. Phys., B 2005, 19, 4645.

[13] W. Xu, B. Peng, J. Chen, M. Liang, F. Cai, J. Phys. Chem., C 2008, 112, 874.

[14] J. B. Asbury, Y. Q. Wang, E. Hao, H. N. Ghosh and T. Lian, Res. Chem. Intermed., 2001, 27, 393.

[15] D. Cahen, G. Hodes, M. Gräetzel, J. F. Guillermoles, I. J. Riess, J. Phys. Chem. B, 2000, 104, 2053.

[16] M. Qiu, R. G. Brandt, Y. Niu, X. Bao, D. Yu, N. Wang, L. Han, L. Yu, S. Xia, R. Yang, J. Phys. Chem. C, 2015, 119, 8501.

[17] W. Shockley, H. J. Queisser, J. Appl. Phys., 1961, 32, 510.

[18] Z-S. Wang, N. Koumura, Y. Cui, M. Takahshi, H. Sekiguchi, A. Mori, T. Kubo, A. Furube, K. Hara, Chem. Mater., 2008, 20, 3993.

[19] Y. J. Chang, Y-J. Wua, P-T. Chou, M. Watanabe, T. J. Chow, Thin Solid Films, 2014, 558, 330.

[20] C. Climent, David Casanova, Chem. Phys., 2013, 423, 157.

Future Scope of Work

Organic semiconducting π-conjugated materials have received a great scientific attention because of their progress in the applications of photovoltaics, light emitting diodes, transistors etc. Stability, good solid state packing, processability rigidity and energy gap is in the semiconducting region are the main requirement for useful organic electronic materials. The physical properties of furan based molecules, like solubility, fluorescence and charge transfer phenomena make them superior over other organic π-conjugated molecules. Easy processability and stability are the advantages of thiophene based molecules over other organic π-conjugated systems. Therefore with the integration of these two properties, sulphur and oxygen based oligomers may enhance the optical and electronic properties and may be used as alternative materials for organic electronics. Our study on organic π-conjugated systems will be continued on electronic and optical properties of thiophene and furan based oligomers and polymers to attain better properties towards material research for application in organic electronics.

List of Publications

1. M. Saisudhakar, T. Vikramaditya, K. Sumithra, J. Phys. Org. Chem. 2015, 28, 695.
2. T. Vikramaditya, M. Saisudhakar, K. Sumithra, J. Mol. Struct. 2015, 1081, 114.
3. T. Vikramaditya, M. Saisudhakar, K. Sumithra, J. Comput. Theor. Nanosci. 2015, 12, 3171.
4. T. Vikramaditya, M. Saisudhakar, K. Sumithra, RSC Adv. 2016, 6, 37203.
5. M. Saisudhakar, T. Vikramaditya, K. Sumithra, Comprehensive evaluation of the effect of various exchange correlation functionals and basis sets on the optical properties of oligothiophenes (under review).
6. M. Saisudhakar, T. Vikramaditya, K. Sumithra, Electronic structure calculations of linear and cyclic isothianaphthenes (under review).
7. M. Saisudhakar, K. Sumithra, Computational modelling of thiophene based donor – acceptor molecules towards photovoltaic applications (under review)

List of International and National Conferences

1. Presented poster: M. Saisudhakar, T. Vikramaditya, K. Sumithra, Electronic structure calculations of linear and cyclic isothianaphthenes at Nascent Developments in Chemical Sciences: Opportunities for Academia-Industry Collaboration, 2015, BITS Pilani, Pilani Campus.
2. Presented poster: M. Saisudhakar, T. Vikramaditya, K. Sumithra, Effect of substituents on electronic properties of oligo- and polythiophenes at 13^{th} Eurasia conference on chemical science, Indian Institute of Sciences, Banglore.
3. Presented poster: T. Vikramaditya, M. Saisudhakar, K. Sumithra, Electronic and structure properties of Oligothiophenes; Chemistry with Computers, IIIT-Hyderabad and IICT-Hyderabad, India (2014).
4. Presented poster: T. Vikramaditya, M. Saisudhakar, K. Sumithra, Diagnostic test to assess the role of Functional, solvent formalism and basis set in determining the optical properties; 13^{th} Eurasia Conference on Chemical Sciences, Indian Institute of Science, Bangalore, India (2014).

Biography of Mr. Saisudhakar: Mr. Saisudhakar has completed his bachelor's degree from DRS degree college, Khammam, affiliated to Kakatiya University. He has received master's degree in chemical sicences from Pondicherry University. He has joined for Ph. D. in computational chemistry at BITS Pilani Hyderabad Campus, Hyderabad under the supervision of Prof. K. Sumithra in the year 2012. His research interests are the of electronic structure properties of oligo, poly and cyclic thiophenes in the application of solar cells, organic light emitting diodes. He also involved in the study of adsorption properties of carbon naotubes.

Biography of Prof. K. Sumithra: Prof. K. Sumithra is presently working as associate professor, Department of Chemistry in Birla Institute of technology and science, Pilani Hyderabad Campus, India where she joined in July, 2009. She received her Doctoral degree from Cochin University of Science and Technology, Cochin, Kerala. After Ph.D. she has worked briefly as a lecturer and has worked in various institutes in Germany as a post-doctoral researcher. After this, she has worked in Martin Luther University on a C1 position equivalent to Junior Professor in the Theoretical Physics division for about six years.

She has been involved in teaching and research for the past 15 years. Her research interest mainly focus on Statistical Mechanics of Polymer in disordered media, Adsorption of polymers on surfaces, Pattern Recognition and Computational Material Science. Her current research concentrates on adsorption on carbon nanotubes, band structure calculations, organic semiconducting oligomeric and polymeric systems etc. She has published several research articles in various peer reviewed international journals. Recently, she has successfully completed two projects funded by DST and CSIR.